5-2020

Vestigial-like 1 is a shared targetable cancer-placenta antigen expressed by pancreatic and basal-like breast cancers

Sherille Denae Bradley

VESTIGIAL-LIKE 1 IS A SHARED TARGETABLE CANCER-PLACENTA ANTIGEN EXPRESSED BY PANCREATIC AND BASAL-LIKE BREAST CANCERS

by

Sherille Denaé Bradley, M.Sc.

APPROVED:

_____
Gregory Lizee, Ph.D.
Supervisory Professor

_____
Chantale Bernatchez, Ph.D.

_____
Amir Jazaeri, M.D.

_____
Dorothy Lewis, Ph.D.

_____
Gheath Al-Atrash, D.O., Ph.D.

APPROVED:

_____
Dean, The University of Texas
MD Anderson Cancer Center UTHealth Graduate School of Biomedical Sciences

VESTIGIAL-LIKE 1 IS A SHARED TARGETABLE CANCER-PLACENTA ANTIGEN EXPRESSED BY PANCREATIC AND BASAL-LIKE BREAST CANCERS

A

Dissertation

Presented to the Faculty of

The University of Texas

Health Science Center at Houston

and

The University of Texas

MD Anderson Cancer Center

Graduate School of Biomedical Sciences

in Partial Fulfillment

of the Requirements

for the Degree of

DOCTORATE OF PHILOSOPHY

By

Sherille D. Bradley, M.Sc.

Houston, Texas, USA

December 2019

ACKNOWLEDGEMENTS

First, giving glory and honor to my Lord and Savior Jesus Christ to whom without I could not have accomplished this project. Secondly, thank you to my loving husband of 7 years, Jeremy Sanders, for being my daily support system. Also, thanks to my family for all of their love, prayers, and support throughout this entire process. Special thanks to my mentor Dr. Greg Lizee for his guidance and exceptional leadership during both my masters and Ph.D. studies. Thank you to Dr. Patrick Hwu for always questioning the relevance of my project and encouraging me to think about the bigger picture as it relates to saving patient's lives.

Thank you to all of my current and past lab mates who have contributed to this project; Amjad Talukder, Brenda Melendez, Kyle Jackson, Arjun Katailiha , and Heather Sonnemann. Huge thanks to Dr. Jason Roszik, Dr. David Hawke, and Dr. Cassian Yee for being integral to the success of this dissertation project. I am incredibly grateful for your help, from teaching me your methodology, processing data, and your intellectual contributions to my project. In addition, special thanks to each one of my committee members for sacrificing their time, providing their insight, encouragement, and challenging me intellectually throughout my Ph.D. studies. Finally, thank you to the MD Anderson Cancer Center UTHealth Graduates School of Biomedical Sciences for your resources and in providing well-experienced researchers to work with at this amazing institution.

VESTIGIAL-LIKE 1 IS A SHARED TARGETABLE CANCER-PLACENTA ANTIGEN EXPRESSED BY PANCREATIC AND BASAL-LIKE BREAST CANCERS

Sherille Denaé Bradley, M.Sc.

Advisory Professor: Gregory A. Lizee, Ph.D.

Cytotoxic T lymphocyte (CTL)-based cancer immunotherapies have shown great promise for inducing clinical regression by targeting tumor-associated antigens (TAA). To expand the TAA landscape of pancreatic ductal adenocarcinoma (PDAC), we performed tandem mass spectrometry analysis of HLA class I-bound peptides from tumors of PDAC patients. This led to the identification of a shared HLA-A*0101 restricted peptide derived from co-transcriptional activator Vestigial-like 1 (VGLL1), a novel putative TAA demonstrating overexpression in multiple tumor types and low or absent transcript expression in normal tissues with the exception of placenta. VGLL1-specific CTL isolated and expanded from the blood of a male PDAC patient showed the capacity to recognize and kill in an antigen-specific manner a majority of HLA-A*0101 allogeneic tumor cell lines derived not only from PDAC, but also ovarian, bladder, gastric, lung and basal-like breast cancers. Gene expression profiling revealed that VGLL1 is a member of a unique group of cancer-placenta antigens (CPA) that may constitute safe immunotherapeutic TAA targets for patients with multiple different cancer types. Additionally, we demonstrate that VGLL1 is associated with poorer patient survival rates in pancreatic cancer. However, its role in cancer remains largely uncharacterized. VGLL1 shares a similar binding motif to the TEAD family of genes with the oncogenes, YAP/TAZ that promote malignancies through the Hippo signaling pathway. We show that VGLL1 may play a significant role in tumorigenesis by inducing tumor cell proliferation, migration, and invasion.

TABLE OF CONTENTS

LIST OF FIGURES

Chapter I. Introduction and background

Chapter II. Tumor antigen discovery and T cell generation

Chapter III. VGLL1-specific T cells recognize and kill both autologous pancreatic tumor lines and other VGLL1-expressing tumor lines

LISTS OF TABLES

Chapter I. Introduction and background

ABBREVIATIONS

MHC: Major Histocompatibility Complex

HLA: Human leukocyte antigen

CTLs: Cytotoxic T Lymphocytes

TILs: Tumor infiltrating lymphocytes

DCs: Dendritic cells

APCs: Antigen presenting cells

MART-1: Melanoma antigen recognized by T-cells 1

NY-ESO-1: New York esophageal squamous cell carcinoma 1

MAGE-A: Melanoma-associated antigen

YAP1: Yes associated protein 1

IL-2: Interleukin-2

IFN-α: Interferon-alpha

PD1: Programmed cell death protein 1

PDL1: Programmed death ligand 1

CTLA-4: Cytotoxic T- lymphocyte antigen-4

VEGF: Vascular endothelial growth factor

OVCA: Ovarian Cancer

PDAC: Pancreatic Cancer

VGLL1: Vestigial-like 1

MUC16: Mucin 16

CHAPTER I:

INTRODUCTION AND BACKGROUND

1.1 Introduction to Immunology

Immunology is the study of the immune system and its role in protecting the body against foreign pathogens and disease [1, 2]. The immune system is comprised of two main subcategories of immunity, innate and adaptive immunity [2, 3]. Innate immunity is the body's first line of defense against foreign entities [4, 5]. The innate response is immediate non-specific protection made to fight against invading bacteria, viruses, and fungus [3]. Adaptive immunity, also referred to as specific or acquired immunity, is created in response to the body's exposure to these foreign substances over time [6]. Adaptive immunity can be further subdivided into humoral and cell-mediated immunity [3, 6]. Humoral immunity is regulated by activated B cells through the production of antibodies, while cell-mediated immunity is carried out by T-lymphocytes cells (T cells). There are three major categories of T cells: helper, regulatory, and cytotoxic [2]. Within each of these three categories, there are multiple T cell subtypes. Helper T cells are primarily $CD4^+$ T cells. Helper T cells produce molecules called cytokines that signal to other immune cells in response to pathogens that the T cell recognizes. In contrast, regulatory T cells (T regs) play a role in the suppression of the immune system. T regs function to protect against the immune system by acting as a shut-off switch when it is no longer needed [2, 7]. Lastly, cytotoxic T cells (CTLs or $CD8^+$ T cells) are the primary effector cells of the immune response. $CD8^+$ T cells produce molecules that destroy foreign pathogens or infected cells once activated.

The power of the immune system can be harnessed to target not just invading microbes and viruses, but it can also be used as a biologic therapy for the treatment of cancer. While both the innate and adaptive immune system can be used as therapeutic

interventions of cancer, the adaptive immune response plays a vital role in anti-tumor immunity. As we will discuss further, this is because CTLs are the critical regulators of the cell-mediated immune response against cancer cells. In the following section, we will briefly discuss the history of immunotherapy, its various forms, and multiple ways that the adaptive immune response can be harnessed to treat cancer.

1.2 Immunotherapy

Immunotherapy aims to induce anti-tumor responses by augmenting immune surveillance and overcoming mechanisms of immune suppression. In recent years, immunotherapy has emerged as a viable treatment option for multiple cancers. However, immunotherapy wasn't used routinely for many years after its initial discovery due to a lack of known mechanisms of action and poor reproducibility [8] [9]. The first attempts to harness the immune system for the treatment of cancer started in the 1890s by William B. Coley. Coley observed disease remission in patients who were injected with mixtures of live and attenuated bacteria [10, 11]. Since Coley didn't know the mechanism of action, and studies yielded mixed results**,** immunotherapy remained dormant for many years after this initial observation (**Figure. 1.1**). In the late 1950s, Thomas and Burnet played a major role in bringing immunology to the forefront. They proposed that lymphocytes were mediators of immunosurveillance by identifying and eliminating somatic cells transformed through mutations. However, it wasn't until the 1970s, that Carswell et al., discovered that the eradication of tumors was a result of tumor necrosis factor production in response to the bacterial endotoxins [12]. Morales et al. went on to publish their findings in the 1970s showing, that Bacillus Calmette-Guerin (BCG) could be used to treat bladder cancer [13]. At this point, immunology was began to be taken seriously as a treatment option [13]. Since then, many further advances in cancer immunotherapy have led to remarkable improvements in response rates, progression-free survival, and overall survival in patients.

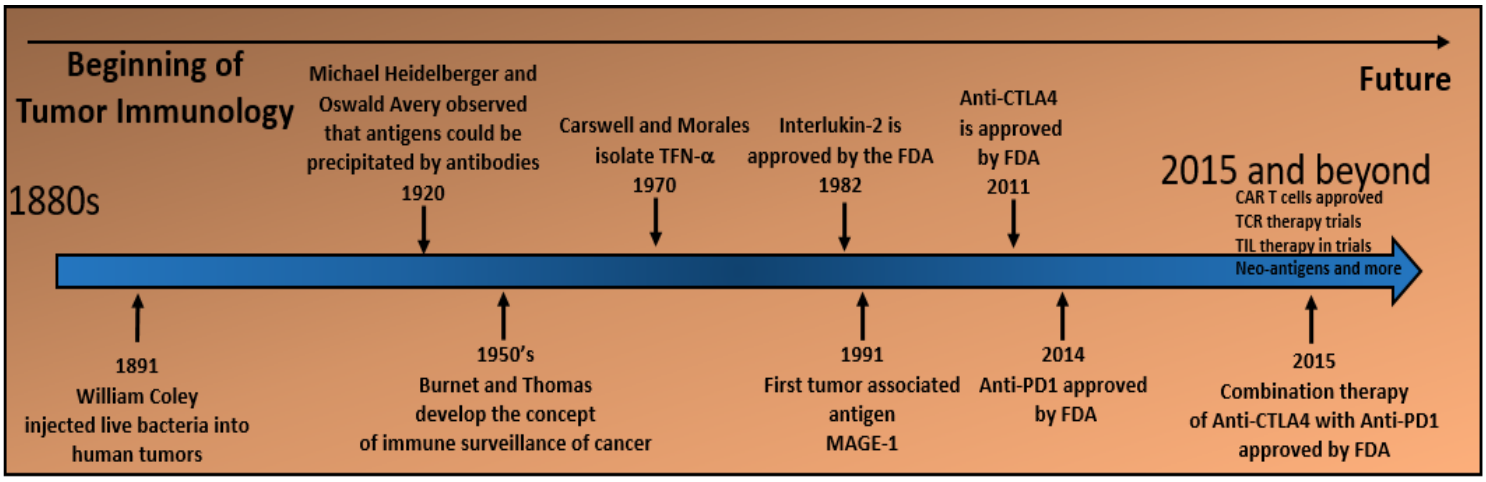

Figure 1.1 History of Tumor Immunology.

Figure 1.1 The History of Tumor Immunology. A timeline of the origins of tumor immunology. The timeline includes some of the major accomplishments and discoveries since its beginnings that has led to advancements in immunotherapy.

There are several forms of immunotherapy that fall into one of two categories: passive immunotherapy and active immunotherapy [14]. Active immunotherapies can be non-specific or specific. Active immunotherapies directly induce an immune response through the eliciting the host's endogenous immune system to fight disease [9, 14]. Passive immunotherapy differs in that it relies on elements constructed in the laboratory, which are then administered to patients to provide exogenous immunity [15, 16]. Cytokines and chemokines, such as interleukin-2 (IL-2) and interferon-alpha (IFN-α), are two common forms of active immunotherapy (**Table 1.1**) [17, 18]. They can be used to boost the immune response and lead to increased proliferation of tumor-eliminating T cells and or activation of disease-fighting cells [17, 19]. Vaccines are another biological agent used to induce anti-tumor responses. These can include peptide, viral, and dendritic cell-based vaccines [20, 21].

One form of passive immunotherapy involves the transfer of monoclonal antibodies into patients to target an array of specific antigen targets [22]. Monoclonal antibodies can bind to surface targets on cancer cells and act as downstream signaling pathway blockers of proliferation [22]. For example, bevacizumab (Avastin) is an FDA-approved monoclonal antibody against the growth factor VEGF-A (**Table 1.1**). However, there are also monoclonal antibodies that can also be used to inhibit receptors that normally act to halt the immune response. Examples of such inhibitors are checkpoint blockade therapies, or immune checkpoint modulators. These antibodies bind to the surface receptors on T cells that effectively "put the brakes" on T cell activation, blocking them and allowing them to continue to be active and attack the tumor [23]. Most recently, the Nobel Prize for Physiology and Medicine was awarded to, Dr. Jim Allison and his colleague Dr. Tasuku Honjo, for their groundbreaking discovery of cytotoxic T-lymphocyte-associated protein 4

(CTLA-4) checkpoint molecules and programmed death (PD-1) respectively [24]. Their discoveries are perhaps one of the most prominent findings in the last ten years and has radically impacted the treatment of metastatic melanoma [25, 26].

No matter the type of immunotherapy used, the key to specific anti-tumor immunity lies within the target. One of the most vital categories of targets of anti-tumor immune responses are tumor-associated antigens (TAAs). These tumor-specific targets are recognized by T cells to induce an immune response for tumor elimination [27]. Tumor-associated antigens are peptides found on the surface of tumors bound to Human Leukocyte Antigens (HLA) molecules (**Figure 1.2**). TAAs come in a variety of forms including, glycolpeptides, viral or bacterial derived-peptides, and phosphopeptides [28]. TAAs can be targeted with multiple therapeutic options, including cancer vaccines and T cell-based immunotherapies [28].

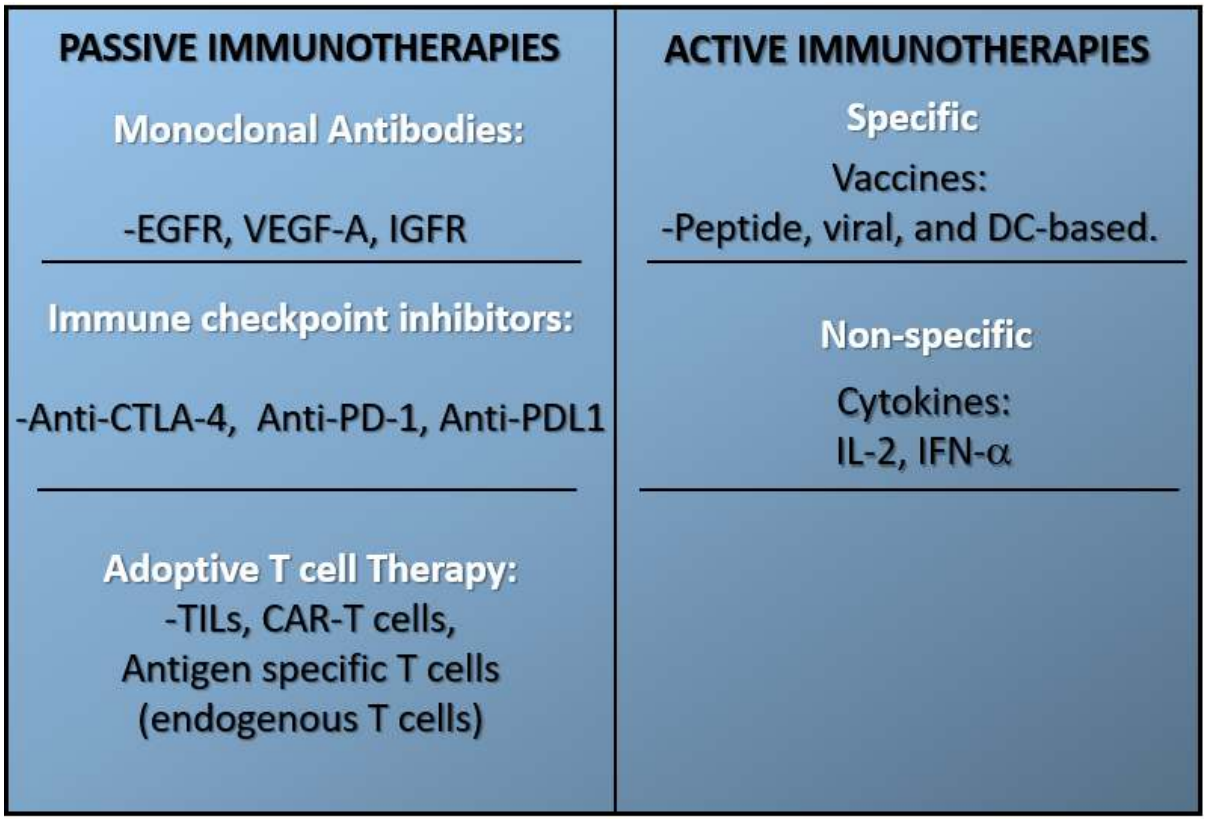

Table 1.1 Forms of Immunotherapy.

Table 1.1 Forms of Immunotherapy. A table displaying current active and passive immunotherapeutic approaches.

1.3 Tumor Associated Antigens

The discovery of tumor-associated antigens in the late 1950s revolutionized our understanding of tumor immunology. Dr. Richmond T. Prehn's research showed in mice that an immune response could be mounted against a carcinogen-induced sarcoma that later protected the mice against future challenges with the same tumor [29] [30]. His work provided evidence that tumors contained specific target antigens that could induce immunity and lasting immune memory [30]. These studies were the foundation for work that has continued to identify human tumor antigen targets. It is known that tumor antigens can be derived from self-proteins that are either over-expressed, tissue-specific, or arise due to mutations [27]. Tumor-associated antigen targets must possess some level of immunogenicity with low immune tolerance in order to be effective targets of CTL-mediated immune responses. **Figure 1.2** demonstrates a "gradient" of tumor- associated antigens ranging from non-targetable self-antigens (high tolerance, low immunogenicity) to antigens (low tolerance, high immunogenicity).

Although most self-antigens are not targetable due to unacceptable toxicity against normal tissues, there are classes of self-antigens that are potentially targetable [31]. Some antigens are expressed in specific normal tissues despite being found abundantly in tumors; these are known as tissue differentiation antigens [31]. One example of a tissue differentiation antigen is the protein enzyme tyrosinase. It is expressed only by melanomas and by normal skin cells known as melanocytes [32]. Another class of self-antigens are cancer-testis antigens (CTAs); these include antigens such as MAGE-A and NY-ESO-1 [33-35]. As the name suggests, they are found in high abundance primarily in testis tissue and in some tumors. Over-expressed tumor-associated antigens are found in

low abundance in multiple normal tissues but are highly over-expressed in tumors. The protein HER2 is an example of an antigen that is expressed by normal tissues but is highly overexpressed in multiple cancers, such as breast, gastric, and lung cancers [36].

Neo-antigens are highly tumor-specific antigens that arise from somatic tumor-associated mutations.

These targets are highly sought are the most sought after because of their unique tumor-specific sequences avoid issues of T cell tolerance and auto-reactivity [37]. Mutated TAAs can originate from frameshifts, deletions, insertions, fusions, and or other structural rearrangements of proteins [38]. Additionally, oncogenic viruses, such as human papillomavirus (HPV), can also induce the expression of unique tumor-specific antigens, which can be exploited as tumor-specific targets [39, 40].

Continued efforts to identify targetable tumor antigens shared by large numbers of cancer patients remain vital to the current and future success of T cell based cancer immunotherapies.

Schematic of tumor associated antigens

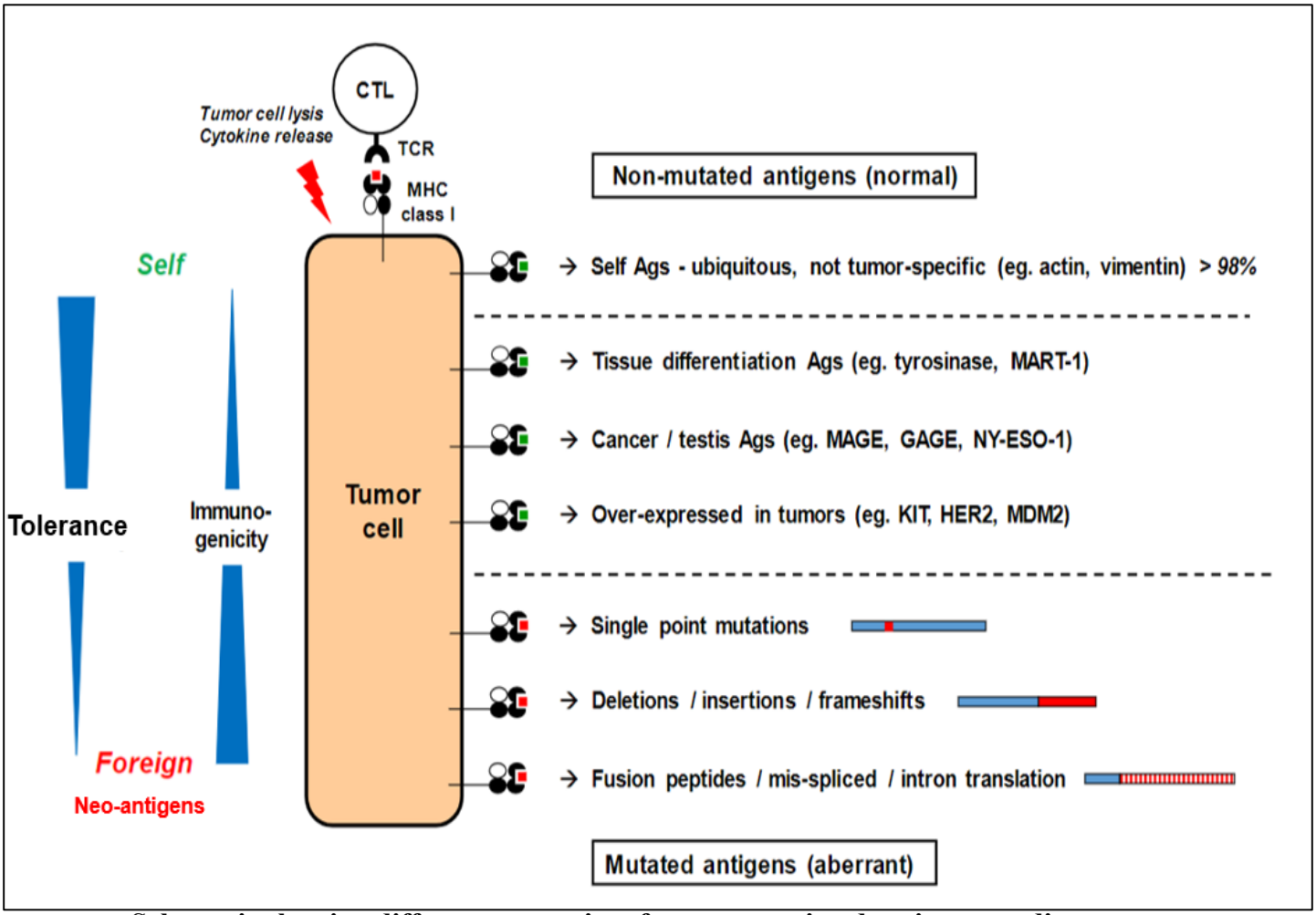

Figure 1.2 Schematic showing different categories of tumor associated antigens gradient.

Figure 1.2 Schematic showing different categories of tumor associated antigens gradient. Tumor cell representing the several tumor associated antigens found on its surface. The figure demonstrates the range from non-mutated (high tolerance, low immunogenicity) to foreign (low tolerance, high immunogenicity) antigens.

The discovery of TAAs has led to the development of multiple cancer immunotherapies, including peptide vaccines and adoptive T cell therapies. For example, cancer vaccines utilize tumor-associated peptides to prime antigen-specific T-cell responses in the body and increase the numbers of TAA-specific CTLs. Adoptive T cell therapy involves the isolation and ex-vivo expansion of tumor-reactive T cells. The benefit that adoptive T cell therapy has over vaccines is the ability to expand T cells to a greater extent, then what vaccines alone can accomplish.

Lymphocytes that infiltrate into the stroma of tumor nodules are referred to as tumor-infiltrating lymphocytes (TILs) [41, 42]. TILs provided the first evidence that the immune system can recognize tumor antigens [43, 44]. In 1988, Wolfel et al. showed that target structures presented by HLA molecules on tumor cells could induce the killing of these cells by CTLs [44]. The target structures identified were later described as the first tumor antigens recognized by T cells [45]. Intracellular proteins are comprised of polypeptide chains, and within a cell, they are degraded into shorter peptides that can be presented at the cell surface when loaded onto HLA-I molecules. HLA class I-bound peptides usually range in size from 8 to 12 amino-acids, and are derived from most cell-associated proteins and are recognized by the T-cell receptor of CTLs [46]. Peptides can only bind to specific HLA alleles that possess particular amino acid binding motif preferences [46, 47]. The targeting of TAAs through T cell mediated immunity has been the foundation of modern-day .cancer immunotherapy. The next section will discuss the role of TAAs in CTL-mediated immunotherapies.

1.4 CTL-mediated immunotherapy

Cancer immunotherapies have grown exponentially in recent years and have made remarkable improvements in patient survival. The adaptive immune response relies heavily on immune effector cells known as cytotoxic t-lymphocytes. Also referred to as CD8+ T cells, CTLs are known to be major players in inducing the regression of tumors (**Figure 1.3B**). $CD8^+$ T cells possess T cell receptors (TCRs) that recognize HLA class I molecules displaying peptide antigens on all cells in the body (**Figure 1.3A**). In addition to distinguishing self-antigens from pathogen-derived antigens, effector CD8+ T cells can also be primed to target tumor antigens [48].

Several different T-cell based immunotherapies have been developed to treat cancer. TILs are have set the foundation for the expansion of adoptive transfer of tumor reactive T cells. The cytokine interleukin-2 (IL-2) is responsible for the growth, proliferation, and differentiation of T cells to become effector cells. T cells also produce IL-2 in recognition of a foreign pathogen or a tumor antigen. Dr. Steven Rosenberg found that IL-2 as a monotherapy was an effective treatment option for metastatic melanoma patients [49, 50]. He also demonstrated that TILs extracted from melanoma tumors could be expanded *ex vivo* with the administration of high dose IL-2 *in vitro* [51, 52]. IL-2 given as either a monotherapy or in combination with TILs were some of the first successful T-cell mediated immunotherapies developed for the treatment of cancers [41, 52].

An alternative form of adoptive T cell therapy involves the isolation and expansion of endogenous tumor-antigen specific T cells (ETCs) from peripheral blood [50]. ETC treatment uses the peripheral blood as a source for the isolation of low-frequency, tumor-

reactive T cells [50, 53]. Much like TILs, these T cells can be isolated, stimulated, and expanded *ex vivo* to high quantities, then re-administered to cancer patients as a robust form of therapy [54]. In TIL therapy the specific tumor antigen target is usually unknown at the time of treatment; thus TIL therapy is usually a highly personalized treatment [55]. ETC targets specific, known tumor targets and has the potential to be a shared immunotherapy that can benefit many patients [50].

Tumor antigen peptides can be used to prime tumor antigen-specific T cells *in vitro*. Cells also found in the peripheral blood, known as antigen-presenting cells (APCs), primarily dedritic cells, monocytes, and B lymphocytes are used to activate antigen-specific T cells and induce proliferation [20, 55]. After *in vitro* stimulation with peptide-pulsed APCs, antigen-specific T cells expand to billions of cells and used for therapeutic purposes [53]. Once a tumor-antigen specific T cell deemed to have good anti-tumor activity, the therapeutic TCR can be cloned and used for TCR engineering, a relatively new treatment [56].

TCRs that have the high affinity for their tumor antigen target can be cloned and transduced into T cells that normally cannot recognize the target antigen [57]. These engineered TCR-T cells can be administered to other patients who share the same antigen target of interest, as well as the presenting HLA molecule. TCR-T based immunotherapy likely has the potential to reach a much broader patient population.

The first clinical trials using T cell therapies were done in the setting of metastatic melanomas [50, 58]. Targeting the tumor antigens, MART-1 and gp100, has shown good clinical activity with TIL and ETC [53, 57]. Some of which have induced complete responders or induced dramatic regressions in tumors [53, 58]. Although, there has been

minimal toxicity noted in these patients, TCR-T therapies against these same antigens have induced unacceptable toxicities, by killing normal melanocytes. Although antigen-specific immunotherapies are available for melanoma, many other tumor types have no known TAA, to target, which represents an important unmet need in the field.

Antigen presentation and T cell Recognition

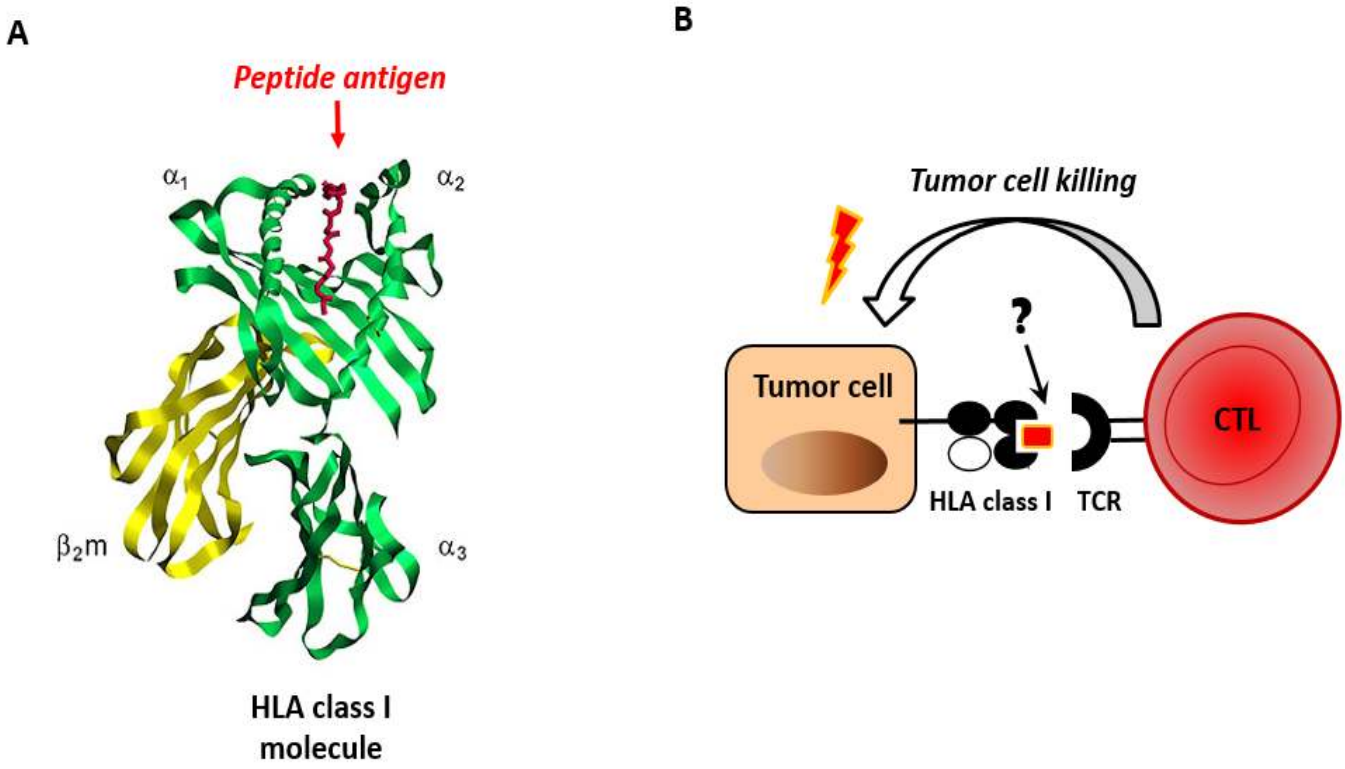

Figure 1.3. T cells recognize antigens bound to and presented by HLA class I molecules.

Figure 1.3. T cells recognize antigens bound to and presented by HLA class I molecules. **A**) Crystal structure of an HLA class I molecule displaying where peptide antigens are bound. **B**) HLA class I molecule presenting an unknown tumor antigen to a T cell for recognition and killing of the tumor.

1.5 The role of HLA class I molecules in CTL-mediated immune responses

HLA molecules constitute the central focus of the T cell mediated immune response. HLA class I molecules display peptides display peptides expressed by all nucleated cells of the body, including self, non-self, pathogen, and tumor-derived to effector T cells. All cells can present endogenously derived peptides on HLA class I molecules. Specialized APC's, such as DC's can also display exogenously-derived peptides in a process called cross-presentation. Mature HLA class I complexes are assembled in the endoplasmic reticulum (ER); they are heterodimers assembled from a polymorphic heavy chain, a light chain called β2- microglobulin (β_2m) and an antigenic peptide (**Figure 1.4**) [59, 60]. Proteasomes degrade cytoplasmic proteins into smaller peptides, which are transported into the ER by the transporter associated with antigen presentation (TAP) and are loaded into the peptide-binding grooves of the HLA-I molecules. The HLA-I binding groove accommodates peptides 8 to 12 amino acids in length [59]. In the ER, HLA-I molecules are stabilized by chaperone proteins such as calreticulin [61]; in addition, the molecule tapasin interacts with TAP to assist in the delivery of peptides to HLA-I molecules. When a peptide is successfully bound to HLA-I heavy chain and β2- microglobulin as a trimolecular complex, it exits the ER via the secretory pathway and travels to the cell surface in vesicles for presentation (**Figure 1.4**). Since HLA-I display these peptides at the cell surface, and then they play an essential role in antigen presentation and T cell surveillance.

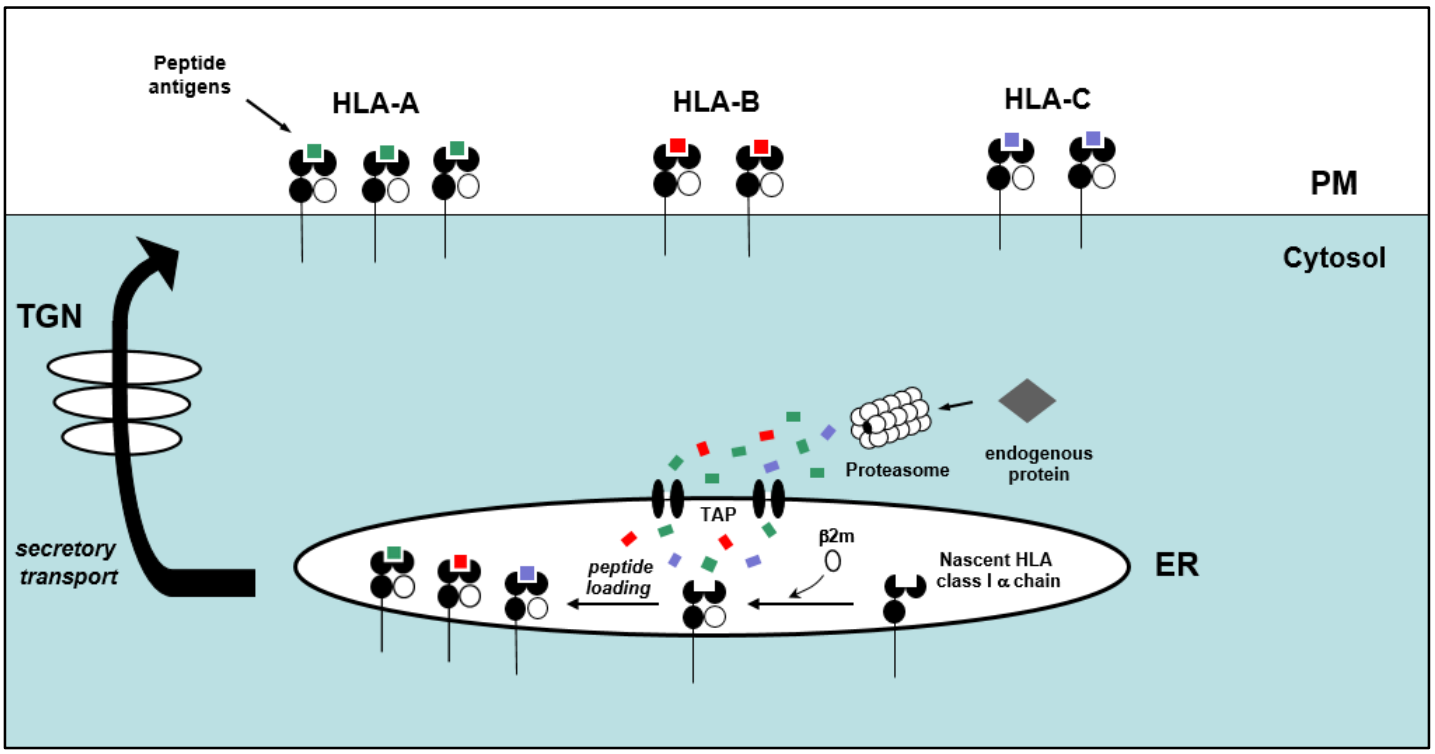

Figure 1.4 HLA Class I processing and antigen presentation pathway.

Figure 1.4 HLA class I processing and antigen presentation pathway. Endogenously derived proteins are degraded, loaded on to HLA molecules, and shuttled to the cell surface for presentation. HLA molecules can fit specific antigens in their binding groove and present to T cells on the surface of cells.

Human CTLs recognize the products of the three classical genes; HLA-A, HLA-B, and HLA-C. Each HLA type can recognize and bind uniquely to many different peptides dictated by the molecular properties of the their peptide binding grooves (**Figure 1.4**) [62]. HLA-A and HLA-B are expressed at higher surface levels in human cells than HLA-C. The extremely high level of HLA polymorphism results in different peptide-binding grooves that recognize and bind characteristic peptide sequences, allowing for each individual to present a wide and distinct array of peptides.

Each HLA-I molecule loaded with peptide is expressed on the cell surface to present peptides to CD8+ T cells. This can induce clonal expansion of effector of T cells, target cell killing, or cytokine release, depending on the APC and T-cell differentiation state. Each T cell contains a unique T-cell receptor that binds to HLA-I/peptide complexes; when this occurs, many more stabilizing receptors bind to one another from each cell, thus allowing the T-cell to stay in close contact with the APC. This induces the release of effector molecules such as Granzyme B and perforin by CD8+ cytotoxic T cells to induce target cell death. Granzyme B is a serine protease and perforin is a pore-forming protein that facilitates it's entry into target cells; once inside, it triggers an increase of intracellular calcium that eventually leads to the apoptosis of target cells [61, 63].

The antigenic landscape of tumors, or immunopeptidome, is the collection of the peptides are presented by HLA molecules [64]. By analyzing the immunopeptidome of cancers, researchers have discovered novel TAA targets to facilitate the treatment of cancer. Multiple methods have been used for tumor antigen discovery, but in recent years mass spectrometry analysis has proven the most useful for high-throughput.The following section,

will discuss how mass spectrometry-based antigen discovery has made major strides in cancer immunotherapy.

1.6 Mass spectrometry-based antigen discovery

In recent years, there have been significant improvements in the field of proteomics, the large-scale study of proteins. Coupled with technological advances in genomics, bioinformatics, and prediction platforms, these tools have greatly facilitated immunopeptidome discovery [64]. For many years, the most commonly used method for tumor antigen discovery was *in-silico* based [65]. The use of computer programs and prediction software has been the primary methodology for HLA-I binding prediction, but these methods as a single form of identification have several limitations.

In-silico approaches to identify tumor antigens rely on peptide sequences that have been eluted from different HLA alleles [66], [65]. Together with binding affinity algorithms that are derived from *in-vitro* binding assays, these tools are capable of predicting potential tumor antigen sequences that may be viable HLA-bound targets. They are also are capable of identifying possible neo-antigens peptides [67]. However, neo-antigen discovery is much more challenging and costly since it requires massive amounts of DNA and RNA sequencing data from both normal and tumor tissues that must be analyzed for non-synonymous mutations [64, 68]. These mutated protein variants are then translated into amino acid sequences *in silico* and analyzed with HLA peptide binding programs against all known HLA alleles [68]. Examples of these programs include NetMHC or EpitoolKit. If potential antigens are identified, synthetic neo-antigens can be used to conduct T cell screening assays for potential reactivity [68, 69].

Mass spectrometry (MS) can be used as a more direct form of tumor antigen discovery that is both unbiased and comprehensively investigates the entire peptide repertoire of a given tumor sample [64]. This sample may be a solid tumor specimen, cell line, or even

bodily fluids. The current process of MS-based antigen discovery starts with immunoprecipitation (IP) of HLA class I complexes from solubilized lysates [64]. IP's are typically conducted with pan-HLA class I or pan-HLA class II antibodies [68]. However, HLA-allele specific antibodies can also be used as well. The peptides are eluted in low PH and are separated by high-pressure liquid chromatography and injected into a mass spectrometer for analysis [68]. The results are searched against publicly-available protein databases, using serch tools such as Mascot or MaxQuant [70].

One of the benefits of MS over *in-silico* methods is the high-throughput [64]. Depending on the size of sample, up to thousands of potential tumor antigen targets can be detected in less than 2 hours. Additionally, targeted-MS, a process that adds a higher level of fractionation of the sample, can increase the depth at which the sample is analyzed and provide greater sensitivity. Targeted-MS enables more accuracy and reproducibility for specific peptides of interest [71, 72]. Typically, target-MS is used as a secondary method after a sample has been analyzed in discovery mode. Thus, it is more suited for peptide validation, rather than discovery.

There are several databases that are used to help to determine the targetability of MS-eluted peptides. The Swiss-Prot is a database that complies the information from scientific literature and computational analyzes on human protein sequences [73, 74]. The database is used to search for MS-eluted peptides to provide any relevant information on proteins. Additional validation and vetting of MS-eluted peptides can be determined by evaluating the expression of peptide-encoding genes in primary tissues and tumors. Normal tissue transcript expression determined by RNA sequencing is found in the Genotype-Tissue expression (GTEx) Portal database. Overall patient tumor tissue expression is available in the The

Cancer Genome Atlas (TCGA) database. TAAs found to be highly expressed in normal tissues according to the GTEx are immediately eliminated as potential therapeutic targets. While, TAAs that are highly over-expressed in tumors with low expression in normal tissues can be further evaluated. HLA-I peptide prediction binding algorithm databases are also used to add another level of confidence that eluted peptides are presented on the surface of the tumor. These HLA-I algorithms provide information on the predicted binding affinity of each peptide, indicating if the peptide weakly or strongly binds to HLA alleles. Together, these databases allow for in-depth analysis of MS-eluted peptides to determine if they are suitable therapeutic targets.

Currently, MS-based antigen discovery has expanded the immunopeptidome landscape many tumor types, including melanoma, hepatocellular carcinomas, leukemia, and renal cell carcinomas [69, 75]. It has primarily been used to discover shared antigens, but now researchers are also using this method to detect neo-antigens for personalized therapies or shared neo-antigen epitopes [76]. This method of detection is currently being developed for neo-antigens but has yielded some positive results in highly mutated cancers, like lung cancer and melanomas [77, 78]. There remain limitations to sensitivity, and these analyses require large sample sizes.

MS-based antigen discovery coupled with *in silico* methods has helped to expand the targetable immunopeptidome landscape of multiple cancers. HLA prediction binding algorithms, in particular have served as an important validation to vet eluted peptides.

MS-based antigen discovery has also helped to improve HLA class I binding algorithms for future researchers. The development of these methods, has allowed us to analyze additional cancers that have historically poor response rates to the current standard of care options.

Cancers types such as ovarian and pancreatic cancer for example have a lack of alternative treatments once patients fail to respond to front line treatments. This forms the rationale for this dissertation work, as will be discussed future in the following section.

1.7 Long term goal and rationale for this dissertation

The long-term goal of this dissertation was to develop a novel and effective cytotoxic T cell-based immunotherapy for cancer patients. Through this work, we aimed to identify shared tumor antigen targets in two cancers that have poor response rates to the current standard of care therapies, ovarian cancer and pancreatic cancer. Although, tumor associated antigen discovery is feasible for these cancers, to date there remains no T cell-based immunotherapeutic options for these patients. Cancer vaccines have been the primary objective of previous studies, but these have not provided benefits in the overall survival rates of these patients. There a few ongoing clinical trials using CAR T cells against a select few antigen targets for ovarian cancer. However, the trials are still very early, and have yet to show any promising results. Thus, there remains an un-met need to identify and validate viable tumor associated antigens in these cancers to faciliate T cell-based immunotherapies.

We chose to focus our efforts on the identification of non-mutated, overexpressed antigens in ovarian and pancreatic cancer. Our goal was to identify a shared tumor-associated antigen with little to no expression in normal tissues. If the TAA was also shared amongst both or additional cancer types, that was also ideal. Finally, we took into consideration the diversity of the HLA types from our patient samples, aiming to find epitopes from HLA alleles expressed at a high frequency in the worldwide if population. Due to our clinical collaborators, we had the rare opportunity to have access to fresh patient tumor samples for our studies. Additionally, we the expertise and knowledge on how to utilize mass-spectrometry based tumor antigen, where we used this method to identify tumor antigen targets in melanoma. Using high-throughput tandem mass spectrometry, we successfully this method to identify the tumor associated antigen, SLC45A2 [79]. In collaboration with a

bioinformatics expert and our clinical collaborator, we also were able to validate the peptide target and then isolate low-frequency endogenous, T cells from the peripheral blood of healthy donors. Furthermore, we were able to show that these SLC45A2-specific T cells could recognize and eliminate tumors that expressed the target gene and the appropriate HLA types. This is now the basis for an ongoing clinical trial for uveal melanoma patients. The work in this dissertation applies the same antigen discovery concepts to ovarian and pancreatic cancers, leading to the discovery of Vestigial-like 1 (VGLL1) as a potentially targetable TAA for multiple tumor types.

1.8 Overall hypothesis and Specific Aims

It was our ***central hypothesis*** that the accurate identification and selection of appropriate tumor associated antigens in ovarian or pancreatic cancer, would provide a foundation on which to develop a novel and effective T-cell based immunotherapy. In this dissertation we tested this hypothesis through fulfilling the following aims:

AIM 1. Identify tumor-associated antigen-encoding genes from patient tumor specimens.

Aim 1.1. Perform HLA class I-bound peptide elution and mass spec analysis of patient specimens to identify potential tumor-associated peptides.

Aim 1.2. Select best shared tumor-associated target peptides utilizing bioinformatics algorithms.

AIM 2. Generate antigen-specific cytotoxic T-cells against validated peptides and expand the shared tumor-associated target repertoire.

Aim 2.1. Validate best peptide candidates and generate antigen-specific CTLs against selected targets.

Aim 2.2. Test the specificity and cytotoxicity of generated CTLs using HLA-matched tumor cell lines and primary cell lines.

Aim 2.3. Identify shared TAA targetable tumors by testing the generated CTLs against additional HLA-matched TAA-expressing tumor types.

AIM 3. Characterize the role of the identified tumor-antigen VGLL1 in cancer progression.

Aim 3.1. Utilize siRNA and lenti-viral vectors to generate knockdown and overexpressed VGLL1 tumor cell lines, and analyze morphological changes in transduced tumor cells.

Aim 3.2 Explore the role of VGLL1 as a promoter of cancer progression by examining VGLL1 over-expressing and knockdown tumor cells for proliferation, migration, and invasion of the tumor cells.

CHAPTER II:

OVARIAN CANCER TUMOR ASSOCIATED ANTIGEN DISCOVERY AND T CELL GENERATION

2.1 Rationale for tumor antigen discovery in ovarian cancer

Our first aim sought to delve into the immunopeptidome landscape of ovarian cancer (OVCA) to identify viable tumor antigen targets. Specifically, we sought to target the most aggressive and deadly form of OVCA, epithelial ovarian cancer (EOC) [80]. Epithelial ovarian cancer is the leading cause of death among gynecological cancers and has been coined the "silent killer" [81-83]. The current five-year survival rate for EOC patients is about 44%, due primarily to its metastatic nature and late-stage diagnosis [80, 83, 84]. The common symptoms of ovarian cancer are similar to other gastrointestinal and gynecological conditions and thus are often are not easily attributed to the early diagnosis of ovarian cancer [81, 85].

The current standard-of-care relies on surgical tumor debulking followed by cisplatin-based chemotherapy [86]. Despite the high rate of initial responses, acquired cisplatin resistance in ovarian cancer remains a significant roadblock to the successful treatment of patients. Currently, immunotherapy for EOC is only considered after patients have failed front-line therapy [81, 87]. Several clinical trials using adoptive T cell including TILs and CAR-T cells have been conducted or are underway. Immune checkpoint inhibitors, anti-VEGF, and poly (ADP-ribose) polymerase (PARP) inhibitors are also being tested clinically [88, 89].

The presence of tumor-infiltrating lymphocytes (TILs) in EOC patient tumor samples does show an increased correlation with progression-free survival and overall patient survival [90]. This suggest that a T-cell based immunotherapy may potentially improve patient outcomes. EOC is known to have a highly immunosuppressive environment, similar to

pancreatic cancer [91, 92]. Therefore, EOC immunotherapies may need to be combined with additional anti-tumor approaches to achieve full treatment efficacy.

Adoptive T cell therapy approaches have been used in clinical trials for EOC [93]. Most notably, TIL therapy has had some mixed but mostly promising results. TILs promote tumor regression in patients with either advanced disease or recurrent platinum-resistant cancer [94]. However, toxicity remains an issue with EOC patients. As a single treatment, platinum-based chemotherapy is very toxic to patients [95]. In clinical trials, the combination of TILs and cisplatin, even without IL-2 still resulted in unfavorable toxicities [95].

Overall, clinical data supports the notion that the presence or absence of TILs does have a significant impact on response rates of patients [96]. This does bring up the question of what exactly are the TILs recognizing? Additionally, how can we boost this anti-tumor response? Are there potentially shared target antigens present in these EOC patient tumors? Having a better understanding of the antigen targets presented by these tumors could improve the outcome for EOC patient survival.

The next section will discuss how tandem mass spectrometry was utilized to analyze fresh ovarian tumor specimens derived from patients at M.D. Anderson Cancer. In collaboration with Dr. Amir Jazaeri in the M.D. Anderson Gynecological Oncology department, we analyzed over 30 ovarian tumor samples derived from patients. To identify tumor-associated antigens, we performed HLA class I immunoprecipitation and acid elution, followed by mass spectrometry analysis to identify HLA-bound peptides found within the tumor samples.

2.2. Ovarian cancer MS-based TAA discovery and antigen-specific T cell generation

2.2a.) Identification of ovarian cancer TAAs from fresh patient tumor specimens.

In the first aim, our goal was identifying appropriate target genes through direct proteomic analysis of OVCA patient tumor samples. To achieve this, we analyzed OVCA tumor samples from freshly excised patient biopsies obtained from our MD Anderson surgical collaborator Dr. Amir Jazaeri. We lysed the tumor specimens, and then performed immunoprecipitation of HLA class I molecules, and followed by acid elution of HLA-bound peptides. Next, we utilized tandem mass spectrometric analysis to identify tumor-associated peptide antigens, as shown in (**Figure 2.1)**.

In tandem mass spectrometry, individual fragmented peptides ions are displayed as a mass spectrum. The full length peptide backbone is fragmented into b and y ions. The spectrum consists of peaks corresponding to each fragmented ions mass-to-charge (m/z) ratio values (**Figure 2.2**). Multiple copies of the same peptide can be within the sample, and the relative intensity of the fragmented ions is depicted on the y-axis. Higher quality spectra contain more of the ion fragments. The spectra fragments are matched against Swiss-port databases to determine the theoretical full-length peptide identity.

In total, we completed peptide elutions on 38 fresh OVCA tumor specimens. Nearly all of the samples were collected from high-grade epithetical ovarian cancer patients, with the exception of two patients (**Table 2.1**). Additionally, the site of where the tumor was collected varied but was mainly derived from the omentum, which is an indication of advanced disease and metastasis (**Table 2.1**). The majority of the patients also underwent HLA typing to determine their HLA allelic expression, an important step in validating our MS results. This allows for peptide binding predictions of eluted peptides (**Table 2.1**).

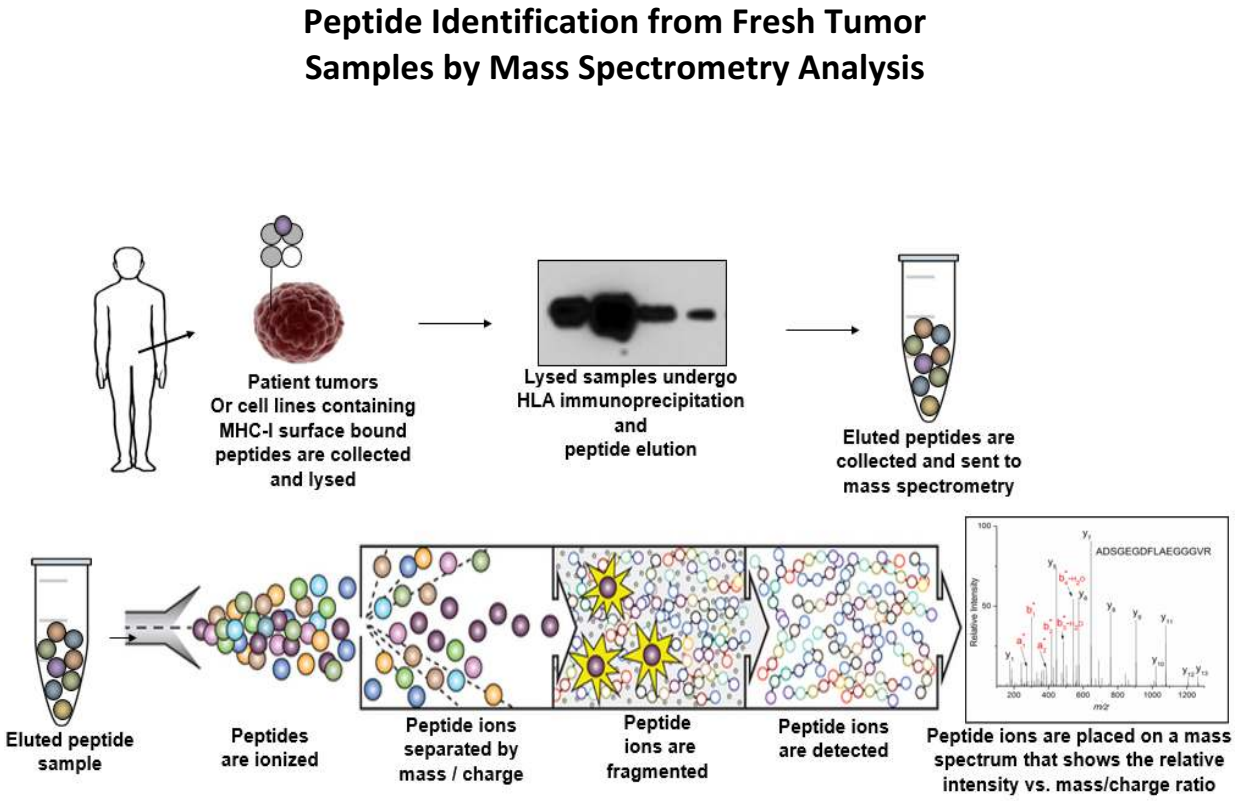

Figure 2.1. Peptide Identification from Fresh Tumor Samples by Mass Spectrometry Analysis.

Figure 2.1. Peptide Identification from Fresh Tumor Samples by Mass Spectrometry Analysis. Patient tumor samples containing surface bound HLA-I molecules were extracted, lysed, and acid washed to eluted the peptides. The eluted peptide samples were then analyzed by mass spectrometry analysis for the identification of peptides found within the sample. The peptide ions are separated by mass/charge, then the ions are fragmented, and laser then detects the ions. A mass spectrum is the final output for fragmented peptides detected within the sample.

MS/MS mass spectrum

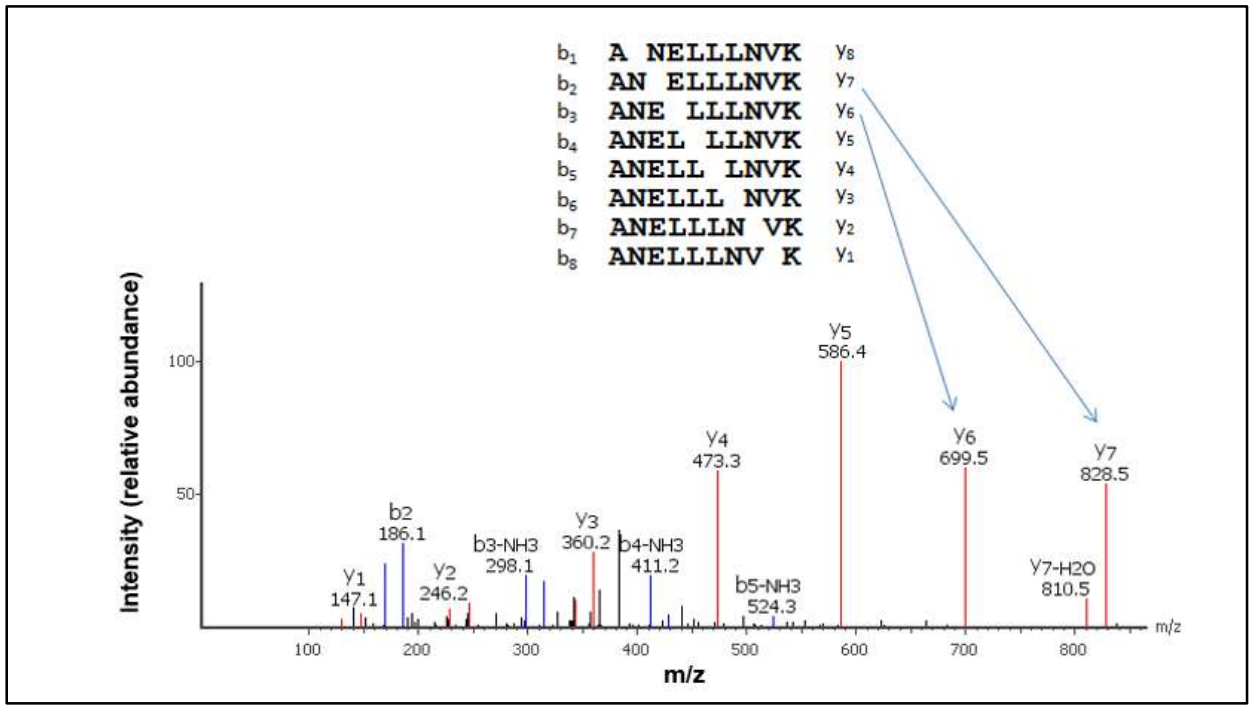

Figure 2.2. Example of a MS/MS mass spectrum.

Figure used with premission from author:

Hughes, C., Ma, B., Lajoie, G.A. De novo Sequencing Methods in Proteomics. Methods Mol Biol. 2010;604:105-21.

Figure 2.2. Example of a MS/MS mass spectrum. The spectrum is a mass spectrometry output that displays the fragmented peptide ions within a sample. The theoretical peptide is fragmented into b and y ions, which are measured by their relative abundance and mass-to-charge ratios.

Tumor ID	Site:	Subtype:	HLA-A-X	HLA-A-Y	HLA-B-X	HLA-B-Y
14-347	Ovary	High grade EOC	02 01	02 01	07 02	08 01
14-370	Ovary	High grade EOC	02 01	11:01	35 03	44 02
14-376	Omentum	High grade EOC	33 01	43 03	34 02	78 01
14-379	Omentum	High grade EOC	02 01	23 01	40 01	49 01
14-530A	Ovary	High grade EOC	02 01	03 01	51 01	52 01
14-530B	Omentum	High grade EOC	02 01	03 01	51 01	52 01
14-535	Omentum	High grade EOC	01 01	25 01	18 01	37 01
14-547A	Pelvic Tumor (Implant)	High grade EOC	01 01	24 02	08 01	44 03
15-028	Omentum	High grade EOC	03 01	11 01	07 02	27 05
15-033	Omentum	High grade EOC	01 01	01 01	15 01	40 01
15-055	Omentum	High grade EOC	02 01	51 01	53 01	30 02
15-059	Right Ovary	High grade EOC	03 01	31 01	49 01	51 07
15-068	Omentum	High grade EOC	02 01	30 01	51 01	13 02
15-166	Omentum	High grade EOC	N/A	N/A	N/A	N/A
15-094	Ovary	High grade EOC	01 01	02 01	44 02	57 01 01
15-069A	Omentum	High grade EOC	01 01	74 01	08 01	57 03
15-069B	Omentum	High grade EOC	01 01	74 01	08 01	57 03
15-097	Left Ovary	High grade EOC	01 01	68 01	08 01	38 01
15-192	Right Ovary	High grade EOC	N/A	N/A	N/A	N/A
15-199	Omentum	High grade EOC	01 01	02 01	08 01	40 01
15-202	Ovary	High grade EOC	01 01	03 01	14 02	57 01
15-124	Ovary	High grade EOC	02 01	24 02	14 02	27 02
15-257	Ovary	High grade EOC	N/A	N/A	N/A	N/A
15-203	Omentum	High grade EOC	02 01	02 05	35 01	58 01
15-290	Omentum	High grade EOC	01 01	29 02	08 01	44 03
15-316	Omentum	High grade EOC	26 01	29 02	44 03	45 01
15-324	Omentum	High grade EOC	N/A	N/A	N/A	N/A
15-330A	Left Ovary	High grade EOC	01 03	30 02	07 02	41 01
15-330B	Pericolonic mass	Carcinosarcoma	01 03	30 02	07 02	41 01
15-356A	Pericolonic mass	Carcinosarcoma	N/A	N/A	N/A	N/A
15-356B	Ovary	High grade EOC	N/A	N/A	N/A	N/A
15-316	Omentum	High grade EOC	26 01	29 02	44 03	45 01
15-391	Omentum	High grade EOC	N/A	N/A	N/A	N/A
15-418B	Ovary	High grade EOC	02 01	02 01	35 01	40 01
15-433A	Omentum	High grade EOC	02 01	24 02	35 12	39 02
15-433B	Omentum	Carcinosarcoma	02 01	25 01	35 01	58 01
16-012	Omentum	High grade EOC	02 01	03 01	07 02	13 02

Table 2.1 Ovarian tumor sample list.

Western Blot of Immunoprecipitated HLA class I

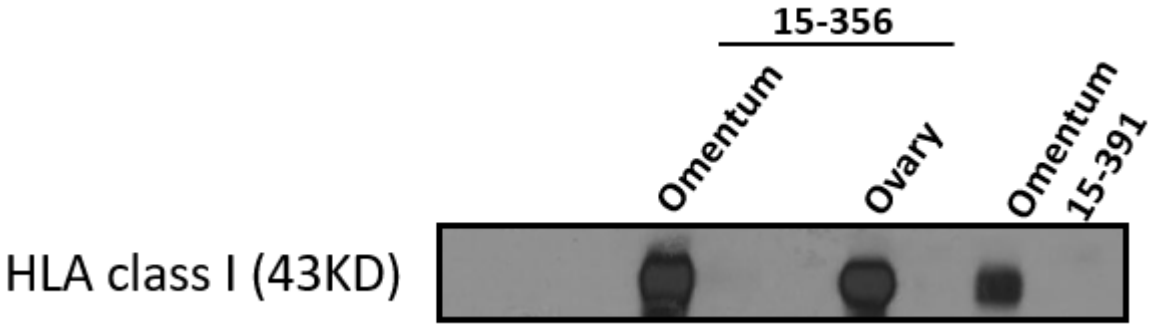

Figure 2.3. Representative image of an HLA immunoprecipitation validation by Western blot analysis from three ovarian cancer patients.

Figure 2.3. Representative image of an HLA immunoprecipitation validation by western blot analysis. Western blot of 3 different ovarian patient tumor sample HLA immunoprecipitations. Samples were stained with the pan-class I antibody W6/32 to determine the relative abundance of HLA-I found within the lysed tumor sample prior to mass spectrometry analysis.

All HLA immunoprecipitations were validated by Western blot analysis to determine if the HLA class I protein concentration was sufficient and was comparable between each sample. **Figure 2.3** is a representative figure of a peptide elution validation by Western blot analysis. We identified roughly 500 to 1500 peptides on average per tumor sample.

To assess the most frequently eluted peptide-encoding genes found in the OVCA immunopeptidome, we analyzed 20 of the best peptide elutions. **Figure 2.4** displays the top 50 most frequently eluted peptide-encoding genes among these samples. Through this unbiased observation of the most frequently eluted peptide-encoding genes, it was revealed that majority of the peptide-encoding genes eluted are not therapeutically safe antigen targets.

Finding TAAs with only limited or no cross-reactivity with primary tissues remained our primary goal in the selection of potential tumor antigen targets. We found that most of the samples expressed peptides from genes that are un-targetable due to their high expression in normal tissues. These peptides may show up in high abundance because of the size of the protein they encode for, or due to the high abundance of the protein in specific tissues. For example, we found that the gene that encodes for the protein Titin (TTN) appeared in our OVCA elutions significantly more than any other gene. Titin is a very large protein found in cardiac and muscle tissues, which is likely why Titin-derived peptides were found so frequently in our elutions. By utilizing the Genotype-Tissue Expression Portal (GTex) database, which contains RNA sequencing on samples collected from 55 primary tissue sites from >3000 individuals, we can further analyze the therapeutic safety of each gene.

The relative RNA transcript expression of a gene in each tissue can be represented in transcripts per million (TPM). TPMs can range from zero, which is essentially no transcript

expression, up to the thousands indicating extremely high gene expression. We were specifically searching for TAAs that have the lowest expression in normal tissues. Zero TPMs represents ideal transcript expression in primary tissues. However, the vast majority of peptides we eluted were derived from genes that also had some level of transcript expression in normal tissues.

Primary tissues from the GTex were split into four safety categories that reflected the potential toxicities expected from off-target killing activity by antigen-specific CTLs (**Table 2.2**). These categories ranged from extremely dangerous (essential), hazardous, dangerous, and likely okay (non-essential). **Table 2.2** contains examples of some of the normal tissues within each category along with the acceptable TPM thresholds for each category transcripts. All peptide-encoding genes were screened based on their TPM expression in each of the GTex normal tissues. Tumor-associated antigen transcript expression up to 30 TPM maximum was allowed in non-essential tissues (such as prostate, breast, and adipose tissues). A maximum expression threshold of 1 TPM was imposed for highly essential tissues such as heart and brain, for which CTL recognition can be lethal [97], [98].

As observed with TC –T targeting of MAGE-A3, lethal cross-reactivity with other peptides that share similar sequences is a serious concern [97, 99]. To provide additional validation for our selected high-confidence peptide matches, they were analyzed by BLAST searches to identify all potential source genes. This helped to eliminate peptide candidates derived from multiple genes that may induce cross-reactivity. However, it is not currently possible to identify all potential peptide cross-reactivies *in silico*.

.

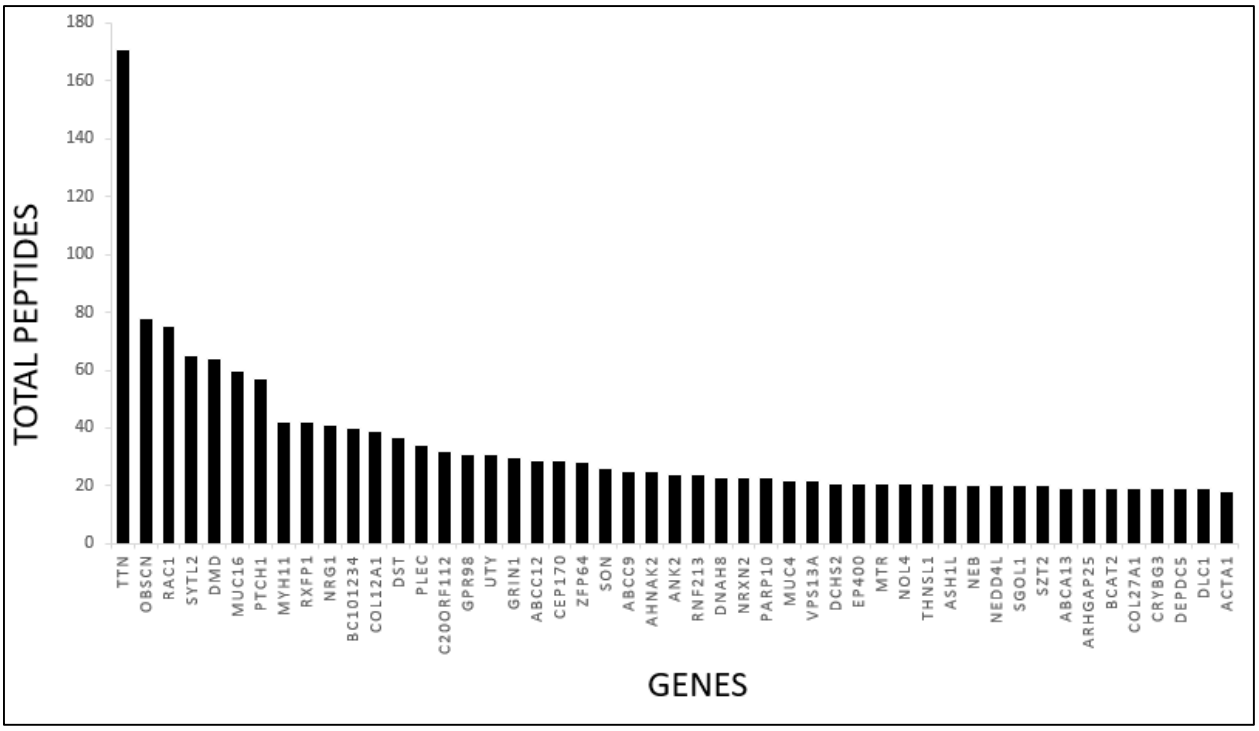

Figure 2.4. Unbiased look at the top 50 genes encoding for the most frequently eluted peptides in OVCA.

Figure 2.4. Unbiased look at the top 50 most frequently eluted peptide-encoding genes in OVCA. Graph displaying the top 50 peptide-encoding genes eluted from 20 ovarian cancer tumor samples.

Maximum RNA Transcript Thresholds for TAA expression in Normal Tissues

Extremely Dangerous Tissues	Hazardous Tissues	Dangerous Tissues	Likely Okay Tissues
Heart, Brain	Liver, Kidney, Colon, Lung, Stomach	Esophagus, Whole Blood , Bladder, Pancreas	Breast, Testis, Skin, Ovaries
1 TPM or lower	3 TPM or lower	10 TPM or lower	30 TPM or lower

Table 2.2 Potential toxicity of TAAs based on primary tissue TPM expression. Table displaying the RNA transcript expression thresholds cutoffs for potential TAA in normal tissues.

Examining GTEx normal tissue gene expression, we concluded that Titin was clearly not a safe targetable tumor antigen [97]. Despite its significant abundance in our OVCA tumor sample elutions (**Figure 2.5**). Titin is expressed >300 TPM in skeletal muscle and >50 TPM in the heart muscle. Since our dangerous threshold cutoff for the heart tissues was 1 TPM the expression of Titin eliminated it as a potentially safe therapeutic TAA.

Although the GTex provided some insights into gene expression for primary tissues, putative TAA genes were also screened for expression and in different cancer types through analysis of The Cancer Genome Atlas (TCGA) RNA sequence database. The TCGA contains whole exosome and RNA sequencing data from over 20,000 patients with over 35 different cancer types (**Table 2.3**).

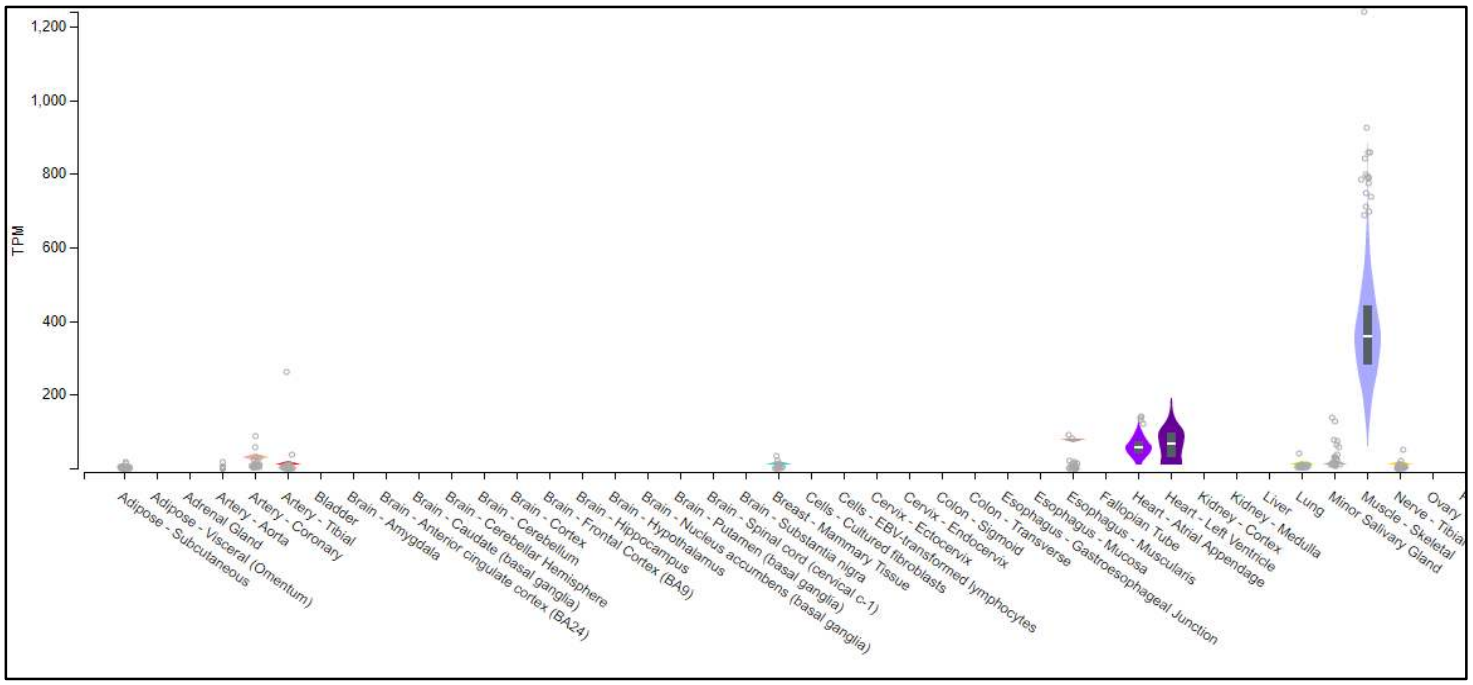

Figure 2.5. Expression of the gene Titin in normal tissues.

Figure 2.5. Expression of the gene Titin in normal tissues. RNA expression of the gene Titin in normal tissues. The x-axis displays the transcripts per million. The y-axis displays the primary tissues. Data Source: GTEx Analysis Release V8.

Abbreviation	Cancer Type
LAML	Acute Myeloid Leukemia
ACC	Adrenocortical carcinoma
BLCA	Bladder Urothelial Carcinoma
LGG	Brain Lower Grade Glioma
BRCA	Breast invasive carcinoma
CESC	Cervical squamous cell carcinoma and endocervical adenocarcinoma
CHOL	Cholangiocarcinoma
LCML	Chronic Myelogenous Leukemia
COAD	Colon adenocarcinoma
CNTL	Controls
ESCA	Esophageal carcinoma
FPPP	FFPE Pilot Phase II
GBM	Glioblastoma multiforme
HNSC	Head and Neck squamous cell carcinoma
KICH	Kidney Chromophobe
KIRC	Kidney renal clear cell carcinoma
KIRP	Kidney renal papillary cell carcinoma
LIHC	Liver hepatocellular carcinoma
LUAD	Lung adenocarcinoma
LUSC	Lung squamous cell carcinoma
DLBC	Lymphoid Neoplasm Diffuse Large B-cell Lymphoma
MESO	Mesothelioma
MISC	Miscellaneous
OV	Ovarian serous cystadenocarcinoma
PAAD	Pancreatic adenocarcinoma
PCPG	Pheochromocytoma and Paraganglioma
PRAD	Prostate adenocarcinoma
READ	Rectum adenocarcinoma
SARC	Sarcoma
SKCM	Skin Cutaneous Melanoma
STAD	Stomach adenocarcinoma
TGCT	Testicular Germ Cell Tumors
THYM	Thymoma
THCA	Thyroid carcinoma
UCS	Uterine Carcinosarcoma
UCEC	Uterine Corpus Endometrial Carcinoma
UVM	Uveal Melanoma

Table 2.3 List of TCGA cancer types

By assessing the TCGA tumor expression data relative to the GTex normal tissue expression, an TAA over-expression index was calculated (**Figure 2.6**) (OV-index). The OV-index took into account the average TPM expression of the eluted peptide-encoding genes in tumors divided by the max TPM expression in essential tissues. This allowed for the filtering out of the high-confidence potentially dangerous peptide targets from the peptides that may be safer to target with T-cell based immunotherapies.

For validation, each eluted peptide was also further assessed for several parameters using bioinformatics algorithms, including Mascot Ion Score, MS1 mass differential (delta mass), and predicted binding to the patient's HLA allotypes, as determined by high-resolution HLA typing [100], [101]. The Mascot Ion score indicated how well the experimentally-derived sequence matches the database sequence. Ion scores typically ranged between 0-90. Only ion scores of 10 or greater were considered, with the best-matched peptides having scores >25. The delta mass is a measure of the deviation between the measured peptide mass and the theoretical mass of the peptide, and is important for quality control. Delta masses between -3 and 3 ppm were considered high quality identifications, and peptides outside of this ran were excluded from further consideration [102].

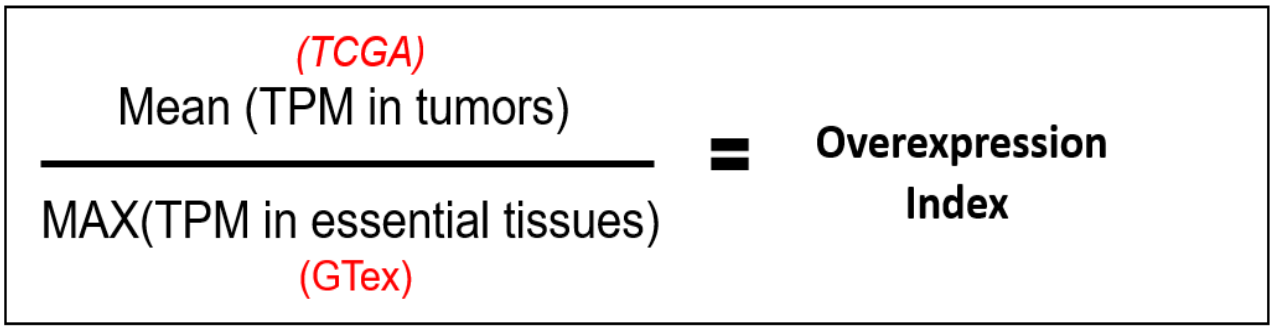

Figure 2.6. Formula used for the calculation of overexpression index.

Figure 2.6. Formula used for the calculation of overexpression index. The average TPM expression of the eluted gene in tumors divided by the max TPM expression in essential dangerous tissues determined the OV-index.

The NetMHC and NetMHCpan algorithms determined predicted HLA binding of the peptides. A low nM affinity score indicates a stronger binding affinity for that peptide to a particular HLA allele. After selecting high-confidence peptides, targeted MS/MS analysis was sometimes performed to confirm the TAA peptide identity. As described in chapter I, targeted MS/MS allows for a more sensitive level of detection with higher-condifidence. To validate peptides, we combined targeted MS/MS with the isotope labeling of the individually selected high-confidence peptides. In this process, we started by synthesizing a $^{13}C/^{15}N$ isotope-labeled synthetic peptide from the high confidence peptide candidates selected.

The isotope-labeled peptide is analyzed by mass spectrometry along with the original unlabeled tumor-derived peptide. The mass spectra of the unlabeled and labeled peptide are matched against each other, while also taking into account the retention-window time. The retention-window time is an output that measures the time from injection to detection of a peptide. For peptide validation, both peptides should have similar, if not exact retention-window times. Additionally, the peptide-derived spectra should be matching with the exception of shifted ion mass-to-charge ratios characteristic of the isotope-labeled peptide.

The following section will discuss the candidate TAAs identified through our OVCA antigen discovery methods, and delve deeper into one specific peptide-derived from MUC16 that was selected as a potentially safe therapeutic target based on the criteria outlined above.

2.2b.) A novel MUC16-derived peptide was identified in ovarian cancer

From our screening and validation method, a total of 8 TAA peptides were identified from the 38 OVCA tumor specimens. Five of these peptides were from the gene, Mucin 16 (MUC16) (**Table 2.3**); however, each peptide identified was from different patient OVCA tumor samples. We also identified three novel peptides encoded by mesothelin (MSLN). Although MSLN has been pursued as a TAA in CTL-based and peptide vaccines trials, we ultimately decided against pursuing it [103-106]. Due to MSLN's elevated expression in normal lung tissue at (88 TPM), Thus it was not deemed a safe target according to our criteria.

From the five peptides that we identified, we chose to pursue the HLA-B*07:02-restricted peptide derived from MUC16. The spectra for this MUC16-derived peptide, TPGGTRQSL, is shown in (**Figure 2.7**). We selected this TAA target for multiple reasons: First, the MUC16-derived peptide TPGGTRQSL was found in an OVCA sample and in a pancreatic tumor specimen from a patient expressing HLA-B*07:02. Additionally, the MUC16-dervided peptide, TPGGTRQSL was also found in another HLA-B*0702 ovarian tumor sample by Schuster et al. [107]. Detecting this peptide in another patient with a different cancer type, suggested that it might be a shared tumor antigen target. This added another level of confidence to this peptide as a potentially valuable therapeutic target. The predicted high binding affinity to HLA-B*07:02 (16nM) also contributed to our confidence that this peptide might be expressed in these tumor types (**Table 2.3**).

MUC16 was first isolated by MD Anderson's own Dr. Robert Bast in 1981 [108]. It is the largest membrane-associated mucin, being over 22,000 amino acids in length. MUC16 is expressed at very low levels in adipose tissue, the cervix, and salivary glands. However,

MUC16 is expressed under 1 TPM for all these tissues, while being highly over-expressed in several cancers, including ovarian, pancreatic, cervical, uterine, mesothelioma and lung (**Figure 2.8**).

Peptide Sequence	Gene	Tumor ID	Ion Score	HLA allele	Predicted HLA binding affinity	Worldwide HLA allele prevelance
RVRELAVAL		14-347	14	HLA-B*07:02	15 nM	8%
YPESVIQHL	**MSLN**	14-370	26	HLA-B*35:01	397 nM	11%
ESAEVLLPR		14-376	25	HLA-A*33:01	25 nM	2%
VSKTTGMEF		14-530A	55	HLA-B*15:01	56 nM	7%
VQRMSISV		14-530B	40	HLA-B*15:01	4266 nM	7%
LFKNSSVGPL	**MUC16**	15-033	18	HLA-B*15:01	1514 nM	7%
SESPSTIKL		15-418B	42	HLA-B*40:01	19 nM	10%
TPGGTRQSL		16-012	50	HLA-B*07:02	16 nM	8%

Table 2.3. List of potential TAA-targets eluted from OVCA tumor specimens.

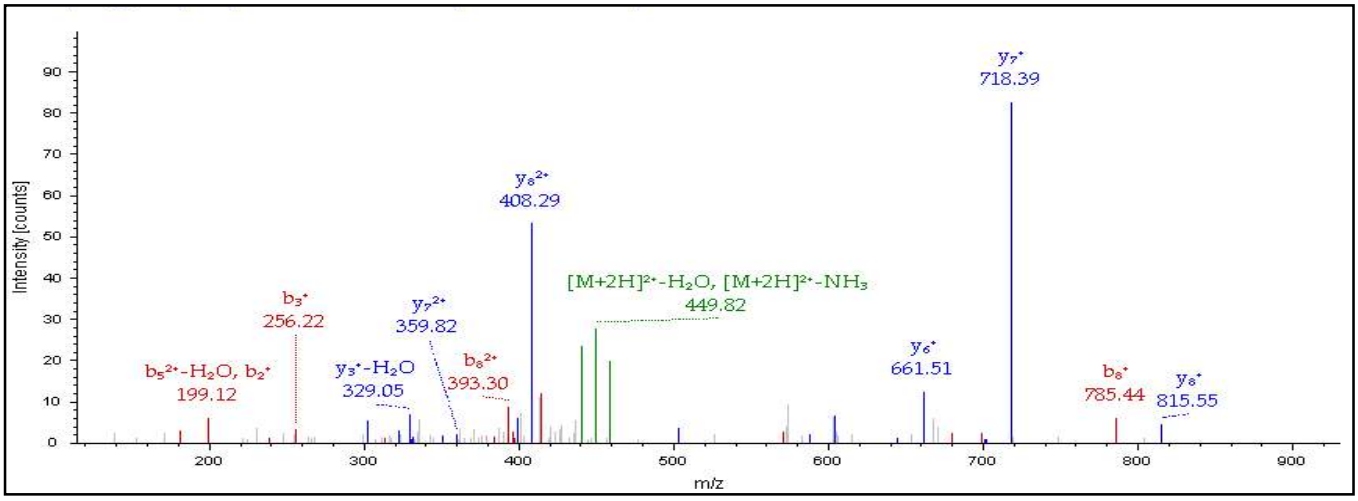

Figure 2.7. Mass spectra of MUC16-derived peptide TPPGTRQSL.

Figure 2.7. Mass spectra of MUC16-dervied peptide TPPGTRQSL. Mass spectra of an HLA-B*0702-restricted MUC16-derived peptide isolated from an ovarian cancer tumor specimen OV16-012.

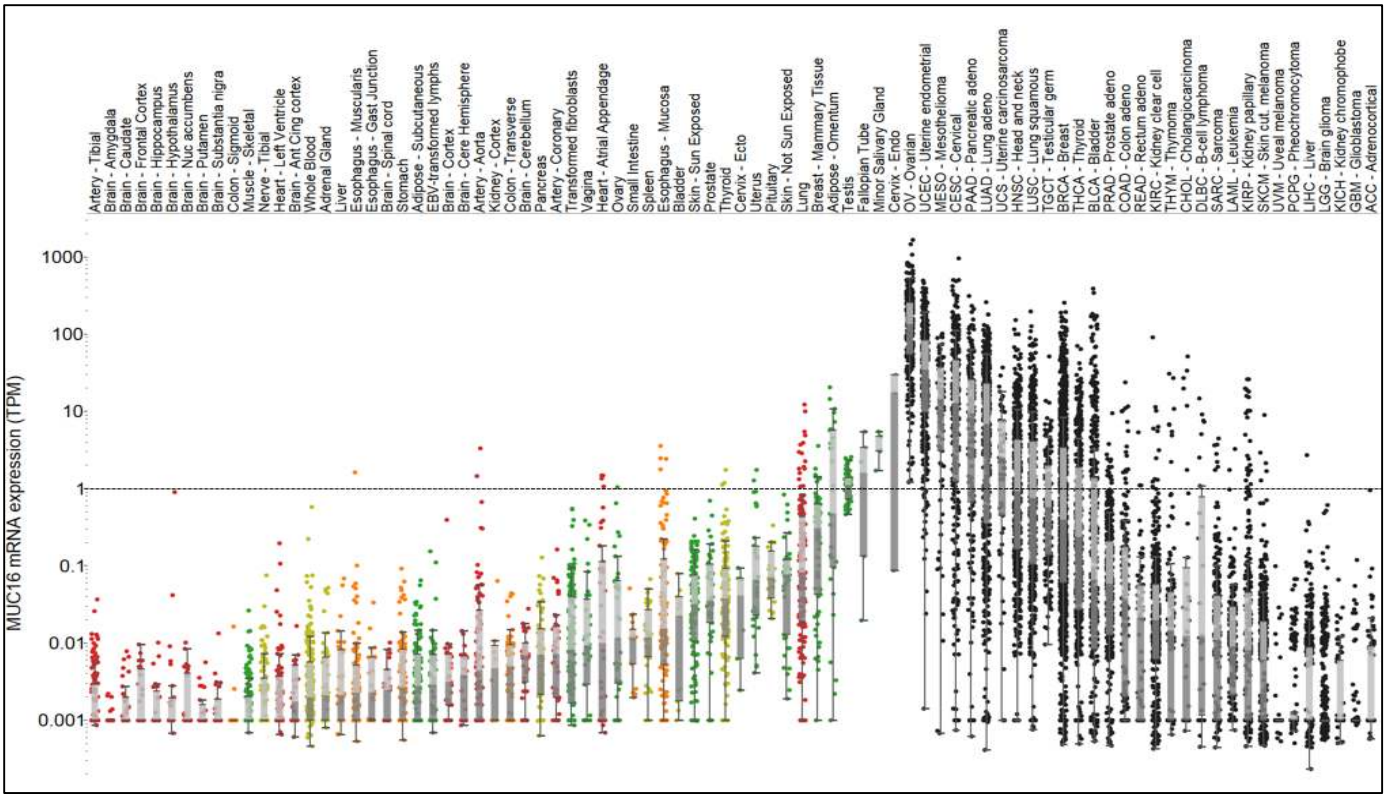

Figure 2.8. MUC16 mRNA transcript expression in normal tissues and tumors.

Figure 2.8. MUC16 mRNA transcript expression in normal tissues and tumors. GTex mRNA transcript expression of MUC16 in normal tissues color-coded by extremely dangerous essential tissues (red), hazardous (orange), dangerous (yellow), and non-essential (green). This is versus the TCGA mRNA expression of MUC16 in multiple tumor types shown in grey.

The MUC16 gene and protein has a long history with ovarian cancer. MUC16 (CA125) is an established biomarker for epithelial ovarian cancer progression [109, 110]. MUC16 also contains a proteolytic cleavage site that allows for a major portion to be released from the cell surface [111]. Circulating serum levels of MUC16 are monitored in EOC patients as a prognostic factor to determine if patients are responding to treatment or if there is a recurrence [112]. Since MUC16 is a self-antigen, the ability for MUC16 to detach from the surface of tissues and circulate may contribute to T cell tolerance. This possibility was something we considered might be a hindrance to our ability to isolate MUC16-specific T cells from the blood. Aside from MUC16 being a biomarker for EOC, it also is linked to ovarian and pancreatic cancer progression through its adhesion to epithelial mesothelin-expressing cells. This interaction promotes the migration, invasion, and metastasis of these cancers [113-115]. This occurs through the upregulation of the cell motility protein, MMP-7, via the MAPK pathway [116]. Since MUC16 appeared to be a safe TAA target based on its low normal tissue expression, combined with its high over-expression in multiple cancers, we next proceeded to attempt to isolate T cells against the peptide TGGTRQSL.

2.2c.) Generation of MUC16-specific T cells from healthy donor peripheral blood

To generate MUC16-specific T cells, we utilized guidance from our clinical collaborator, Dr. Cassian Yee, who has previously developed this protocol [114]. Our MUC16-derived peptide was restricted to HLA-B*07:02, but we also utilized an HLA-A*02:01 MART-1 peptide as a positive control. The MART-1 peptide was used to generate MART-1 specific T cells alongside the generation of MUC16-specific T cells to ensure the protocol worked as expected. We began with a leukapheresis obtained from a healthy donor who expressed both HLA-A*02:01 and HLA-B*07:02 positive alleles.

Donor PMBCs were stimulated twice with autologous dendritic cells (DCs) pulsed with either the MART-1 or MUC16 (TPGGTRQSL) peptide in the presence of IL-21. Following the two stimulations, the cultured cells were stained and sorted with either a MART-1/HLA-A*02:01 or MUC16/HLA*B07:02-PE-conjugated custom tetramer. The cells were also stained with CD8+ antibody to sort out tetramer-positive CD8+ T cells. The cells were analyzed by flow cytometry for double-positive cells. Following the stimulation double-positive MART-1 cells presented at frequency of 18% , a relatively high frequency (**Figure 2.9**). This indicated that this donor might possess a higher than normal frequency of MART-1-specific T cells, compared to the average person. By contrast, after the stimulation, MUC16-specific T cells were barely detectable at, 0.069% (**Figure 2.9**).

We sorted cells from multiple culture wells for each peptide and pooled the wells together to expand the sorted cells in a 12-day Rapid Expansion Protocol (REP). We obtained a total of 34,000-sorted MART-1 cells and 4,300 cells for MUC16. After REP and an additional sort for double-positives (DPs), we were able to expand the MART-1-specific T-cells to 35% DPs, but did not detect any MUC16-specific cells (**Figure 2.9**). Since

MUC16-specific T cells did not expand (**Figure 2.9**). This was an indication that potential high tolerance and low immunogenicity could be hindering our ability to isolate MUC16-specific T cells. Despite these results, we opted to repeat this protocol with modifications using the same PBMC donor.

MART-1 and MUC16-specific T cells Generation

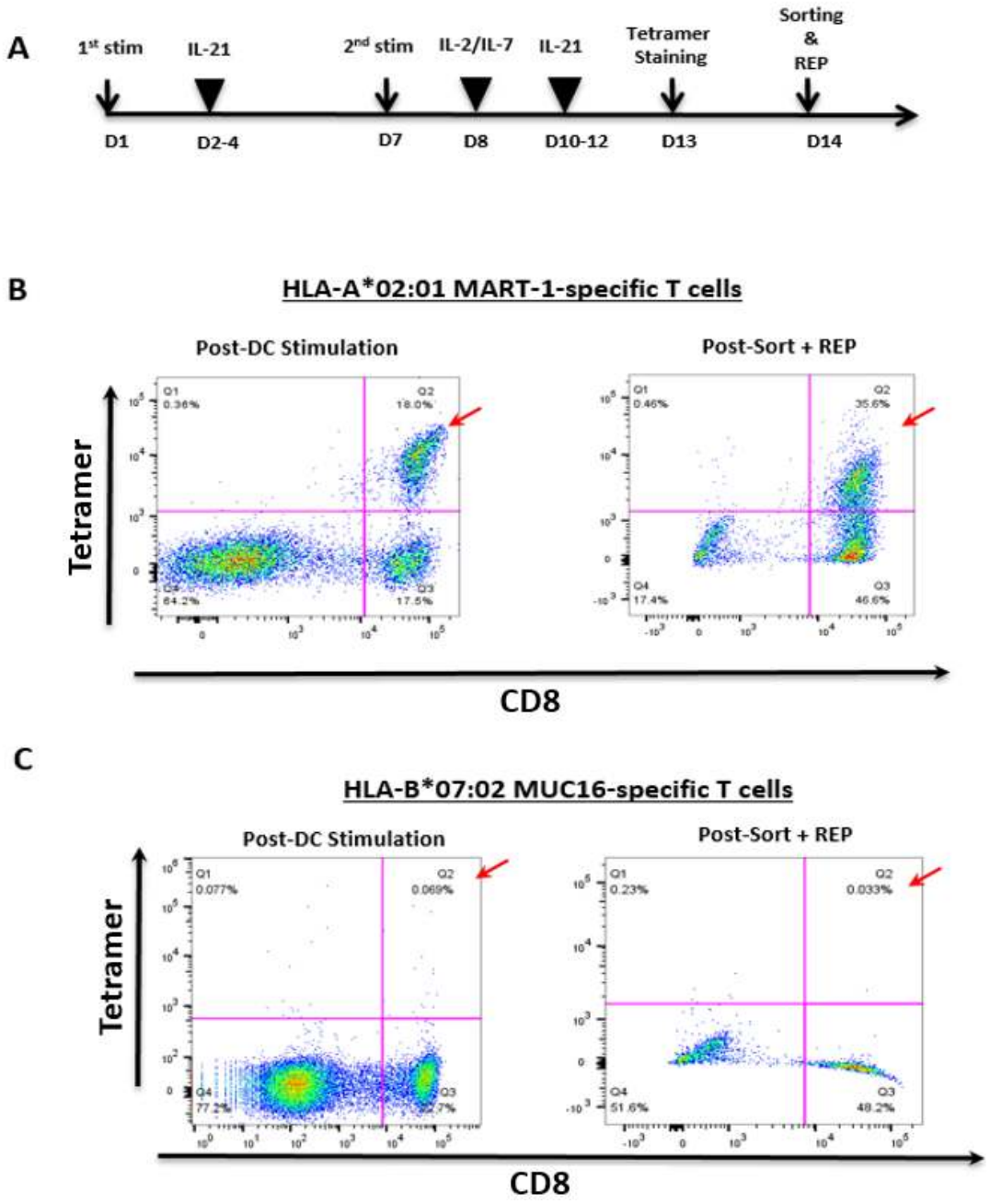

Figure 2.9. First approach for the generation of MART-1 and MUC16-specific T cells.

Figure 2.9. First approach for the generation of MART-1 and MUC16-specific T cells. (A) Schematic outlining the experimental procedure for generating antien-specific $CD8^+$ T-cells from human donor PBMCs. **(B)** PBMCs isolated by leukapheresis were stimulated with autologous MART-1 and MUC16-peptide-pulsed dendritic cells (DCs). After two stimulations CD8+ and MART-1 (middle row) and MUC16 (bottom row) tetramer-positive cells were sorted and expanded using a standard rapid expansion protocol (REP).

To increase the activation and expansion of low-frequency CD8+ T cells within the donor PBMCs, Lipopolysaccharide (LPS), a TLR4 ligand, was added during the two DC stimulations. Following the stims, the cells were stained for double MART-1 or MUC16 tetramer and anti-CD8. Based on the MART-1 staining (13.6%) it appeared that the LPS did not make a significant difference in the amount of MART-1 specific cells isolated. In this experiment a total of 42,000 MART-1 HLA-A*02:01 CD8+ T cells were collected. For the TAA MUC16, we still were not able to isolate very many double-positive cells. In total, we collected 9,826 MUC16-specific CD8+ T cells for the REP. After the 12-day REP, we successfully generated >95% tetramer-positive MART-1 specific T cells (**Figure 2.10**). This was a significant improvement over the initial attempt. However, MUC16-specific T cell generation did not fare as well, as we were unable to isolate substantial amounts of MUC16 tetramer-positive CD8+T cells (**Figure 2.10**). However, after the initial REP we did proceed to undertake a second REP. Unfortunately, upon completion of the second 12-day REP, the number of double-positive MUc16-speific T cells was still inadequate for the purposes of studying their antitumor activity and therapeutic potential.

MART-1 and MUC16-specific T cells Generation

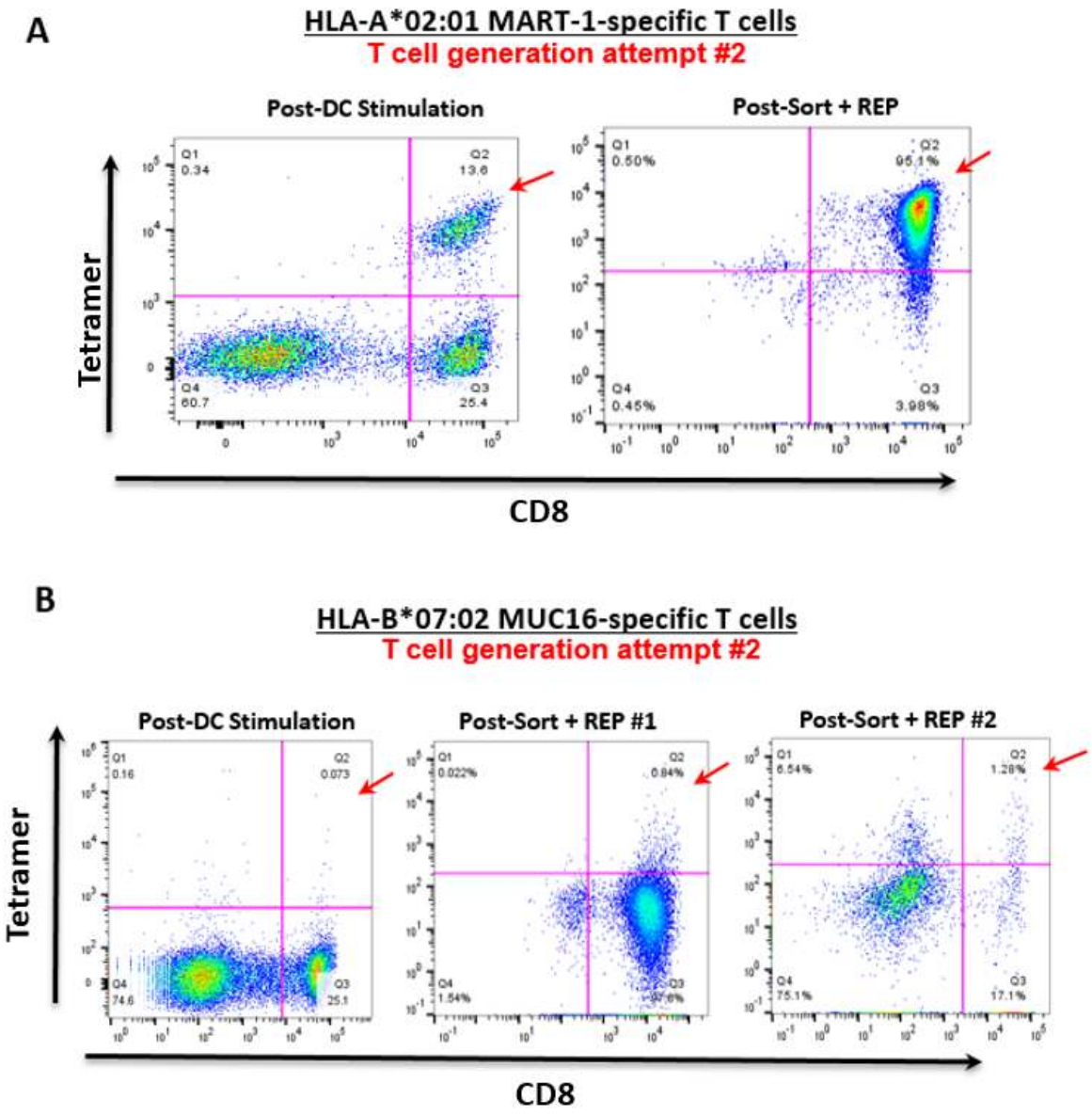

Figure 2.10. Second attempt at the generation of MART-1 and MUC16-specific T cells.

Figure 2.10. Second approach for the generation of MART-1 and MUC16-specific T cells.

Generation of MART-1 and MUC16-specific T cells. (A) PBMCs isolated by leukapheresis were stimulated with autologous MART-1 and MUC16-peptide-pulsed dendritic cells (DCs). After two stimulations, CD8+ and MART-1 tetramer-positive cells were sorted and expanded using a standard rapid expansion protocol (REP). (**B**) MUC16 1 tetramer-positive cells were sorted and expanded using a standard rapid expansion protocol (REP). A second REP was conducted following a low yield of the first REP.

2.2d.) Discussion

MUC16 is a well-characterized tumor-antigen originally discovered in ovarian cancer [108]. That has been a biomarker for the disease several for years. In addition, it is also a biomarker for multiple other cancers including, fallopian tube, endometrial, non-small lung, breast, gastrointestinal, and pancreatic cancers [117-119]. MUC16 plays a critical role in ovarian and pancreatic tumor invasion and metastasis [109, 115]. For several reasons, MUC16 fits the criteria of a safe therapeutic target for T-cell based immunotherapy. It has extremely low expression in normal tissues across the body while having elevated levels in a number of different cancer types. However, attempting to isolate low-frequency T cells from the peripheral blood of a healthy donor, was challenging, which may explain why there are no currently-approved TCR therapies that target MUC16 [120], [121].

MUC16 presents some of the same challenges we face in targeting non-mutated, over-expressed tumor antigens. MUC16 is unique in that happens to be the largest known cell surface glycoprotein (at over 22,000 amino acids), with >50 extracellular tandem repeat domains [122],[123]. This presents a potential explanation for difficulties we experienced in breaking tolerance. Due to the large size of MUC16, it may share similar or matching stretches of amino acids with other mucins or proteins that are not safely targetable. All these factors may be contributing to the lack of immunogenicity of MUC16.

Isolating high-affinity CTLs that recognized MUC16 proved too to be unsuccessful, even after adding LPS to help boost the activation of those low frequency MUC16-specific T cells. MUC16 is known to be expressed at low levels, primarily in female reproductive tissues, such as the fallopian tubes and cervix. We therefore used healthy male donor PBMCs to try to isolate MUC16-specific T cells, which we reasoned would increase our chances of

isolating T cells. Since not every person necessarily possess high-affinity MUC16-specific T cells, repeating the isolation approach different donors might yield a greater chance of success. Using PBMCs from a tumor-bearing patient to isolate T cells may also have been a plausible approach. It is possible that they could possess some TAA-specific T cells that have been exposed to MUC16 on tumors, but could be suffering from an immunosuppressive tumor microenvironment. If we could isolate T cells directly from these tumors, we may have better success at expanding them. Due to the unsuccessful generation of T cells specific for MUC16, we chose to end our pursuit of this TAA target. We instead began working on the isolation of T cells against a different TAA, VGLL1, in collaboration with Dr. Cassian Yee's laboratory, as described in the next chapter.

CHAPTER III:

IDENTIFICATION OF THE SHARED CANCER PLACENTA ANTIGEN VESTIGIAL-LIKE 1 IN PANCREATIC CANCER

3.1 Rationale for tumor antigen discovery in pancreatic cancer

Pancreatic ductal adenocarcinoma (PDAC), the most aggressive form of pancreatic cancer, remains notorious for its poor prognosis and high mortality rate, with its overall 5-year survival rate of 8% being amongst the lowest of all cancer types [124, 125]. Early detection is unusual, with 85% of patients presenting with locally advanced or metastatic disease [126]. Progress towards effective treatment has been slow and the incidence of PDAC-related deaths has continued to rise [127],[128]. Despite some encouraging recent improvements in survival achieved through optimizing the sequencing of surgery and chemotherapy treatment regimens, developing new and effective therapeutic options remains a dire need for advanced-stage PDAC patients [129].

Checkpoint inhibitor (CPI) therapies that act through non-specific activation of T lymphocytes have made a significant positive impact on long-term patient survival [130]. However, the benefits of CPI have mainly been limited to highly mutated tumor types like melanoma and lung adenocarcinoma that can express a large array of potential neo-antigen peptides in the context of surface HLA molecules [131],[128]. Tumor-infiltrating lymphocyte (TIL) therapy, in which individual cancer patients are re-infused with T cells expanded from their own tumors, has also shown great promise for inducing the regression of bulky tumors.[132],[133] TIL are polyclonal and can recognize both patient-specific neo-antigens as well as shared tumor-associated antigens (TAA) such as melanocyte differentiation antigens (MDA) or cancer-testis antigens (CTA)[134], [135],[136]. Targeting of individual validated HLA class I-restricted TAAs through infusion of antigen-specific endogenous T-cells (ETC therapy) or genetically engineered TCR-T cells has also proven successful at

inducing clinical responses in patients with melanoma and other solid cancers [137], [138] ,[139] ,[140] ,[141].

CPI- and CTL-based immunotherapies have unfortunately not shown the same beneficial impact in treating PDAC patients [142], [143]. This lack of success has been attributed to the highly immune suppressive tumor microenvironment (TME) of PDAC, in addition to the relatively low mutational burden that contributes to a dearth of potential neo-antigen targets [144], [120], [145], [146]. A number of potentially targetable HLA class I-restricted peptide antigens have been identified in PDAC, most notably those derived from carcinoembryonic antigen-related cell adhesion molecule (CEACAM), mucin 16 (MUC16), mesothelin (MSLN), and mutated *KRAS*, among others [147], [106], [148], [149], [150]. Although promising, therapies targeting these TAAs have faced inherent limitations, including the induction of toxicities in non-tumor tissues, low prevalence of target antigen expression, or inability to break self-tolerance mechanisms that often hinders the generation of high-affinity CTL [142], [104], [151]. With limited exceptions, clinical trials targeting these antigens have yielded disappointing results, underscoring the need to identify immunogenic targets that demonstrate higher prevalence in PDAC patients.

3.2 Pancreatic cancer MS-based TAA discovery and antigen-specific T cell generation

3.2a.) Immunopeptidome analysis of PDAC patient tumors identifies tumor-associated peptides

To identify peptide targets for CTL-based immunotherapy of PDAC, we analyzed 39 tumor specimens derived from 35 PDAC patients treated at M.D. Anderson Cancer Center. This included 34 freshly-excised surgical specimens (20 metastatic and 14 primary tumors), in addition to 3 patient-derived xenografts (PDX) and 2 organoid cell lines derived from metastases. Tumor cells were lysed and subjected to total HLA class I immunoprecipitation and acid elution, followed by tandem mass spectrometry (MS) to analyze the HLA-bound peptides. Eluted peptide fragmentation spectra were searched against the Swiss-Prot database (updated 9/2018) to identify matches encoded within the human proteome. Individual peptide matches were assessed using several orthogonal parameters, including Mascot Ion score, MS1 mass differential (delta mass), and predicted binding to the patient's HLA allotypes as determined by high-resolution genetic sequencing [100], [101]. Further validation and potential suitability as therapeutic TAA targets was determined by evaluating all peptide-encoding genes for (1) patient tumor tissue transcript expression as determined by RNAseq, (2) normal tissue transcript expression (GTex Portal database), and (3) overall expression in tumor tissues (TCGA database) (**Figure 3.3A**). (http://www.gtexportal.org/home/, http://cancergenome.nih.gov/)

The amount of immunoprecipitated HLA class I correlated with the size of the fresh tumor specimens analyzed ($R^2 = 0.79$), with the exception of 8 tumors (21.6%) that showed low HLA class I expression as assessed by Western blot analysis (**Figure 3.1, Table 3.1**). As expected, HLA class I protein levels also correlated with the number of Swis-Prot database

matches to eluted peptides (R^2 = 0.62, **Figure 3.2**). Overall, the 39 tumor specimens analyzed yielded a total of 23,245 unique, high confidence peptide identities, of which 7,966 peptides (34.3%) were 8- to 13-mer peptides predicted to bind to one or more patient HLA class I allotypes. Fresh tumor specimens yielded a highly variable number of peptides, ranging from 238 to 1657 (mean = 542). For 3 patients, PDX derivation resulted in larger tumor specimens, yielding an increased number of eluted peptides in all 3 cases. One of the two patient-derived organoid cell lines (MP015) yielded the highest number of eluted peptides overall (n = 1903), underscoring the quantitative advantage provided by expanding tumor specimens *in vitro* prior to MS analysis (**Table 3.1, Figure. 3.2**).

Quantity of immunoprecipitated HLA class I correlates with PDAC tumor specimen weight.

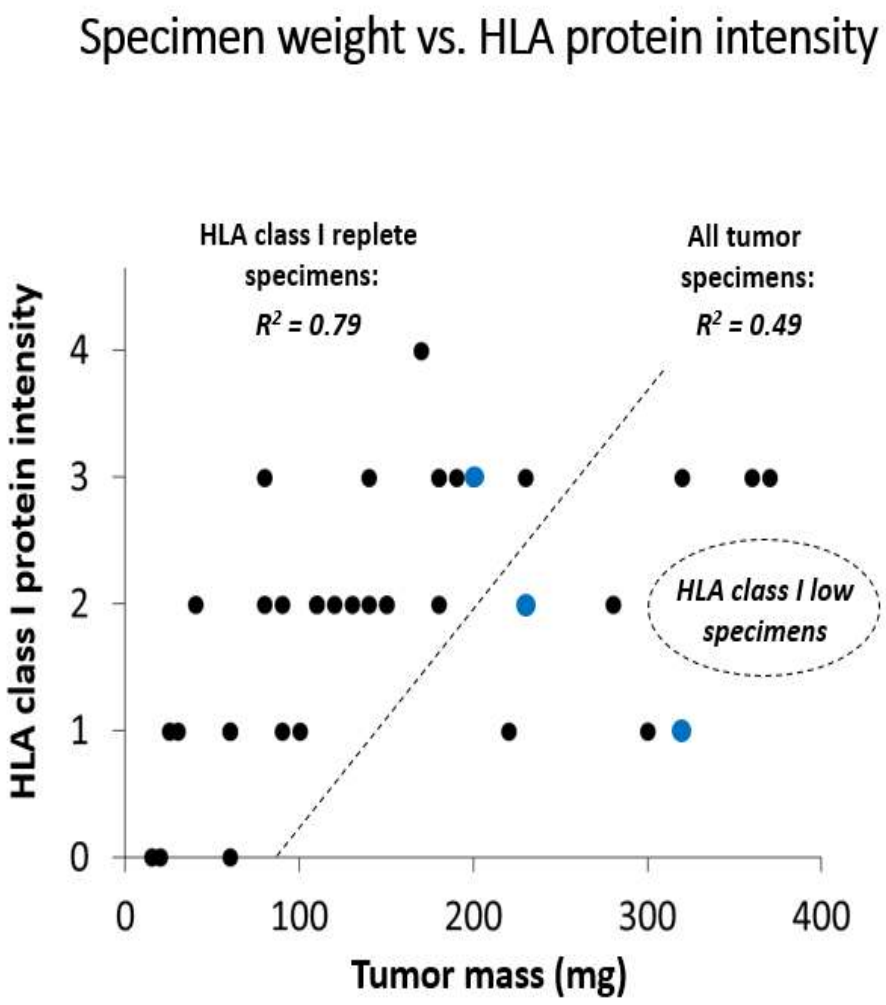

Figure 3.1 Quantity of immunoprecipitated HLA class I correlates with PDAC tumor specimen

Figure 3.1 Quantity of immunoprecipitated HLA class I correlates with PDAC tumor specimen weight. Surgical tumor resections from PDAC patients (n=36) or patient-derived xenografts (n=3) was weighed prior to tissue lysis and immunoprecipitation of total HLA class I using mAb W6/32. Recovered HLA class I was quantitated based on Western blot analysis by assessing the HLA class I band intensity (expected size 42 - 44 KD) on a scale of 0 (none detected) to 4 (highest level detected). Graph shows specimen weight plotted by Western blot band intensity; the dotted line delineates samples with lower than expected HLA class I recovery, indicating reduced tumor HLA expression.

Total number of detected PDAC-associated peptides correlates with quantity of recovered HLA class I.

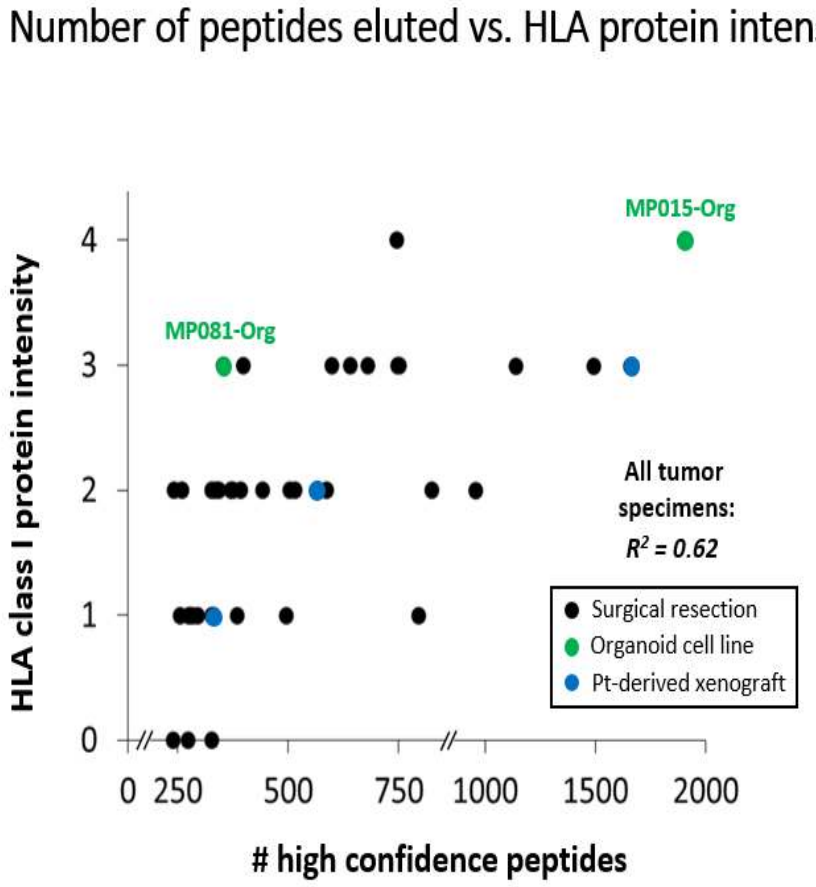

Figure 3.2 Total number of detected PDAC-associated peptides correlates with quantity of recovered HLA class I.

Figure 3.2 Total number of detected PDAC-associated peptides correlates with quantity of recovered HLA class I. HLA class I recovered from patient-derived surgical resections (n=36), xenografts (n=3), or organoid cell lines (n=2) was quantitated by Western blot analysis by assessing the HLA class I band intensity (size 42 - 44 KD) on a scale of 0 (none detected) to 4 (highest level detected). Peptides eluted from immunoprecipitated HLA class I were analyzed by tandem MS and searched against the SwissProt human proteome database. Graph shows number of unique, high quality peptide matches (Mascot Ion score of 20 or higher) plotted against HLA class I intensity, as analyzed by Western blot.

Patient Identifier	Eluted peptide	Source gene(s)	Match Rank	Tumor RNA expression (RNAseq, TPM)	Predicted HLA binding affinity (nM)					
MP015	LSELETPGKY	VGLL1	1	77.53	A*0101	A*2601	B*3502	B*3801	C*0401	C*1203
					51	12558	33903	29369	30164	6181
MP081	LSELETPGKY	VGLL1	1	56.39	A*0101	A*0101	B*3502	B*5701	C*0401	C*0602
					51	51	33903	11936	30164	35852

Table 3.1 VGLL1-derived peptide eluted from two HLA-A*0101^{+} PDAC patient tumor organoids

3.2b.) Expression profiling of peptide-encoding genes identifies VGLL1 as a novel pancreatic cancer TAA

To evaluate if any of the eluted peptides constituted safe therapeutic CTL targets, peptide-encoding genes were individually assessed for normal tissue transcript expression with reference to the GTex Portal database containing RNAseq data of 42 different human tissues. Normal tissues (excluding testis) were categorized into 4 groups that reflected the potential toxicities expected from off-target killing activity by antigen-specific CTLs (**Table 2.2**). Peptide-encoding genes were then screened using four corresponding expression filters of increasing stringency in order to eliminate candidate TAAs most likely to elicit autoimmune toxicity in the context of CTL therapy (**Figure 3.3B**). Thus, while TAA transcript expression up to 30 TPM maximum was allowed in non-essential tissues (such as prostate, breast, and adipose tissues), a maximum expression threshold of 1 TPM was imposed for highly essential tissues such as heart and brain, for which CTL recognition can be lethal.[97], [98]. Using these stringent criteria, 12 TAA peptides were deemed safest to target, the genes encoding these peptides being *MUC16* (encoding 5 unique peptides), *MUC19, ZNF717, EIF5AL1, RGPD1, SLC30A8, MIA2,* and *VGLL1* (each encoding 1 unique peptide). Peptides encoded by TAAs MSLN and IDO1 were also detected, but were excluded in the screening due to elevated RNA transcript expression in normal lung tissue (88 TPM and 16 TPM, respectively, **Figure 3.3B**). Amongst the TAAs deemed safest to target, only 2 peptides (derived from *MIA2* and *VGLL1)* were found to be presented by tumors of more than one PDAC patient (**Table 3.1**).

The 10-mer peptide LSELETPGKY, uniquely encoded by *VGLL1*, was eluted from both PDAC patient-derived organoid cell lines MP015-Org and MP081-Org. This peptide was predicted to bind with high affinity to HLA-A*0101 (51 nM), and RNAseq analysis

confirmed high *VGLL1* transcript expression in both organoid lines (**Table 3.1**). Peptide identity was confirmed by targeted LC-MS, in which a synthetic peptide was analyzed as part of a mixture with organoid tumor-associated peptides. As shown in **Figure 3.3C**, the synthetic isotope-labeled peptide LSELETPGKY generated a highly similar fragmentation spectra to the native VGLL1 peptide detected from PDAC organoid lines MP015-Org and MP081-Org, and was also detected at nearly identical LC-MS retention times. Targeted MS analysis on 2 additional HLA-A*0101-expressing cell lines (PANC10.05 and BXPC3) demonstrated that the same peptide was also presented by PANC10.05, providing further evidence that LSELETPGKY might constitute a widely shared TAA (**Figure 3.4**).

Immunopeptidome analysis reveals a VGLL1-derived peptide expressed by two PDAC patient-derived organoid lines.

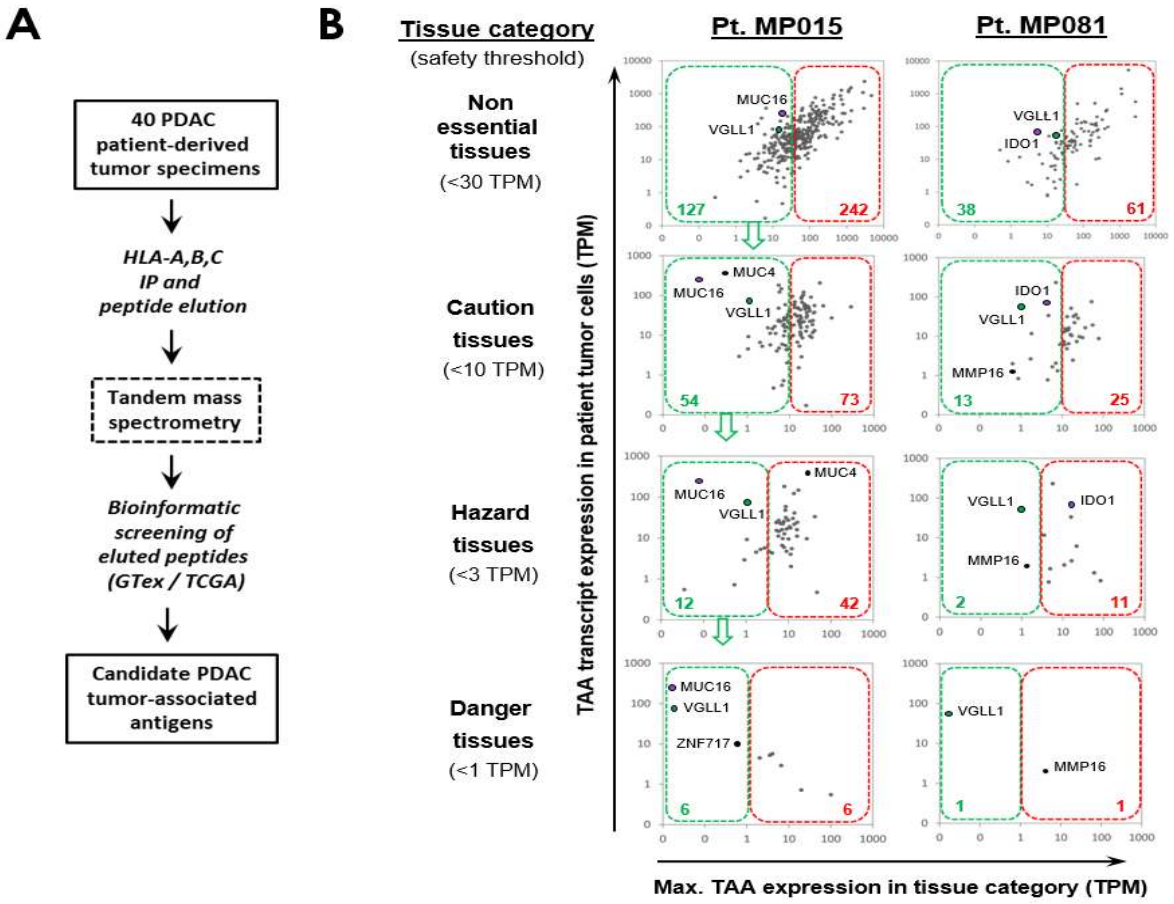

Figure 3.3. Immunopeptidome analysis reveals a VGLL1-derived peptide expressed by two PDAC patient-derived organoid lines.

Immunopeptidome analysis reveals a VGLL1-derived peptide expressed by two PDAC patient-derived organoid lines.

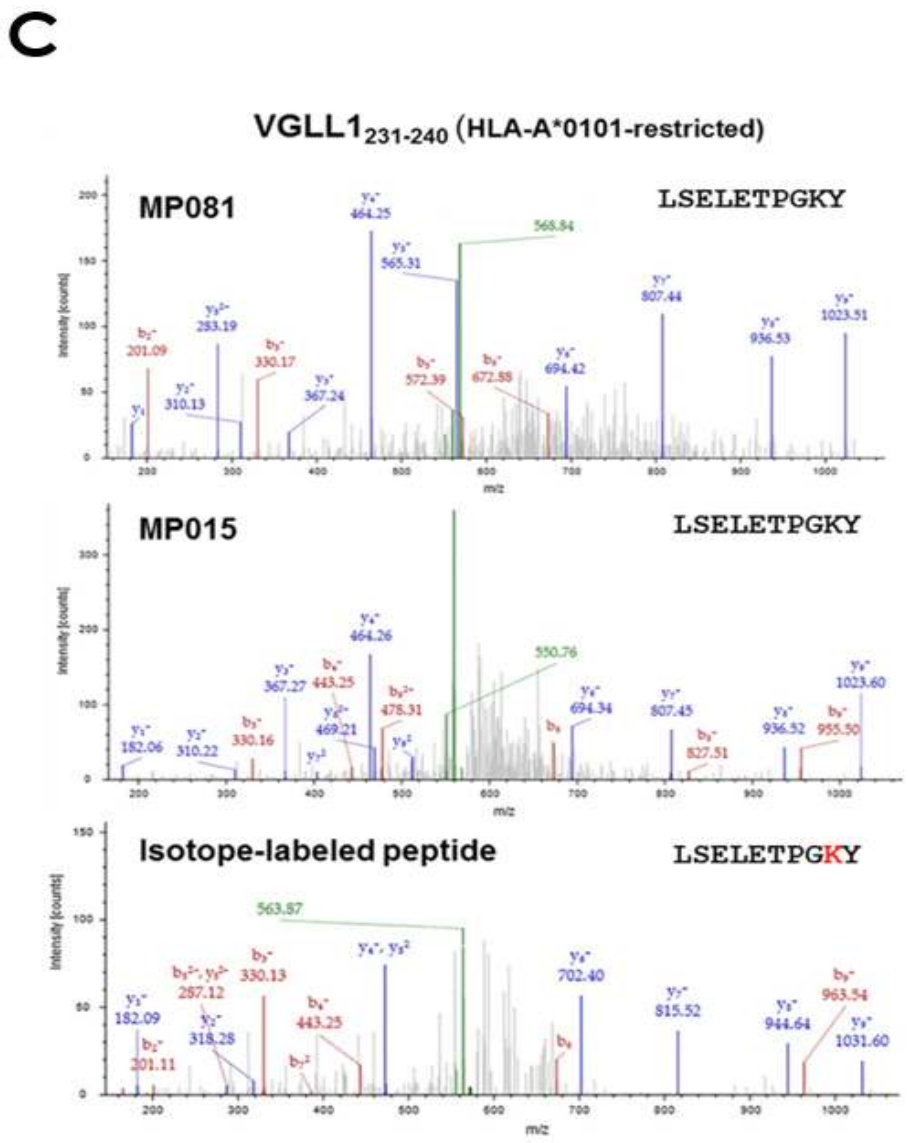

Figure 3.3. Immunopeptidome analysis reveals a VGLL1-derived peptide expressed by two PDAC patient-derived organoid lines.

Figure 3.3. Immunopeptidome analysis reveals a VGLL1-derived peptide expressed by two PDAC patient-derived organoid lines. (A) Experimental strategy to identify PDAC tumor-specific, HLA class I-bound peptides from 41 tumor specimens derived from 36 M.D. Anderson PDAC patients. **(B)** Bioinformatics screening strategy to identify potentially targetable TAAs from amongst the eluted PDAC-associated peptides. Peptide-encoding genes were assessed for PDAC tumor RNAseq expression compared with transcript expression in 42 GTex Portal normal tissues. Excluding testis, normal tissues were separated into 4 categories (non-essential, caution, hazard, and danger tissues) that reflected the potential toxicities expected from off-tumor killing activity against different tissues (**Table 2.2**). All peptide-encoding genes were filtered successively using four corresponding expression thresholds of increasing stringency (30, 10, 3, and 1 TPM, indicated by green dotted lines) to eliminate candidate TAAs most likely to elicit autoimmune toxicity in the context of CTL therapy (red dotted lines). Screening of high-confidence peptides isolated from tumor organoid cell lines of PDAC patients MP015 and MP081 is depicted, showing that only a few eluted peptides met these stringent safety criteria. **(C)** Mass spectra of an HLA-A*0101-restricted VGLL1-derived peptide isolated from two different organoid cell lines, MP015 and MP081 (top 2 panels). The patient-derived peptides co-eluted with and matched the MS fragmentation spectra of the synthetic isotope-labeled VGLL1 peptide LSELETPGK̲Y (containing a $^{13}C/^{15}N$-labeled lysine residue), with the labeled y^+ fragment ion series demonstrating an expected shift of 8 atomic mass units (bottom panel).

VGLL1-derived peptide was eluted from the PANC-1005 cell line

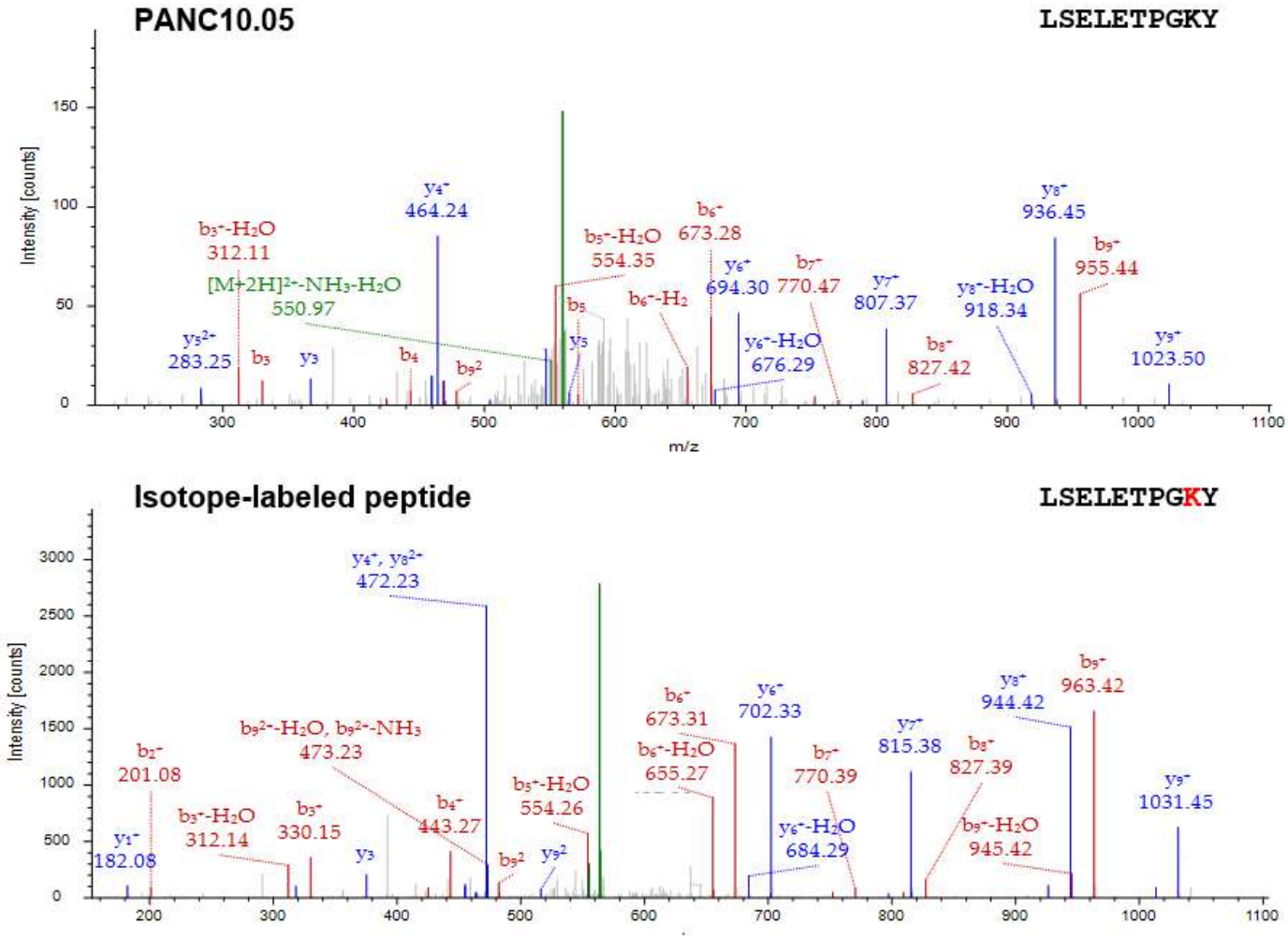

Figure 3.4 VGLL1-derived peptide was eluted from the PANC-1005 cell line.

Figure 3.4 VGLL1-derived peptide was eluted from the PANC-1005 cell line. Mass spectra of HLA-A*0101-restricted VGLL1-derived peptide isolated from PDAC cell line PANC-1005 (top panel). This native peptide co-eluted with and matched the MS fragmentation spectra of the synthetic isotope-labeled peptide LSELETPGKY containing a $^{13}C/^{15}N$-labeled lysine residue (bottom panel).

3.2c.) VGLL1 is expressed by multiple cancer types and is associated with poorer overall survival

VGLL1, also known as TONDU, was first identified as the human homolog of the Vestigial (Vg) protein in *Drosophila*, a key regulator of wing development [152], [153]. Since VGLL1 is a transcriptional co-activator that binds to the TEA domain family of transcription factors (TEFs) implicated in cancer development, we further examined *VGLL1* transcript expression in the 31 cancer types listed in The Cancer Genome Atlas (TCGA). As shown in (**Figure 3.5A)**, in comparison to most normal tissues, *VGLL1* is overexpressed in a number of different cancer types, including PDAC, bladder, ovarian, breast, lung, and stomach cancer. Interestingly, *VGLL1* appears to be preferentially expressed in basal-like breast cancers while demonstrating a relatively low prevalence in other breast cancer subtypes (**Figure 3.6**). A similar tumor-associated expression profile was confirmed by microarray gene expression analysis of tumor cell lines listed in the Cancer Cell Line Encyclopedia (CCLE, **Figure 3.7**). According to the GTex RNAseq database, the highest median *VGLL1* transcript expression was found in 3 non-essential tissues: bladder (15.3 TPM), salivary gland (3.9 TPM), and breast (1.3 TPM). The highest level of *VGLL1* transcript expression in essential tissues was in normal lung (1.0 TPM), esophagus (0.73 TPM), and kidney (0.34 TPM), while *VGLL1* expression in heart and brain tissues was virtually undetectable (**Figure 3.5A**). Collectively, this data suggested that VGLL1 may constitute a safe, targetable TAA for multiple cancer types.

We next assessed if tumor *VGLL1* transcript expression was associated with cancer patient survival. As shown in Figure 2B, TCGA PDAC patient survival (n = 175) was found to be inversely correlated with *VGLL1* expression: patients with high expression had a

significantly shorter overall median survival compared to patients with low or absent expression (16 months vs. 37 months, p=0.001). This was confirmed in a independent cohort of 37 M.D. Anderson PDAC patients for whom PDX tissues could be derived: patients showing an overall survival of less 18 months demonstrated a significantly higher mean PDX *VGLL1* expression compared to patients that survived longer than 36 months (57.3 TPM vs. 9.6 TPM, p=0.003, Figure 2C). It is worth noting that *VGLL1* transcript expression was found to be considerably higher in PDAC tumor cell lines and PDX tissues compared with surgically resected PDAC tumors, perhaps due to the high stromal content of many PDAC tumors *in situ* (**Figures. 3.5A, 3.5C, Table 3.1**). Highly elevated *VGLL1* expression was also associated with shorter overall survival time in breast cancer (p = 0.037) and stomach cancer (p = 0.047), but showed no association with survival in ovarian cancer (**Figure 3.8**) [154]. Interestingly, low or absent *VGLL1* expression was associated with shorter survival time in bladder cancer (p = 0.036). One possible explanation is that loss a normal bladder tissue antigen like VGLL1 may indicate tumor dedifferentiation, which has been associated with poorer prognosis in bladder cancer and other tumor types [155].

VGLL1 is overexpressed in multiple tumor types and is associated with reduced pancreatic patient survival

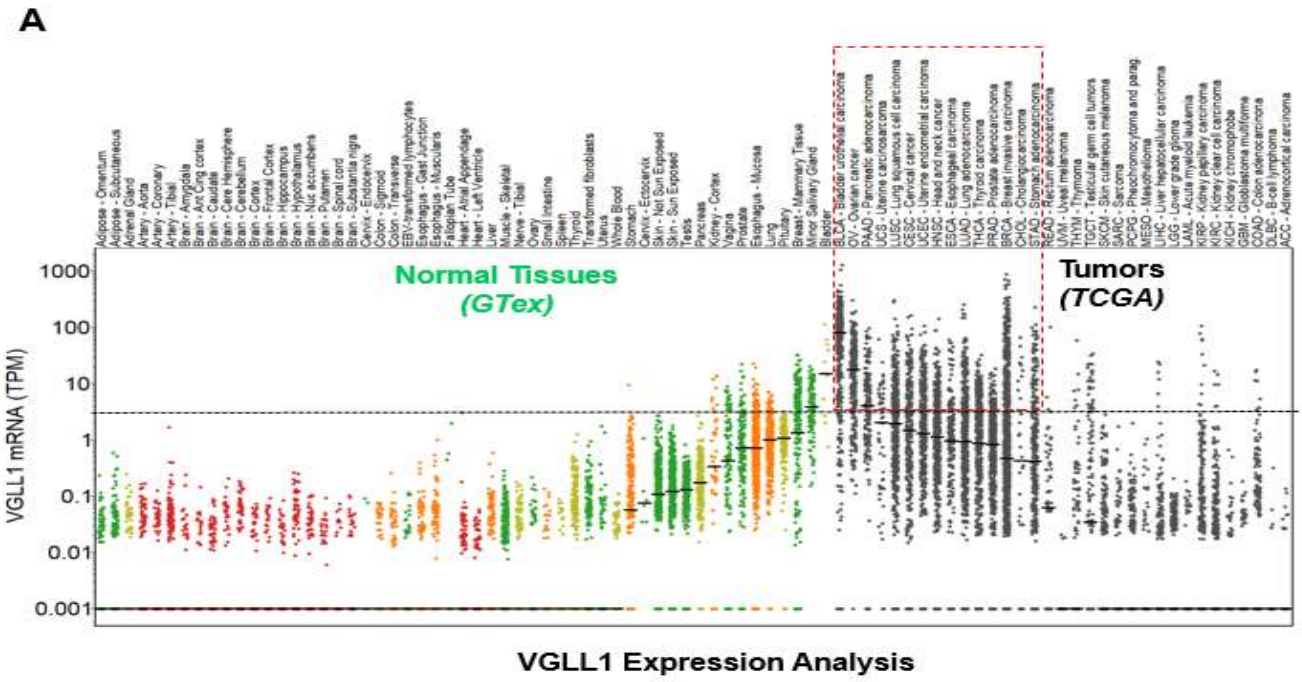

Figure 3.5 VGLL1 is overexpressed in multiple tumor types and is associated with poor pancreatic patient survival.

VGLL1 is overexpressed in multiple tumor types and is associated with reduced pancreatic patient survival

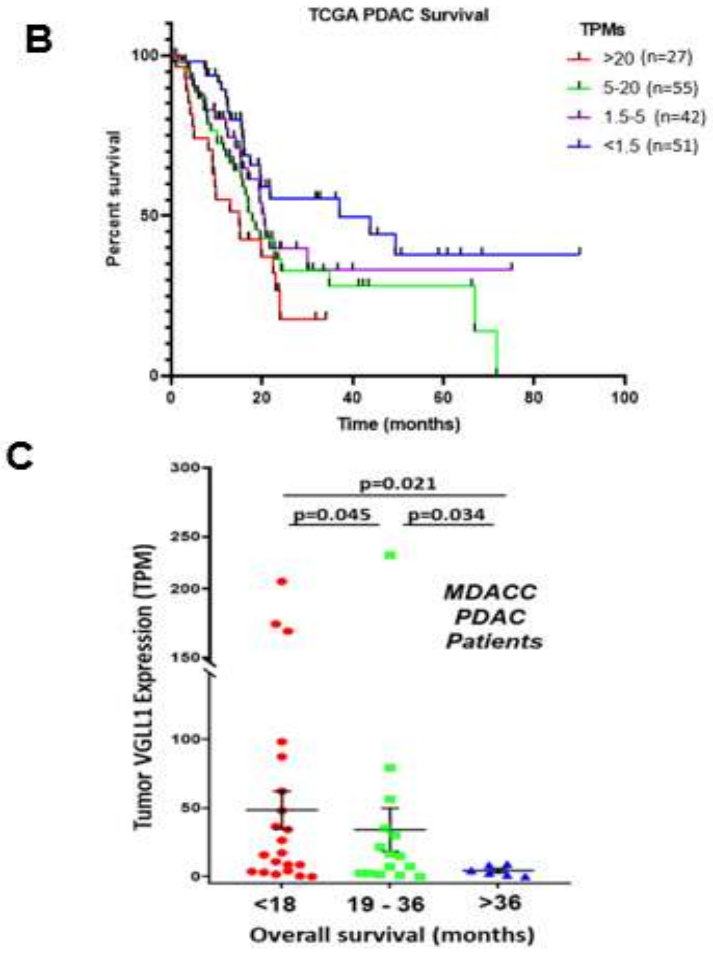

Figure 3.5 VGLL1 is overexpressed in multiple tumor types and is associated with poor pancreatic patient survival.

Figure 3.5 VGLL1 is overexpressed in multiple tumor types and is associated with poor pancreatic patient survival. (A) VGLL1 transcript expression in normal tissues (colored dots, GTex Portal database) and human cancers (black dots, TCGA database), as determined by RNAseq analyses. Each dot represents one normal donor or patient tumor sample. Colors correspond to the 4 normal tissue categories defined in Figure 1: Green, non-essential tissues; Yellow, caution tissues; Orange, hazard tissues; Red, danger tissues. Although >95% of analyzed normal GTex caution, hazard, and danger tissue samples fell below 3 transcripts per million (TPM, dotted line), many TCGA cancer specimens demonstrate VGLL1 expression well above this threshold. **(B)** Kaplan-Meier curves showing TCGA PDAC patient overall survival (OS) stratified by tumor VGLL1 transcript expression (n = 175). P-values indicate log-rank significance test results comparing the OS of 3 groups of VGLL1-expressing patients to those patients with low or absent VGLL1 expression. (**C)** Patient-derived xenografts (PDX) from an independent cohort of MD Anderson metastatic PDAC patient tumors (n = 37) underwent RNAseq analysis after being grown in immunodeficient mice. Stratification of these PDAC patients into 3 groups corresponding to OS time showed that mean VGLL1 transcript expression was significantly associated with shorter patient survival time.

Basal-like subset of Breast Cancer shows elevated VGLL1 Expression

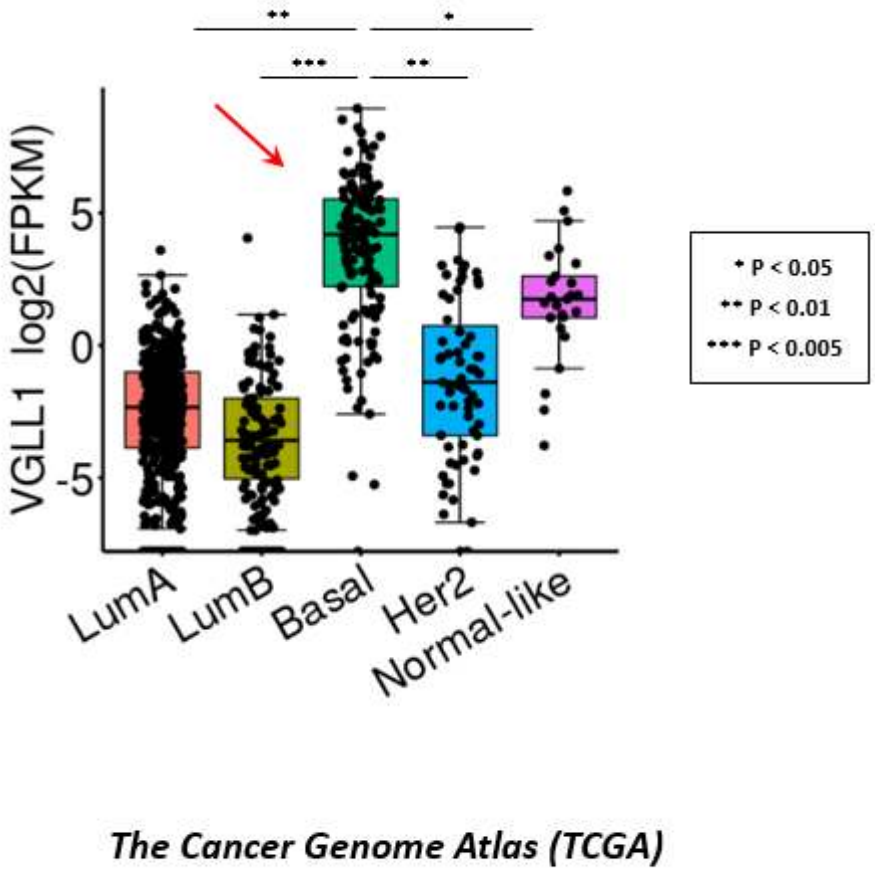

Figure 3.6 VGLL1 is preferentially expressed in basal-like breast cancer compared to other breast cancer subtypes.

Figure 3.6 VGLL1 is preferentially expressed in basal-like breast cancer compared to other breast cancer subtypes. TCGA breast cancer patients were subdivided into 5 major sub-types (LumA, LumB, Basal-like, HER2 overexpressing, and normal-like) and analyzed for tumor VGLL1 expression by RNAseq analysis. Each dot represents one TCGA patient sample, and VGLL1 transcript expression is expressed in fragments per kilobase of transcript per million mapped reads (FPKM).

VGLL1 prevalence and expression in CCLE tumor cell lines

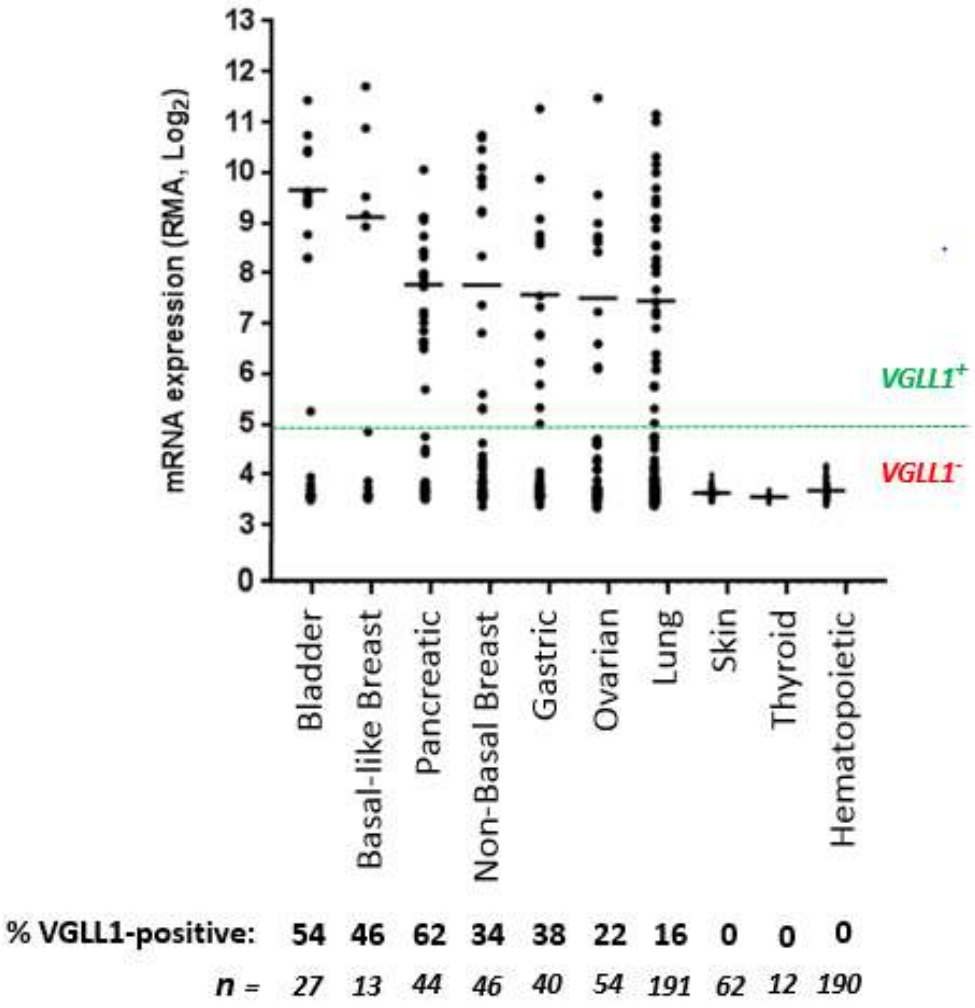

Figure 3.7 VGLL1 gene expression in tumor cell lines derived from a variety of cancer types.

Figure 3.7 VGLL1 gene expression in tumor cell lines derived from a variety of cancer types. Gene expression microarray analysis of a diverse array of tumor cell lines (n=679) from the Cancer Cell Line Encyclopedia (CCLE) showed that VGLL1 is expressed by a majority of PDAC and bladder cancer cell lines, in addition to a significant percentage of breast, gastric, ovarian, and lung cancer cell lines. No VGLL1 expression was found in cell lines derived from melanoma, thyroid, or hematopoietic cancers. Threshold for VGLL1 antigen positivity was 3-fold above background signal.

High tumor VGLL1 expression is associated with reduced survival in stomach and breast cancers

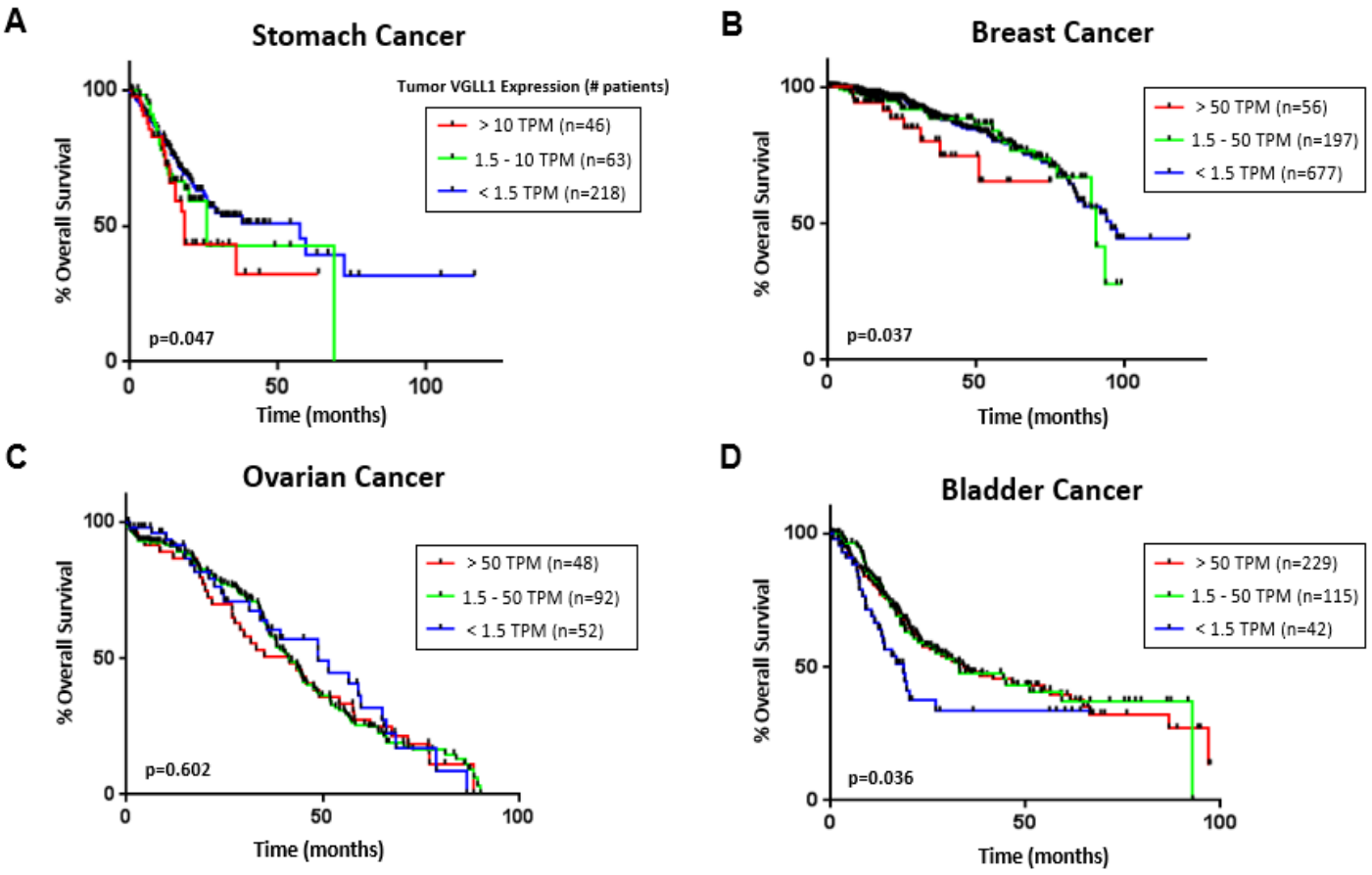

Figure 3.8 High tumor VGLL1 expression is associated with reduced survival in multiple cancer types.

Figure 3.8 High tumor VGLL1 expression is associated with reduced survival in multiple cancer types. TCGA cancer patients were stratified into three groups according to tumor VGLL1 expression as determined by RNAseq analysis. Kaplan-Meier curves show overall survival (OS) of each group for **(A)** Stomach adenocarcinoma, **(B)** Breast carcinoma, **(C)** Ovarian serous adenocarcinoma, and **(D)** bladder urothelial carcinoma patients. P-values indicate log-rank significance test results comparing the OS of the groups with the lowest and highest VGLL1 expression (blue vs. red).

3.2d.) VGLL1 is part of a unique group of Cancer-Placenta Antigens (CPAs) with therapeutic potential

VGLL1 had been previously identified as having a regulatory role during early events in human placental development, and is a specific marker of proliferative cytotrophoblast [156]. In accordance with this, RNAseq gene expression data from 7 human placenta samples showed that *VGLL1* demonstrates the highest expression in this tissue by a large margin (mean = 302.7 TPM), nearly 20-fold higher than its expression normal bladder (**Figure 3.9A**). This led us to explore the notion that cancer-placenta antigens (CPA) may constitute a distinct category of targetable TAAs analogous to cancer-testis antigens (CTAs), which have been successfully targeted with CTL-based therapies. To identify other CPAs with similar expression profiles to VGLL1, we searched the GTex, TCGA, and other RNAseq databases for genes that demonstrated the following attributes: (1) highest normal tissue expression in placenta; (2) low to absent expression in other normal tissues; and (3) elevated expression in pancreatic, breast, bladder, and/or ovarian cancer. This search yielded 9 additional genes, including Placenta-specific 1 (*PLAC1*), previously identified as a target of humoral antitumor immunity in cancer patients[157]. Interestingly, Chorionic Gonadotropin (CG) Beta subunits 3 and 5 (*CGB3/CGB5*), components of the CG hormone complex produced by placental trophoblasts during pregnancy, were also identified as potential CPAs due to their overexpression in a subset of pancreatic, testicular, uterine, and bladder cancers (**Figure 3.10B**). The other 6 putative CPAs demonstrated diverse expression profiles, ranging from those found only in a restricted set of cancer types (*IGF2BP3, ADAM12*), to those overexpressed in most cancer types but also demonstrating elevated expression in normal female reproductive tissues (*CAPN6, MMP11*) (**Figure 3.9, Figure 3.10**.). Although we did not detect peptides derived from these genes in this set of PDAC specimens, epitopes from

several of these putative CPAs have been identified in multiple tumor types and are listed in the Immune Epitope Database (IEDB) [157].

VGLL1 is a cancer-placenta antigen (CPA) demonstrating high expression in placenta and tumors

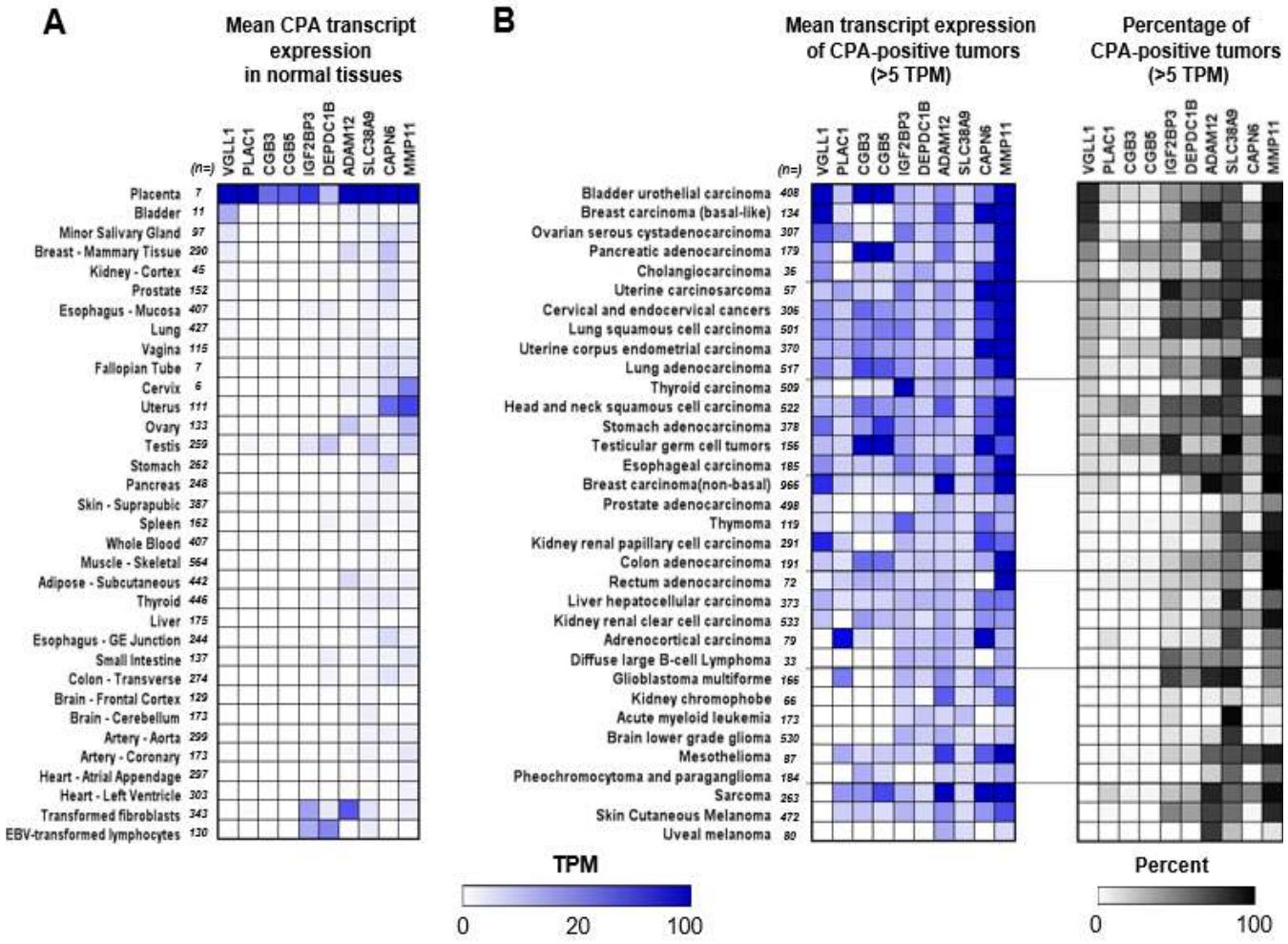

Figure 3.9 VGLL1 is a cancer-placenta antigen (CPA) demonstrating high expression in normal placenta and tumors.

Figure 3.9 VGLL1 is a cancer-placenta antigen (CPA) demonstrating high expression in normal placenta and tumors. Gene expression profiling uncovered 9 additional putative CPAs with similar expression profiles to VGLL1. **(A)** Heatmap depicting the mean transcript expression of different CPAs in normal placenta (top), GTex normal tissues, and transformed lymphocytes and fibroblasts (bottom). Tissues are listed in order of highest to lowest VGLL1 expression, as determined by RNAseq analysis. **(B)** Heatmaps displaying the mean CPA transcript expression (left) and frequency (right) of CPA-positive tumor specimens in 34 different TCGA cancer types as determined by RNAseq. CPA-positive specimens were defined as having tumor CPA transcript expression >5 TPM. Tumor tissues are listed in order of highest to lowest VGLL1 prevalence.

Mean expression of cancer-placenta antigens in all TCGA tumor specimens

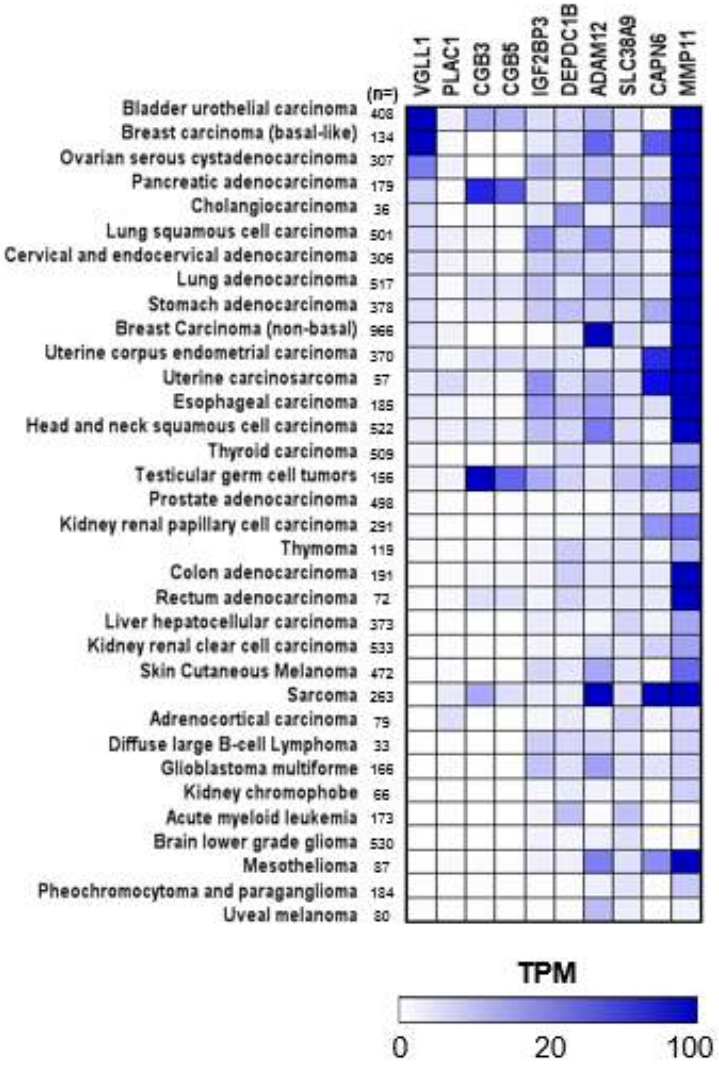

Figure 3.10 Expression of cancer-placenta antigens (CPAs) in all TCGA tumor specimens.

Figure 3.10 Expression of cancer-placenta antigens (CPAs) in all TCGA tumor specimens. Gene expression profiling to search for potential TAAs with similar expression profiles to VGLL1 uncovered nine additional putative CPAs. Heatmap depicts the mean transcript expression of all 10 CPAs in 34 different TCGA cancer types, as determined by RNAseq. Tumor tissues are listed in order of highest to lowest mean VGLL1 transcript expression.

3.3 Generation and validation of VGLL1-specific T cells

3.3a.) VGLL1-specific cytotoxic T cells were expanded from the peripheral blood of PDAC patient MP015

Patient MP015 was a previously healthy 50-year old male first diagnosed with primary PDAC in December 2011. Two years following surgical removal of the primary pancreatic tumor, a thorascopic wedge resection of a left lung lesion was performed in November 2013 and used to derive organoid cell line MP015-Org [158]. The disease was kept in check for nearly 2 more years through a series of chemotherapeutic regimens, but following progression he was enrolled in an IRB-approved cell therapy protocol at M.D. Anderson to receive autologous, expanded tumor-antigen-specific CTLs. Immunopeptidome analysis performed on the expanded organoid cell line MP015-Org in May 2015 led to the identification of 6 HLA class I-bound peptides (4 derived from MUC16 and 1 each from ZNF717 and VGLL1) that met our criteria as safe, targetable TAAs (**Table 2.3**). Custom clinical-grade tetramers were available for 3 of the 6 potential targets: two HLA-B*3502-restricted MUC16 peptides and the single HLA-A*0101-restricted VGLL1 peptide.

Following leukapheresis, patient MP015 PBMCs were stimulated twice with individual peptide-pulsed DCs in the presence of IL-21, followed by tetramer-based sorting of antigen-specific CD8+ T cells (**Figure 3.11A**). Although MUC16-specific CTLs failed to expand from patient PBMC, VGLL1 CTLs expanded successfully, with VGLL1 tetramer-positive T cells comprising 3.4% of CD8+ after 2 weeks of DC-peptide stimulation (**Figure. 3.11B**). Cell sorting followed by employment of the rapid expansion protocol (REP) was repeated twice, resulting in nearly 20 billion expanded CTLs, of which >90% were VGLL1 tetramer-positive and demonstrated restricted Vβ usage (**Figure 3.11B and C**). VGLL1-

specific CTLs were also successfully expanded from 2 of 2 healthy HLA-A*0101-positive blood donors, demonstrating the general immunogenicity of the LSELETPGKY peptide (**Figure 3.12**).

Expanded CTLs from patient MP015 were tested functionally using standard ^{51}Cr release assays. Mel888 melanoma cells (VGLL1-negative, HLA-A*0101 positive) pulsed with titrated amounts of VGLL1 peptide elicited CTL recognition and killing at peptide concentrations as low as 10 nM, indicating relatively high affinity for cognate peptide (**Figure 3.11D**). Importantly, expanded patient-derived CTLs also showed robust recognition of the autologous organoid cell line MP015-Org from which the VGLL1 peptide was originally detected by MS (Figure **3.11A**). In October 2015 following a pre-treatment regimen of Cytoxan, Patient MP015 was infused with 19.6 billion autologous, expanded VGLL1-specific CTL, subsequently receiving interleukin-2 and pembrolizumab. Although the patient experienced a transient fever (a frequent side effect of T-cell infusion-induced cytokine release), they experienced no adverse events indicating potential CTL-mediated toxicities. Unfortunately, scans in late November 2015 showed rapid disease progression manifested as an interval increase in lung lesions and pleural-based metastatic disease [158]. Surprisingly, biopsy of a pleural-based nodule at this time revealed a poorly differentiated neuroendocrine tumor. DNA sequencing analysis of serial liquid biopsies collected over the previous 18 months provided evidence of an extremely rapid evolution of Patient MP015's cancer due to numerous progressive genetic amplifications, deletions, re-arrangements, and epigenetic changes. RNAseq analysis also demonstrated that a dramatic reduction in VGLL1 transcript expression (35.1 TPM to 1.6 TPM) had occurred between December 2013 and December 2015, providing a potential explanation for the lack of clinical response to ETC

therapy (**Figure 3.14**). Patient MP015 expired in January 2016 due to extensive complications deriving from progression of his lung metastases [158].

Mean expression of cancer-placenta antigens in all TCGA tumor specimens

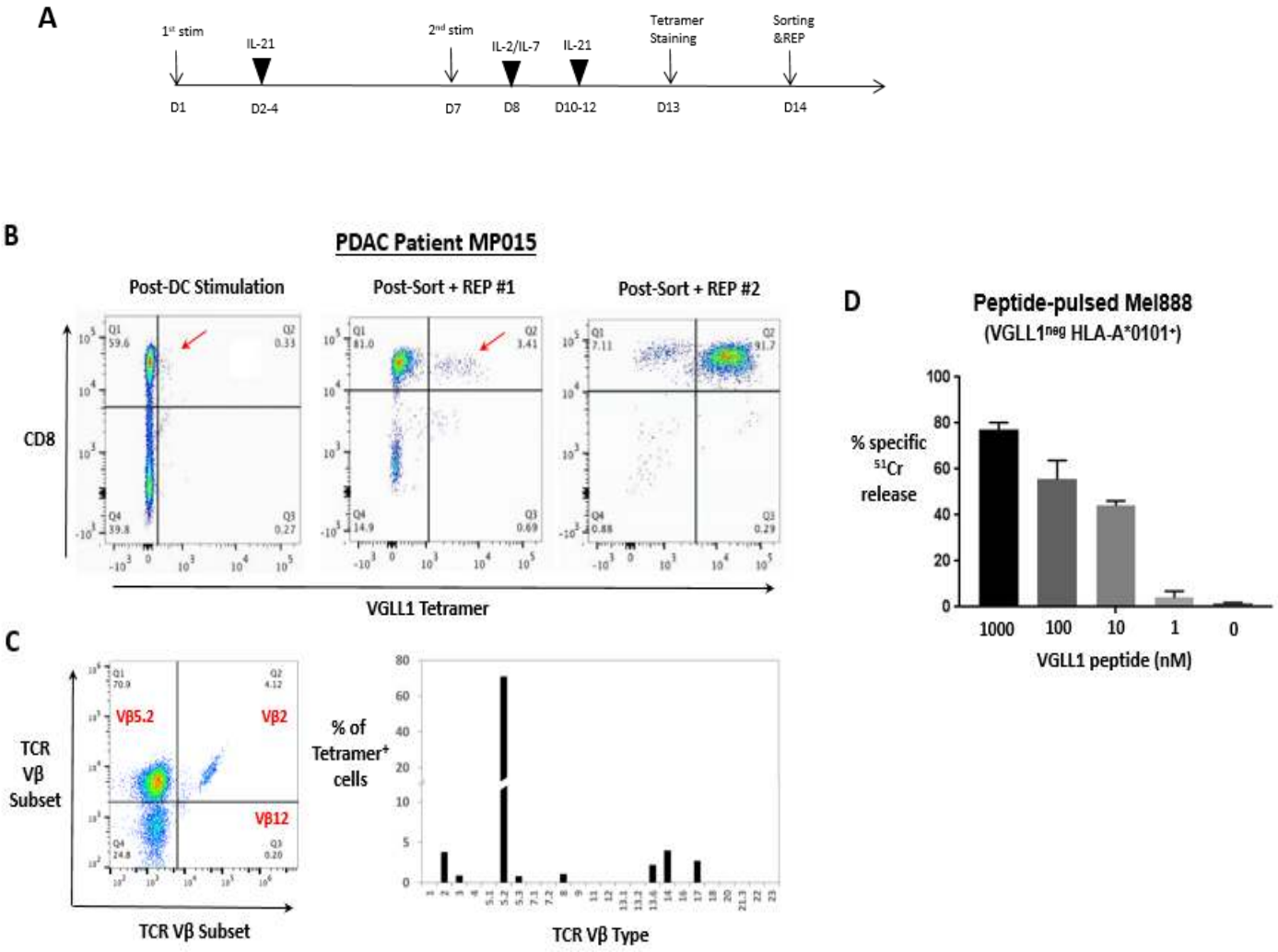

Figure 3.11. Generation of VGLL1 antigen-specific CTLs from peripheral blood of Patient MP015.

Figure 3.11. Generation of VGLL1 antigen-specific CTLs from peripheral blood of Patient MP015.

(A) Schematic outlining the experimental procedure for generating VGLL1-specific $CD8^+$ T-cells from human donor PBMCs. **(B)** PBMC isolated from PDAC Patient MP015 by leukapheresis were stimulated with autologous LSELETPGKY peptide-pulsed dendritic cells (DCs). After two stimulations (top row), CD8+ and VGLL1 tetramer-positive cells were sorted and expanded using a standard rapid expansion protocol (REP). VGLL1-specific T-cells were re-sorted and expanded a second time due to low numbers of antigen-specific cells following the first REP. The second REP yielded 19.6 x 10^9 VGLL1-specific CTLs, which Patient MP015 safely received as an infusion under a personalized ETC therapy Compassionate IND protocol. TCR repertoire analysis of expanded VGLL1-specific CTLs was also performed using Vβ antibodies corresponding to 24 different specificities (bottom panels). **(C)** VGLL1-specific T-cells expanded from Patient MP015 were tested for functionality in a standard ^{51}Cr release assay to assess specific lysis of Mel888 melanoma tumor cells (VGLL1-negative HLA-A*0101-positive) pulsed with titrated amounts of LSELETPGKY peptide at a 5:1 effector-to-target (E:T) ratio.

VGLL1-specific CTLs were expanded from PBMC of multiple donors

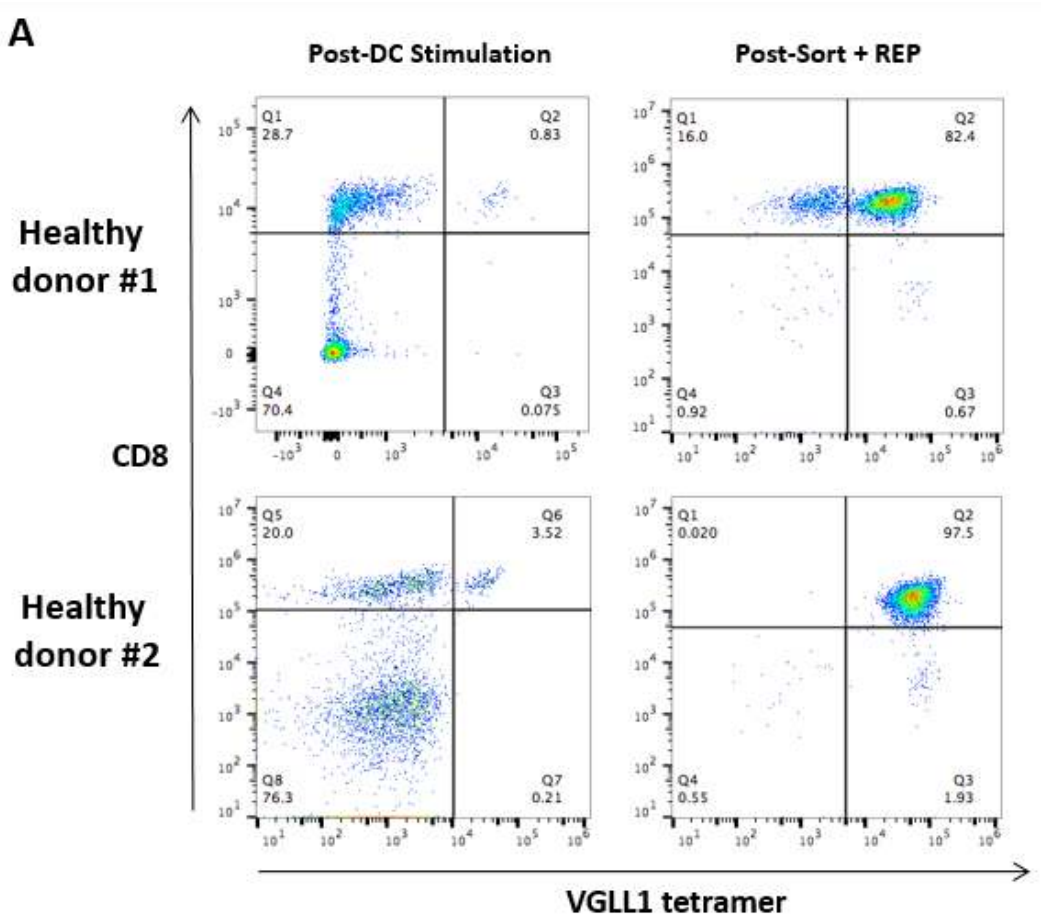

Figure 3.12 Generation of HLA-A*0101-restricted VGLL1 antigen-specific CTLs from multiple normal donor PBMC.

VGLL1-specific CTLs were expanded from PBMC of multiple donors

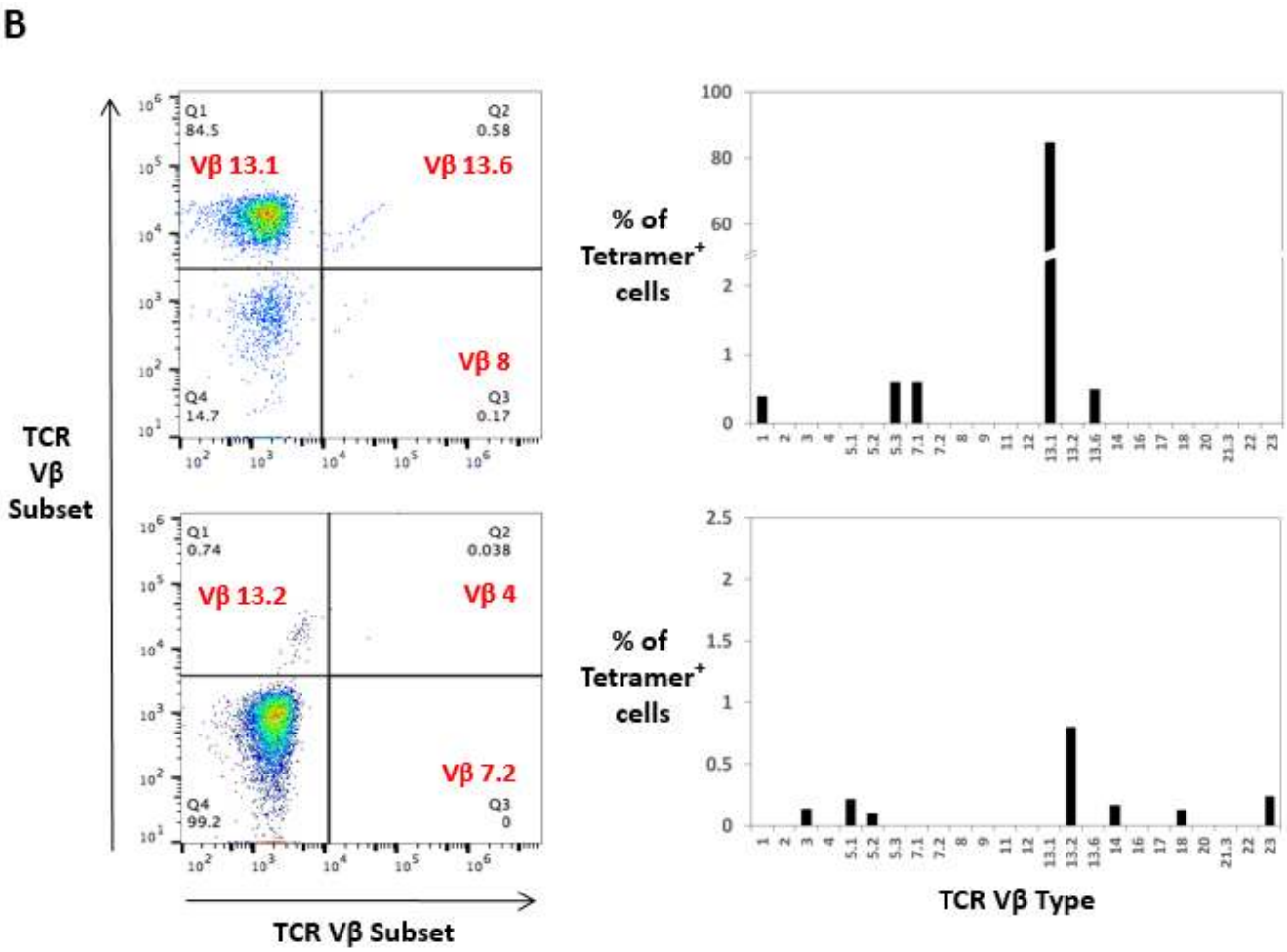

Figure 3.12 Generation of HLA-A*0101-restricted VGLL1 antigen-specific CTLs from multiple normal donor PBMC.

Figure 3.12. Generation of HLA-A*0101-restricted VGLL1 antigen-specific CTLs from multiple normal donor PBMC. (A and B) Induction of VGLL1-specific CD8 T cells from PBMC of two healthy donors. HLA A*0101-expressing donor PBMC were stimulated with LSELETPGKY peptide-pulsed dendritic cells for 2 weeks. VGLL1 tetramer-positive CD8 T cells were sorted by ARIA sorter after 2 stimulations (top panels) and the sorted T cells were expanded using a standard rapid expansion protocol (REP). TCR repertoire analysis of expanded VGLL1-specific CTLs was performed using Vβ antibodies corresponding to 24 different specificities (bottom panels).

RNAseq analysis of lung tumor biopsies revealed loss of VGLL1 expression in PDAC Patient MP015

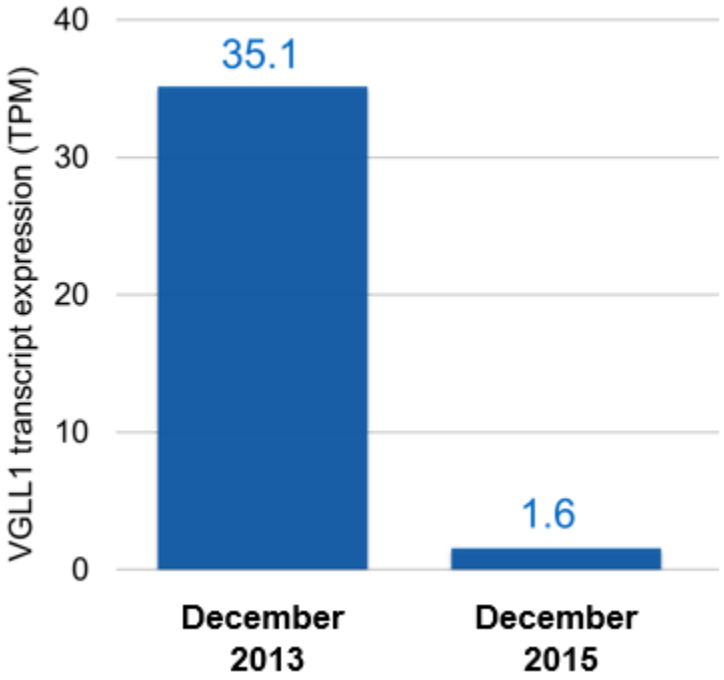

Figure 3.13 PDAC patient MP015 showed loss of VGLL1 antigen expression prior to VGLL1-CTL therapy.

Figure 3.13. PDAC patient MP015 showed loss of VGLL1 antigen expression prior to VGLL1-CTL therapy. Serial liquid biopsies were acquired from the lung metastases of PDAC Patient MP015 at different time points during treatment at M.D. Anderson. Retrospective longitudinal RNAseq analyses of these samples revealed that VGLL1 transcript expression was lost in the months prior to receiving VGLL1-specific ETC therapy.

3.3b.) VGLL1-CTLs demonstrate cytotoxicity against multiple allogeneic PDAC tumor cell lines.

Although Patient MP015 did not experience clinical benefit from adoptive transfer of his own VGLL1-specific CTLs, the robust antitumor activity demonstrated by these T-cells *in vitro* led us to explore whether they may possibly benefit other PDAC patients. HLA-A*0101 was expressed by ~30% of our PDAC patient cohort, and RNAseq analysis of TCGA and MDACC PDAC surgical specimens and PDXs showed that 43.2% to 62.5% of patients express VGLL1 transcript at a level > 5 TPM. From these data, we estimate that 12% to 15% of PDAC patients present the LSELETPGKY peptide target in the context of HLA-A*0101 and therefore could potentially benefit from VGLL1-CTL therapy.

To determine if VGLL1-CTLs derived from Patient MP015 could recognize allogeneic PDAC tumors, we tested a panel of HLA-A*0101 expressing PDAC tumor cell lines as targets for killing using a ^{51}Cr release assay. Western blot analysis was used to confirm VGLL1 protein expression, and flow cytometry confirmed surface expression of HLA-A*0101 in cell lines (**Figure 3.15**). While control cell line WM793 (VGLL1-negative, HLA-A*0101-positive) was not recognized, VGLL1-specific CTLs recognized autologous MP015-Org cells and 4 out of 4 allogenic PDAC lines tested, including inducing robust killing of PANC-1005, CAPAN-1, and BXPC3 (**Figures 3.14A and B**).

The PDAC organoid cells derived from Patient MP081 were also lysed by VGLL1-CTLs but with reduced efficiency, likely due to an outgrowth of VGLL1-negative cells within the culture (not shown). VGLL1-CTL specificity was demonstrated by co-incubation with the pan-MHC class I antibody W6/32, which resulted in blockade of PANC10.05 recognition and lysis (**Figure 3.16**). Collectively, these results provide evidence that the

LSELETPGKY peptide constitutes a shared PDAC tumor antigen that can be effectively targeted with VGLL1-specific CTLs.

RNAseq analysis of lung tumor biopsies revealed loss of VGLL1 expression in PDAC Patient MP015

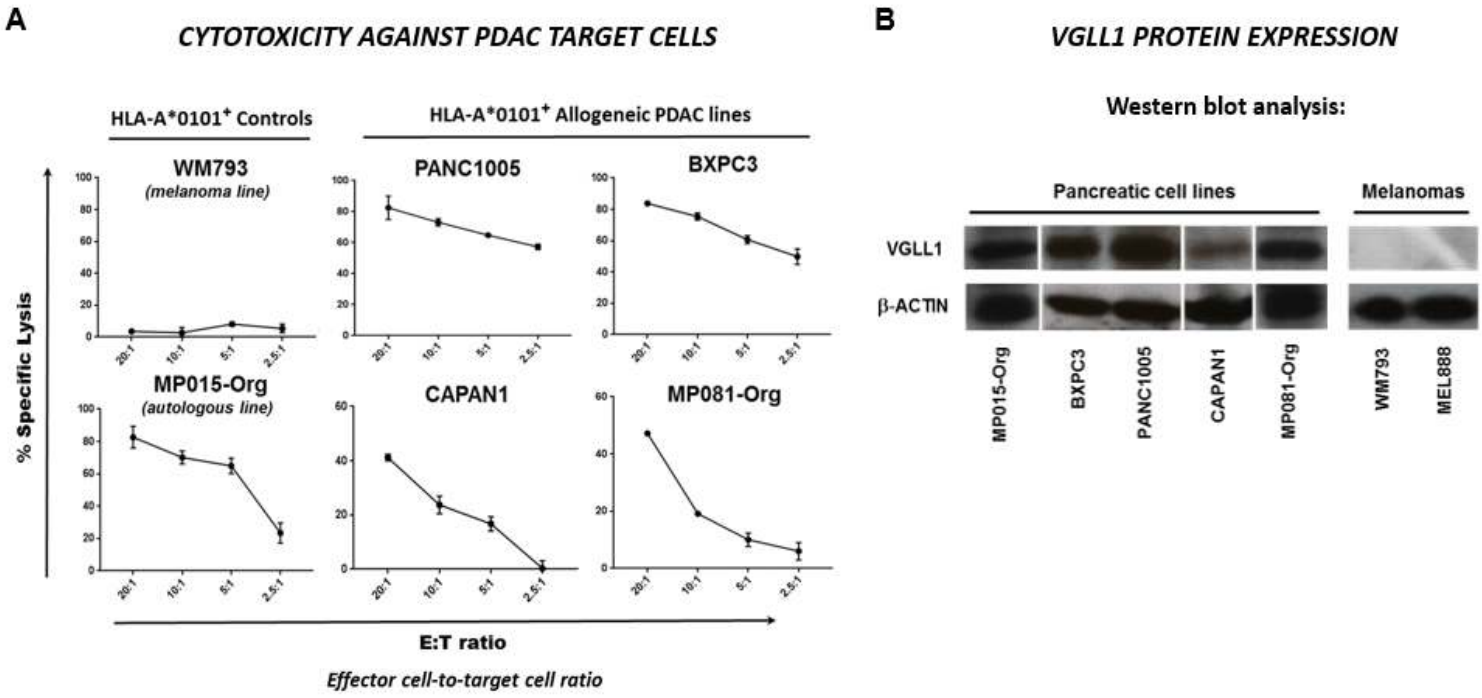

Figure 3.14. VGLL1-specific CTLs recognize and kill multiple allogeneic pancreatic cancer cell lines.

Figure 3.14. VGLL1-specific CTLs recognize and kill multiple allogeneic pancreatic cancer cell lines. (A) Expanded VGLL1-specific $CD8^+$ T cells from Patient MP015 were co-cultured with a panel of HLA-A*0101-positive PDAC tumor cell lines in a standard ^{51}Cr release assay to measure cytotoxic activity at different effector-to-target (E:T) cell ratios. WM793 melanoma cells (VGLL1-negative HLA-A*0101-positive) were used as a negative control line. VGLL1-CTLs robustly killed the autologous organoid cell line MP015 from which the VGLL1 peptide was originally isolated, and also demonstrated cytotoxic activity against four allogeneic, HLA-A*0101-expressing PDAC cell lines. Results show the means and standard deviations of six replicate samples, and data is representative of a minimum of 4 replicate experiments. **(B)** Western blot analysis confirmed expression of VGLL1 protein in all five PDAC cell lines tested.

HLA-A*0101 surface expression on tumor cells and primary cell lines

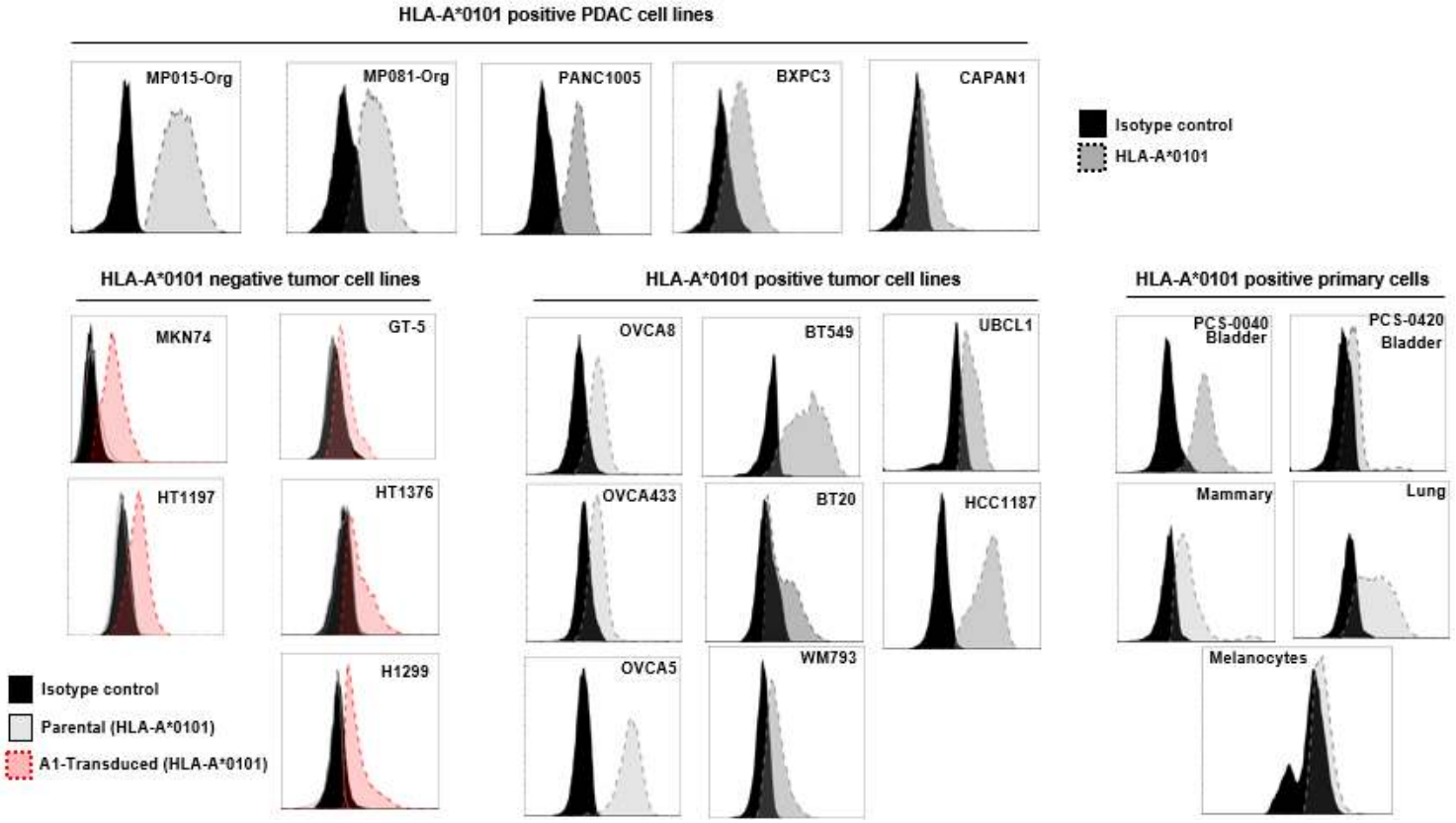

Figure 3.15. HLA-A*0101 surface expression confirmed on target cell lines by flow cytometry.

Figure 3.15. HLA-A*0101 surface expression confirmed on target cell lines by flow cytometry. All tumor cell lines and normal primary cells used in this study were stained with fluorophore-labeled HLA-A*0101-specific mAb and analyzed by flow cytometry to confirm natural endogenous HLA-A*0101 surface expression (grey histograms) prior to use as targets in VGLL1-specific CTL assays. Five tumor cell lines were transduced to express HLA-A*0101 using a lentiviral expression vector (red histograms).

HLA Class I Blockade abrogates VGLL1-CTL recognition of PDAC cell line PANC10.05

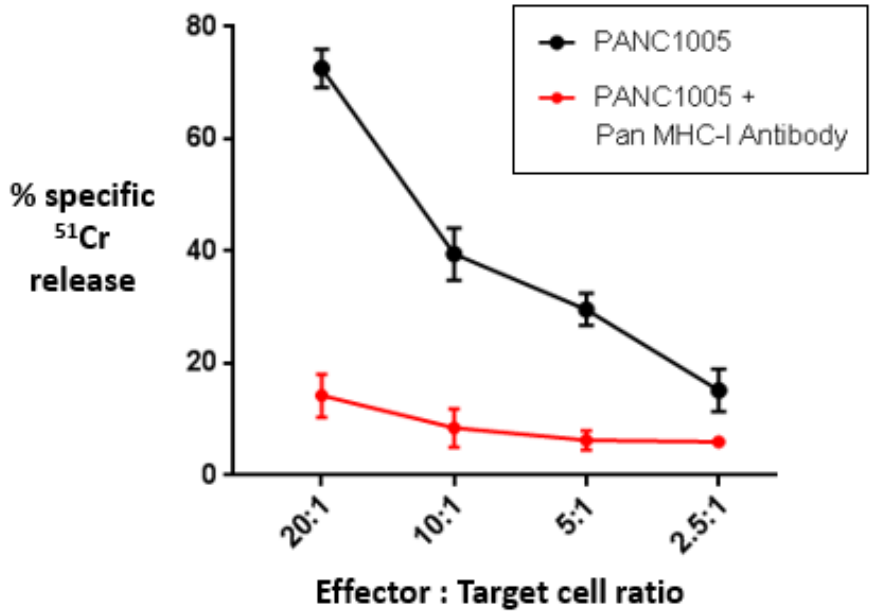

Figure 3.16. VGLL1-CTL killing is blocked with an HLA-class I-specific antibody.

Figure 3.16. VGLL1-CTL killing is blocked with an HLA-class I-specific antibody. Expanded VGLL1-specific CD8+ T cells were co-cultured with HLA-A*0101-positive PDAC tumor cell line PNAC-1005 in a standard ^{51}Cr release assay to measure cytotoxic activity at different effector-to-target (E:T) cell ratios. Addition of the HLA class I blocking antibody W6/32 largely abrogates VGLL1-CTL killing, demonstrating that antitumor activity is HLA class I-restricted.

3.3.c) VGLL1-CTLs show activity against multiple tumor types and reduced recognition of primary cells

TCGA patient RNAseq data analysis indicated that VGLL1 is expressed by several cancer types (16 of 31), most notably in 75 - 80% of patients with bladder, ovarian, and basal-type breast cancers, and 15 - 20% of patients with lung and gastric cancers (**Figure 3.4**). We therefore set out to determine whether cell lines derived from these cancer types could be targets for VGLL1-specific CTLs (**Figure 3.17A**). Western blot analysis of a panel of ovarian, basal-type breast, bladder, gastric, and lung cancer cell lines showed high VGLL1 expression in 12 of 14 lines analyzed (**Figure 3.17B**). Of the 8 cell lines that naturally expressed HLA-A*0101, VGLL1-CTLs killed 2 of 3 ovarian lines, 2 of 3 breast lines, and 2 of 2 bladder and lung cancer lines (**Figure 3.17A**). Five additional HLA-A*0101-negative cell lines (2 gastric, 2 bladder, and 1 lung line) were transduced to express HLA-A*0101 prior to testing them as targets for VGLL1-CTLs. As shown in Figure 6A, all five HLA-A*0101-transduced cell lines were rendered susceptible to killing by VGLL1-CTLs, indicating presentation of the LSELETPGKY peptide from processed, endogenously-expressed VGLL1 protein. Taken together, these results suggest that VGLL1-CTLs have potential therapeutic value for at least five additional cancer types besides PDAC.

To assess the safety of VGLL1-CTLs for potential therapeutic use, we tested them against a panel of normal primary cells most likely to elicit VGLL1-specific reactivity according to the GTex normal tissue expression profile. Since bladder demonstrated the highest normal tissue *VGLL1* transcript expression, we tested two different HLA-A*0101 positive primary bladder cell lines as targets for VGLL1-CTL killing. As shown in **Figure 13.8C**, specific lysis was very low, detectable in one bladder line but only at the highest E:T

ratio. The GTex database indicated that VGLL1 transcript is also expressed at low levels in normal breast and lung (**Figure. 3.3A**). We therefore tested VGLL1-CTL killing activity against HLA-A*0101-expressing primary mammary and lung airway cells, along with primary melanocytes as a negative control. Of this panel, mammary cells elicited moderately high levels of killing by VGLL1-specific CTL, results that were consistent with VGLL1 levels as assessed by Western blot (**Figure 3.17D**). By contrast, lung airway epithelial cells were not killed by VGLL1-CTLs, despite demonstrating ample HLA-A*0101 surface expression (**Figure 3.15**). These results provide supporting evidence that VGLL1-specific T cells are unlikely to recognize any essential normal tissues; however, safety concerns may be warranted due to the potential for reactivity against some non-essential tissues.

VGLL1-CTLs kill cell lines derived from multiple cancers but show reduced recognition of normal primary cell lines

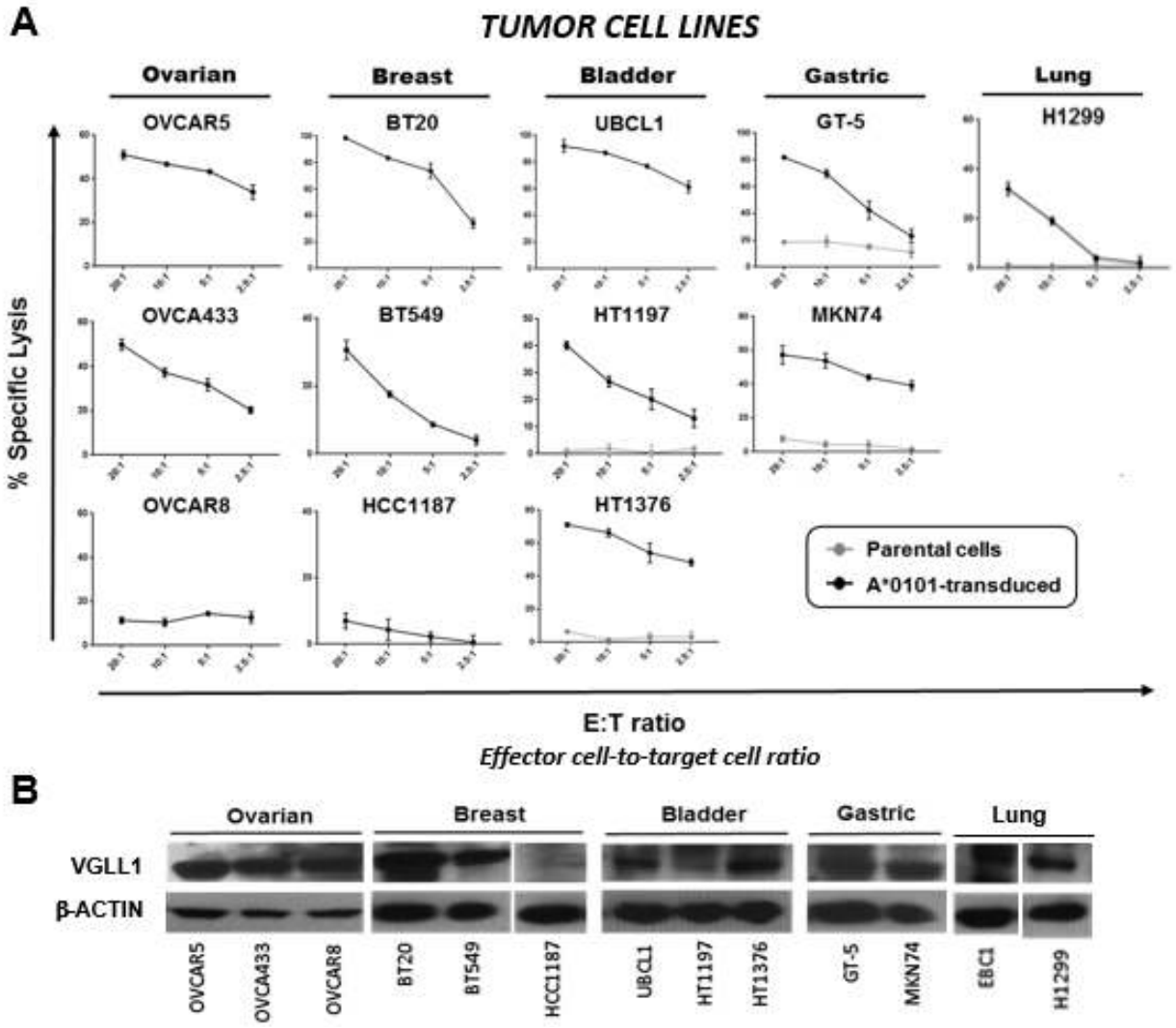

Figure 3.17 VGLL1-specific T cells recognize and kill multiple tumor types, but have reduced recognition of primary tissue cell lines.

VGLL1-CTLs kill cell lines derived from multiple cancers but show reduced recognition of normal primary cell lines

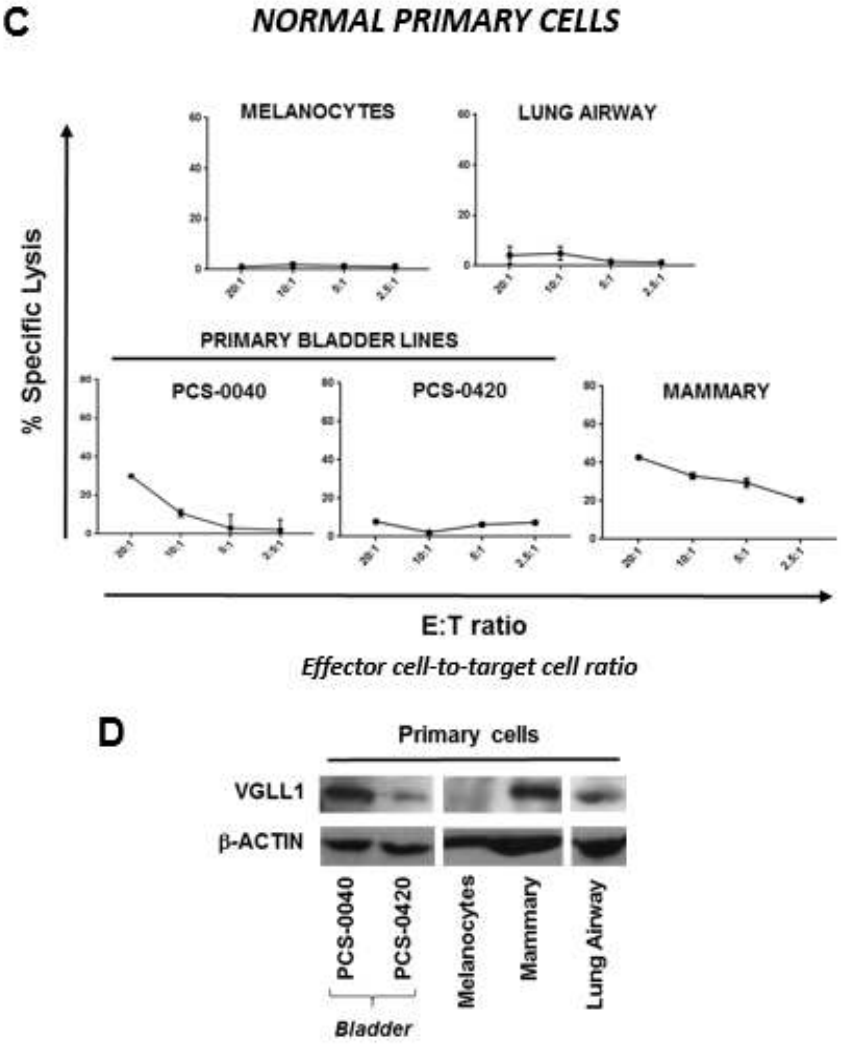

Figure 3.17 VGLL1-specific T cells recognize and kill multiple tumor types, but have reduced recognition of primary tissue cell lines.

Figure 3.17. VGLL1-specific T cells recognize and kill multiple tumor types, but have reduced recognition of primary tissue cell lines. (A) VGLL1-specific CD8+ T cells were co-cultured with 12 different HLA-A*0101-expressing tumor cell lines derived from ovarian, lung, breast, bladder, or gastric cancer in a standard ^{51}Cr release assay to measure cytotoxic activity at different effector-to-target (E:T) cell ratios. Five HLA-A*0101-negative cell lines (EBC1, HT1197, HT1376, GT-5, and MKN74) were lentivirally transduced to stably express HLA-A*0101; VGLL1-CTL killing of the parental cell lines (grey lines) are shown in comparison to HLA-A*0101-transduced counterparts (black lines). **(B)** Western blot analysis confirmed VGLL1 protein expression in 11 of 12 tumor cell lines derived from ovarian, lung, breast, bladder or gastric cancer. **(C)** VGLL1-specific CTLs were co-cultured with HLA-A*0101-expressing primary tissue cells derived from bladder, breast, kidney, lung airway, or skin melanocytes in a standard ^{51}Cr release assay to measure cytotoxic activity. VGLL1-CTL assay results show the means and standard deviations of six replicate samples, and data is representative of a minimum of 2 replicate experiments. **(D)** VGLL1 protein expression in primary cell lines, as accessed by Western blot analysis.

3.3d.) Discussion

The benefits of immunotherapy have been slow to translate to PDAC, likely due to the relatively low mutational burden, highly suppressive tumor microenvironment, and a lack of known TAA targets for CTL therapies [159], [151]. Oncogenic driver mutations in KRAS represent particularly promising target epitopes due to their tumor specificity and high prevalence in PDAC, colorectal cancer (CRC), and lung cancer. In an exciting recent case study, CTLs expanded from TIL of a CRC patient specifically recognized an HLA-C*0802-restricted KRAS peptide containing the G12D mutation; furthermore, these TIL were shown to mediate an objective tumor regression of multiple lung metastases in the patient following infusion [147]. While highly promising, the low worldwide prevalence of HLA-C*0802 predicts that only ~1.5% of PDAC patients could benefit from targeting this mutated epitope. TCRs recognizing mutated KRAS epitopes restricted to HLA-A*1101 have also been reported; although not yet tested in clinical trials, the relatively high prevalence of A*1101 predicts a significantly larger potential patient population that would be centered largely in Asia [160]. The lack of shared mutations beyond KRAS suggests that identification and targeting of non-mutated TAAs may represent the most promising opportunity for advancing immunotherapies for PDAC. Two well-studied TAAs for PDAC and ovarian cancer, MUC16 and MSLN, illustrate the two principal challenges of targeting non-mutated TAAs: difficulty in breaking T-cell tolerance and, conversely, the potential for induction of on-target off-tumor toxicities. Based on low overall normal tissue and relatively high tumor expression, MUC16 appears to be an ideal TAA; however, isolating high affinity CTLs that recognize non-mutated MUC16 epitopes has proven elusive [120], [121]. This lack of immunogenicity may be attributed to tolerogenic attributes of MUC16: being detectable at low levels in

healthy patient serum, and also being a very large protein (>22,000 AA) containing >50 extracellular tandem repeat domains [122].

Employing an unbiased immunopeptidome analysis of tumor specimens derived from 35 PDAC patients, VGLL1 was identified as a novel putative shared TAA, ranked second only to MUC16 in terms of tumor overexpression in comparison to essential normal tissues. However, in contrast to MUC16 epitopes, the HLA-A*0101 restricted VGLL1 peptide was considerably more immunogenic, capable of eliciting antigen-specific CTLs from multiple PBMC donors, including one PDAC patient. Such immunogenicity provides a significant advantage in the context of developing endogenous T-cell (ETC) therapies for cancer patients. HLA-A*0101 is expressed at a relatively high prevalence (25 to 30%) in Western European and North American countries, suggesting that these patient populations would be most likely to benefit from targeting this epitope [161]. Expanded VGLL1-specific CTLs not only recognized and killed a panel of allogenic PDAC tumor lines, but also demonstrated reactivity against A*0101-expressing tumor cells derived from five other cancer types. We estimate that targeting this single VGLL1 epitope could potentially benefit a large number of Western cancer patients, including over 20% of patients with ovarian, bladder, or basal-like breast cancers, ~12% of patients with PDAC, and 5 - 10% of patients with lung, stomach, cervical, uterine, or head and neck cancers.

Higher VGLL1 expression has been associated with shorter patient survival in multiple cancer types, including triple-negative breast and endometrial cancers [154], [162]. However, its negative impact on survival is most striking in PDAC (**Figures 3.5 and 3.6**), suggesting that VGLL1 may play a role in driving tumor aggressiveness. VGLL1 is a co-

transcriptional activator and a marker of proliferating cytotrophoblasts during early human placental development where it is co-expressed with the transcription factor TEAD4 [156], [163].

The discovery of VGLL1 prompted us to search for other putative CPAs that demonstrated overexpression in placenta and tumors, and thus may constitute potential TAA targets. This search uncovered Placenta-specific 1 (PLAC1), initially identified as a target of autologous humoral immunity in gastric cancer and hepatocellular carcinoma patients, and the first CPA reported to represent a class of TAAs distinct from CTAs and oncofetal antigens [164], [165]. A TCR recognizing an HLA-A*0201-restricted peptide derived from PLAC1 was recently isolated and shown to possess antitumor activity against human breast cancer cells in pre-clinical models, but have not yet been tested in clinical trials [166]. As shown in Figure 3, *PLAC1* shows low normal tissue expression, but also demonstrates low overall prevalence in cancer. By contrast, Insulin-Like Growth Factor 2 mRNA Binding Protein 3 (IGF2BP3) was also identified as a promising CPA in our screen, showing relatively high prevalence of expression in ~15 different cancer types, including glioblastoma, uterine, testicular, and lung cancers (**Figure 3.7**). The high level of *IGF2BP3* expression in normal testis, transformed lymphocytes and transformed fibroblasts suggests that this protein may also play a role in driving cancer progression, consistent with its identification as a poor prognostic factor [167], [168]. Unfortunately, IGF2BP3 shows a significant degree of amino acid identity with IGF2BP2, which is expressed at elevated levels in several essential normal tissues, thus limiting the number of safely targetable epitopes. Of the 10 putative CPAs identified, matrix metallopeptidase 11 (*MMP11*) showed the most striking expression and prevalence, being expressed at high transcript levels in 25 different cancer types (**Figure 3.8**). However, in addition to normal placenta, *MMP11* is also

expressed at relatively high levels in uterus, cervix, and ovary, suggesting that CTL-based targeting of MMP11 epitopes may result in reproductive toxicities for women.

In terms of safety profile, cancer prevalence, and immunogenicity, VGLL1 compares favorably with other known TAA targets. Moreover, one male PDAC patient treated with autologous, high-affinity VGLL1-specific CTLs experienced no apparent autoimmune toxicities, providing evidence that VGLL1 can be safely targeted *in vivo*. However, *in vitro* testing did show significant VGLL1-CTL reactivity against cultured primary mammary cells, suggesting that gender-specific safety considerations should be taken into account when targeting CPAs. Immediate clinical applications of these findings include a planned clinical trial to treat HLA-A*0101^{+}/VGLL1^{+} PDAC patients with VGLL1-specific ETC therapy, with future cohorts to potentially include bladder, ovarian, and/or breast cancer patients. VGLL1-specific TCRs derived from Patient MP015 have been cloned and are currently undergoing validation for future potential clinical applications, including TCR-T cell therapies. MS-based identification of additional VGLL1 epitopes restricted to other HLA allotypes is also ongoing, with the promise of expanding the number of treatment-eligible cancer patients [79]. Although single antigen-based CTL targeting can demonstrate limited clinical utility due to selection of antigen-loss variants, tumor debulking and subsequent epitope spreading constitute important aspects of immunotherapeutic success, processes that may be further augmented when combined with other modalities such as checkpoint blockade [137],[138]. Collectively, our study shows that VGLL1 is a promising TAA target that can be used in immune-based therapies to address a clear unmet need in patients with PDAC and multiple other cancers.

CHAPTER IV:

CHARACTERIZING THE ROLE OF VGLL1 IN CANCER PROGRESSION

4.1.) VGLL1 is an important regulator of placental growth during embryo development and is associated with poor prognosis for pancreatic cancer patients.

Through examining the immunopeptidome of pancreatic cancer, we identified VGLL1, as a novel cancer placenta antigen shared by multiple cancer types. However, the role of VGLL1 in cancer progression remains to be elucidated. In total, there are only 15 peer-reviewed publications on VGLL1, and only a subset of these address the role of VGLL1 in cancer. However, we can gleam some insights into its role from studies on primary tissues, since tumors often "hijack" normal functions of cells to benefit their growth and survival. In other words, by studying the role of VGLL1 in primary tissues, we may be able to infer what role it could play in cancer progression.

As previously discussed in chapter 3, VGLL1 is a co-transcriptional activator and an important regulator of the proliferation of cytotrophoblasts during early human placental development. VGLL1 is co-expressed with the transcription factor TEAD4 in the hippo pathway [156], [163]. The hippo-signaling pathway controls organ size, tissue hemostasis, and regeneration [169]. The Human Protein Atlas (http://www.proteinatlas.org) contains IHC staining of placenta tissues, in which VGLL1 is most highly expressed (>200TPM), mostly in the leading edge of the tissues **(Figure 4.1**). The outer edge of the placenta is where cytotrophoblasts are found. Cytotrophoblasts are both highly proliferative and extremely invasive. There are two forms of villous cytotrophoblast stem cells [170]. One form of cytotrophoblasts are the cells responsible for invading the mother's tissue to help the placenta implant into the uterus [171]. The other form of trophoblasts spread to the arteries of the mother and bore into the vessels to create the blood flow connection between the mother and fetus during pregnancy [172].

Due to the known invasive VGLL1-expressing cytotrophoblasts, the expression of VGLL1 in tumor cells may and contribute to the aggressiveness of cancer. As shown in chapter 3, pancreatic cancer patients with elevated levels of VGLL1 had the shortest overall survival (**Figure 3.5**). Additionally, the most aggressive breast cancer subtype, basal-like breast cancer, possesses the highest expression of VGLL1 out of all breast cancer types (**Figure 3.6**).

These two cancers are highly metastatic, and known to spread quickly to neighboring tissues [173]. Suggesting that VGLL1 expression may play a role in tumor metastasis. Furthermore, there appears to be a strong homology VGLL1 with the well established oncogenes YAP and TAZ within in the hippo pathway. In the next section, we will explore how the oncogenes YAP/TAZ may provide a blueprint to understand the role of VGLL1 in cancer progression.

Cytothrophoblasts express VGLL1 in placenta tissue

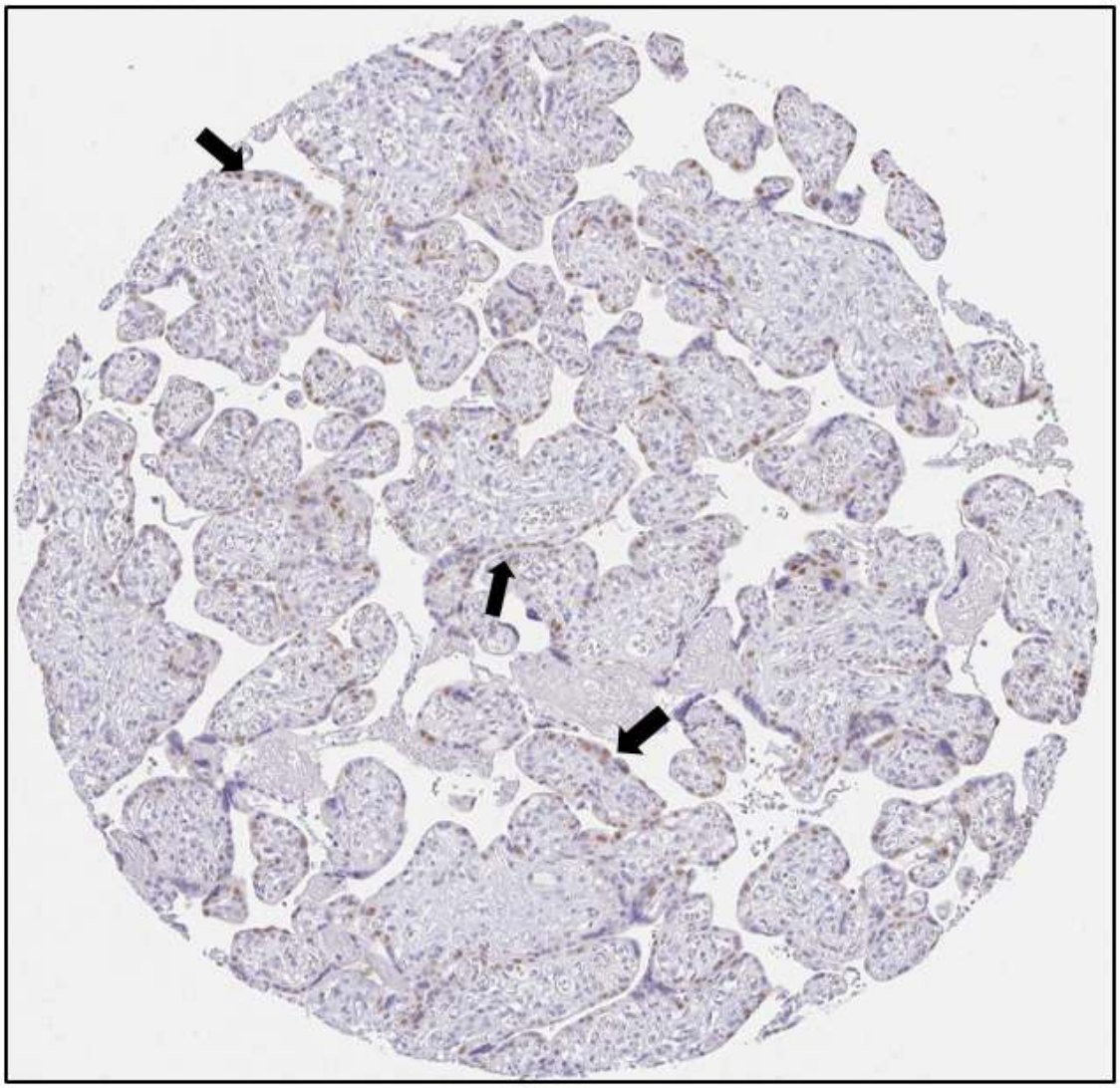

Figure 4.1 IHC staining of placenta tissue from the Human Protein Atlas database.

https://www.proteinatlas.org/ENSG00000102243-VGLL1/tissue/placenta#img

Figure 4.1 IHC staining of placenta tissue from the Human Protein Atlas. VGLL1 is expressed in the outer edge of the cells in placenta tissue by IHC staining. These VGLL1-positive cells are cytothrophoblasts.

4.2.) VGLL1 shares similar binding motif to TEADs with the oncogenes YAP/TAZ in the hippo pathway.

The Hippo signaling pathway is a highly conserved intracellular-signaling network that regulates cell proliferation, organ size, and regeneration [169]. The Hippo signaling pathway is co-opted in multiple cancers to drive tumor progression [174], [175]. Two well-characterized oncogenes, YAP1 (Yes associated protein 1) and TAZ/WWTR1 (WW Domain Containing Transcription Regulator 1), function as co-transcriptional activators of the Hippo signaling pathway, and in cancers they, also bind to TEAD proteins, leading to the upregulation of several cancer-promoting genes (**Figure 4.3**) [152], [176], [177]. It is important to note that YAP and TAZ are two distinct proteins, but are often referenced together because they share mostly redundant functions within the Hippo signaling pathway [178].

YAP is over-expressed in pancreatic cancer and has been linked to promoting factors such as tumorigenesis and chemoresistance (**Figure 4.2**). YAP has also been shown to promote EMT transition in pancreatic cancer, increasing cell motility, invasion, and tumorigenesis through hyperactivation of AKT signaling [176, 179, 180]. Additionally, YAP/TAZ were identified as partners to mutant KRAS in pancreatic cancer [169]. *In vivo* experimental models show that YAP/TAZ act as transcriptional activators downstream of KRAS, resulting in the upregulation of genes that promote proliferation and invasiveness [181]. These two genes have been well characterized in multiple cancers as also being associated with pro-inflammatory responses, migration, and immune evasion [182-184]. The interaction of YAP/TAZ with TEADs was shown to induce PD-L1 upregulation and inhibited T cell function when overexpressed in breast epithelial cells [185].

Oncogenes YAP/TAZ role in the Hippo signaling pathway in pancreatic cancer

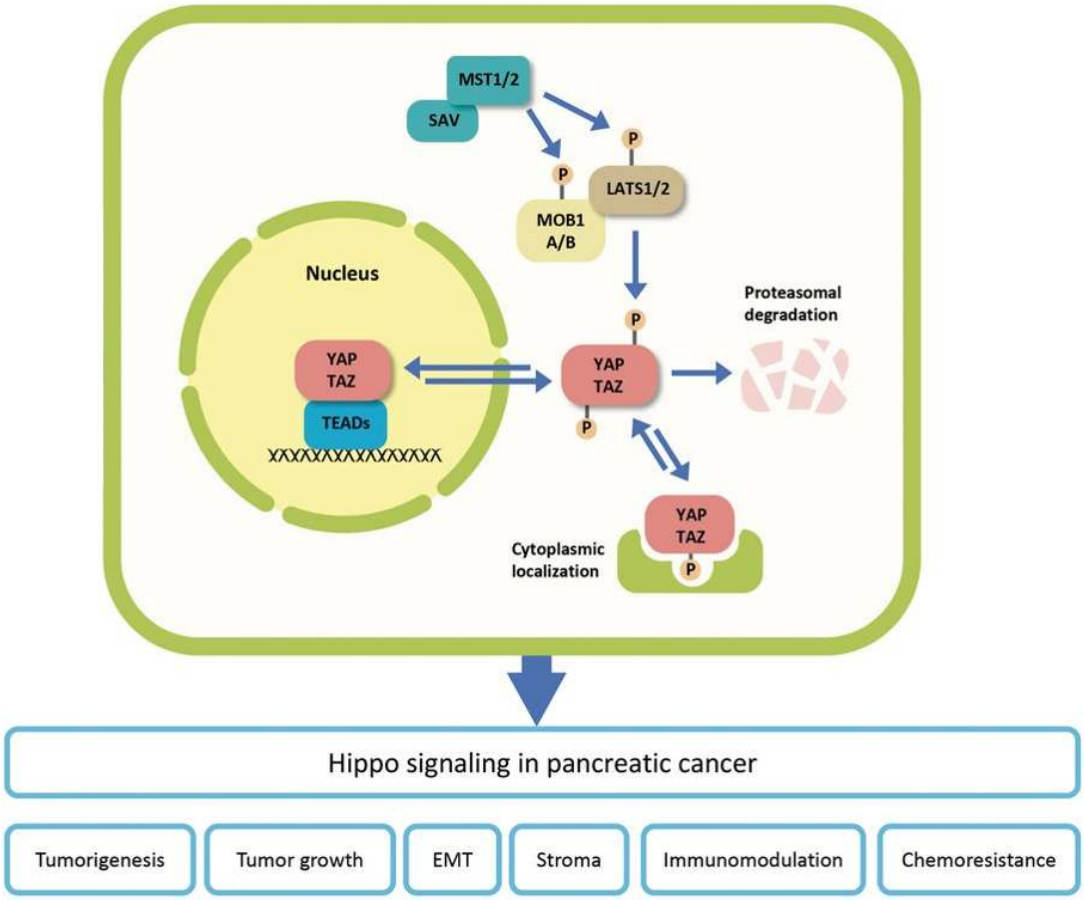

Figure 4.2 The Hippo signal pathway in pancreatic cancer.

Figure used with premission from author:

Ansari D, Ohlsson H, Althini C, Bauden M, Zhou Q, Hu D, Andersson R: **The Hippo Signaling Pathway in Pancreatic Cancer**. *Anticancer Res* 2019, **39**(7):3317-3321.

Figure 4.2 The Hippo signal pathway in pancreatic cancer. Upstream signaling in the hippo pathway results in the phosphorylation of YAP, and its co-activator (TAZ). When YAP and TAZ are held in the cytoplasm, they are degraded to prevent their entry into the nucleus. In the nucleus, they bind to TEADs 1-4, and are responsible for the upregulation of genes involved in proliferation. However, aberrant signaling of the hippo pathway in pancreatic cancer is associated with cancer promoting factors**.**

VGLL1 has been shown to interact with TEAD4 in a manner similar to that of YAP/TAZ, resulting in the upregulation of the proliferation-promoting gene IGFBP5 and facilitating anchorage-independent cell growth (**Figure 4.3**) [163]. These studies suggest that VGLL1 may promote cancer progression directly, which would increase its potential value as a therapeutic target. Although the *VGLL1* transcript loss observed in Patient MP015 could argue against a role as an essential driver gene, the degree of tumor evolution documented in this patient's cancer progression was exceptionally high [158].

The function of VGLL1 in healthy tissues, points to a critical role in placenta cell proliferation. In addition, (**Figure 3.5)**, high VGLL1 expression in pancreatic and basal-like breast cancer patients is associated with a poorer prognosis [154]. Furthermore, cancer cells are known to co-opt the Hippo signaling pathway and upregulate YAP/TAZ to increase tumor- promoting factors. Based on the current evidence on YAP/TAZ within the Hippo signaling pathway and the connection with VGLL1, we hypothesized that VGLL1 may play a role in cancer tumorigenesis through promoting proliferation, migration, and/or invasion. In the following section, we will discuss how we aimed to test our hypothesis and demonstrate why VGLL1 is a promising therapeutic target in pancreatic cancer.

VGLL1 shares similar interaction with TEADs as the oncogenes YAP/TAZ

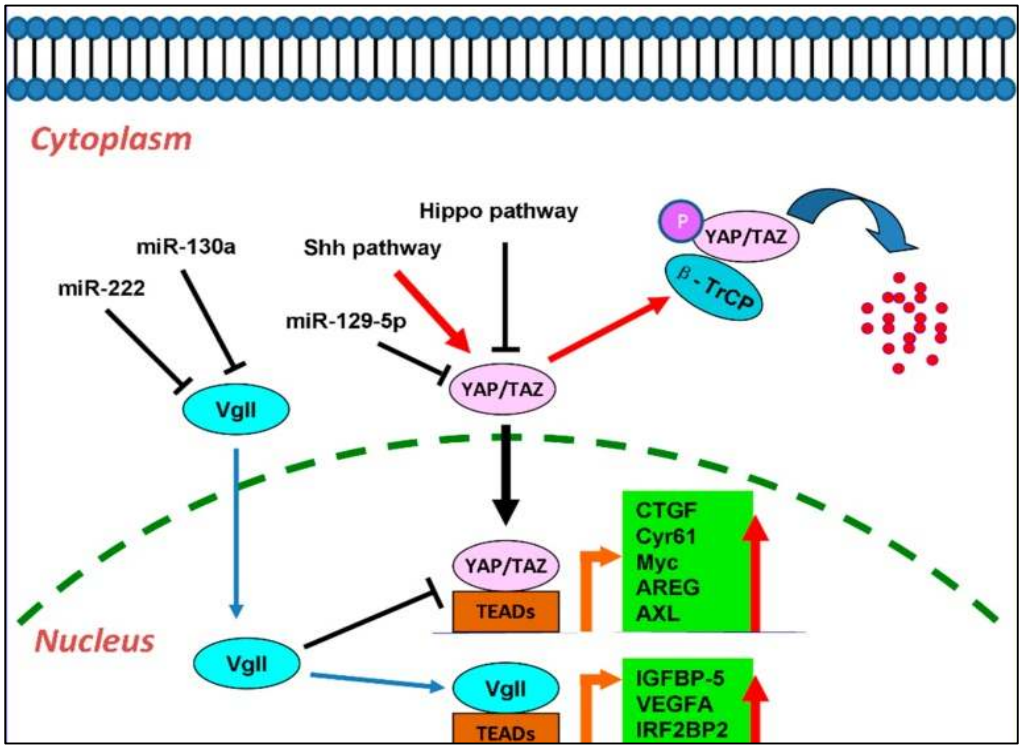

Figure 4.3 VGLL1 and YAP/TAZ share similar interaction with TEADs in the hippo pathway.

Figure used with premission from author:

Pobbati AV, Chan SW, Lee I, Song H, Hong W: **Structural and functional similarity between the Vgll1-TEAD and the YAP-TEAD complexes**. *Structure* 2012, **20**(7):1135-1140.

Figure 4.3 VGLL1 and YAP/TAZ share similar interaction with TEADs in the hippo pathway. The well-established YAP/TAZ oncogenes bind to TEADs in cancer cells to activate cancer-promoting factors. VGLL1 appears to also bind to the TEADs and perform a similar function, by upregulating genes that are also known to promote cancer progression such as; VEGF-A and the anchorage-independent growth factor IGFBP-5.

4.3.) VGLL1 overexpression leads to increased proliferation, migration, and invasion of cancer cells *in vitro*.

To access any potential changes that VGLL1 expression may induce in tumors, we first generated two VGLL1-overexpressing lines. VGLL1 lenti-viral vectors were used to transduce tumor cells that did not express VGLL1, as assessed by western blot. We utilized the cell lines PANC1, a pancreatic tumor cell line, and H1975, a lung cancer line. The cells were transduced to express VGLL1, and VGLL1 protein expression was validated by Western blot analysis, as shown in **Figure 4.4A**. PANC10.05, a naturally-expressing VGLL1-postive cell line was used as a positive control. We next generated transient knockdowns of the VGLL1 transduced H1975 lung cancer cells. To create the transient knockdowns, we used esiRNA vectors (MISSION® esiRNA Cat. #EHU042561); this allowed for increased chances of knocking down VGLL1 expression to a greater degree than standard siRNA. Mission esiRNA works by targeting the same mRNA sequence with multiple siRNAs, and thus guarantees at least a 70% knockdown efficiency. We confirmed reduced VGLL1 expression in the knockdown cells by Western blot analysis (**Figure 4.4B**).

Following the validation of the VGLL1- transduced cell lines, we proceeded to observe morphological changes in the cells. Evident growth and phenotypic differences were found in the H1975 cell lines post-VGLL1 transduction. Cells were plated and analyzed using microcopy at 24, 48, 72, and 96 hours. As shown in **Figure 4.5** at the 72hr mark, VGLL1 over-expressing H1975 lung tumor cells had formed multiple clusters despite growing in a 2D culture (**Figure 4.5C**). The clusters resembled similar growth patterns to 3D spherical organoid cell culture, similar to the MP015 organoid cell line from which the VGLL1 peptide was derived.

This may indicate ability of VGLL1 to induce growth in an anchorage-independent matter [186, 187], which is also an indication of metastatic potential [186]. The colonies were alive; some were attached to the flask and some were floating in the supernatant. However, once they were collected and re-plated, all cells survived and continued to grow and expand in a similar matter. Knocking down VGLL1 in the overexpressed lung cancer cells returned the cells to a similar phenotype of parental H1975 cells and GFP-transduced control cells (**Figure 4.5D**).

Simultaneously we counted the H1975 tumor cells to assess proliferation counts. On day one, we plated 30,000 cells in triplicates, and the cells were observed at 24, 48, 72, and 96hr mark, using a Nexcelom cellometer (**Figure 4.6**). As expected, the VGLL1 overexpressed cells proliferated faster than the WT VGLL1-negative cells, $P > 0.001$ (**Figure 4.6**). Additionally, the VGLL1 knockdown cells grew similarly to the parental line (**Figure 4.6**). We failed to reject our hypothesis that VGLL1 plays a role in tumor cell proliferation. The upregulation of VGLL1 may be used by tumor cells to promote growth.

The few papers that have been published on VGLL1 hint at its potential role in tumor cell migration and invasion. Migration and invasion differ from one another, in that migration refers only to a cell's ability to fill-in an area or move from one point to another [188]. Invasion defers from migration; in that it looks at the ability to migrate coupled with the cell's ability to move past an extracellular matrix. We first accessed the ability of PANC1 VGLL1 overexpressing cells migration in comparison to VGLL1-negative cells, by performing a wound healing assay. Cells were plated at 500,000 cells per well in triplicates in the Cytoselet wound healing plates (Cell biolabs, Cat.#CBA-120). Each well contained a pre-placed insert that creates 0.9mm gap for measuring migratory cells. After 24hrs the insert

was removed and migration of the cells were observed for an additional 48hrs. At the 48hr mark, VGLL1 over-expressing cells had nearly filled in the entire wound area (**Figure 4.7A**). While WT and GFP-transduced control PANC1 cells, had migrated at a significantly slower rate (**Figure 4.7A**). By analyzing multiple images and comparing the wound-healing area, we concluded that the VGLL1-expressing cells migrated significantly faster than the other two cell lines, P>0.0001 (**Figure 4.7B**). We also noted again in this assay that VGLL1-transduced cells formed clusters that grew in three dimensions.

Based on the survival data of pancreatic and basal-like breast cancer patients (**Figure 3.5 and 3.6**), we reasoned that VGLL1 may have an effect on the aggressiveness of tumors *in vivo* [154]. We next set out to determine if VGLL1 expression increased the invasiveness of tumor cells *in vitro*. The invasiveness of a cell is determined by its ability to degrade and migrate through an extracellular membrane barrier. We utilized PANC1 VGLL1-overexpressing cells, along with WT parental, and GFP transduced controls cells. The CHEMICON cell invasion kit by Millipore was used to conduct this assay. An invasion chamber, containing a thin layer of an extracellular membrane (ECM) was inserted into a well. The cells were placed inside of the invasion chamber in serum-free media, and RPMI with 10% FBS was placed into the well below. The tumor cells were plated at 50,000 cells per well and allowed to migrate for 48hrs. At the 24 and 48hr mark, cells attached to the ECM were harvested. The invasive cells were stained and dried, following the collection of the chambers, and counted by microscopy. The assay was performed in triplicates, a mean of all invasive cells was derived from total cell counts. As shown, PANC1 VGLL1-expressing cells had significantly more invasive cells than VGLL1 non-expressing PANC1 parental cells (**Figure 4.8A**). Quantification of the total cells counts indicated that VGLL1-expressing

cells demonstrated >10X the number of invasive cells after 48hrs, P >0.0001 (**Figure 4.8B**). This data provides strong evidence that VGLL1 expression can drive tumor cell invasiveness, and is consistent with the poor survival noted in patients with tumors demonstrating high VGLL1 expression.

VGLL1 protein expression in a pancreatic and lung cancer line

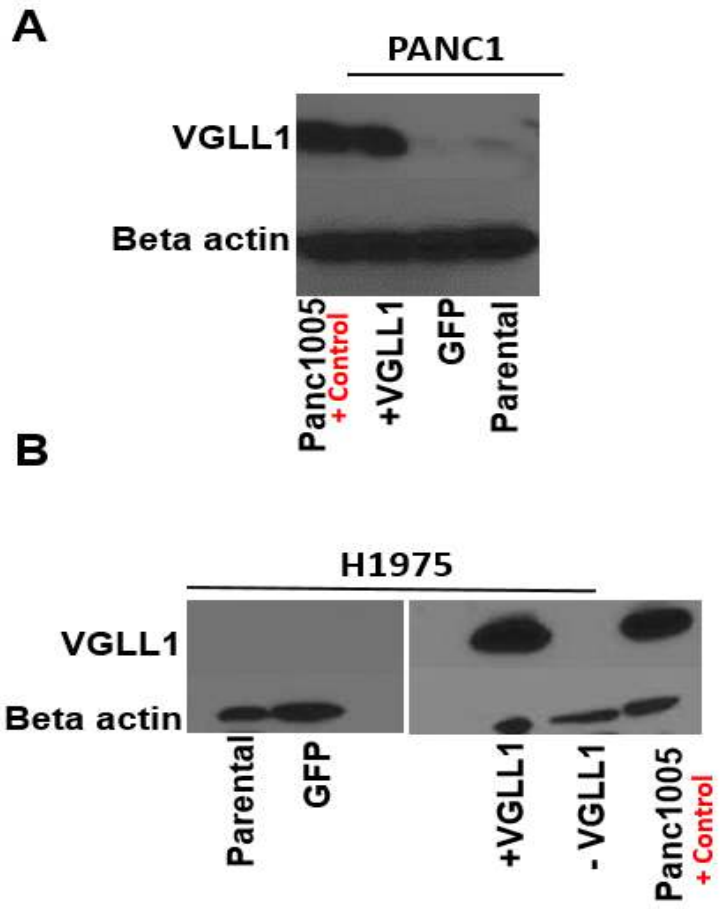

FIGURE 4.4. Transduction of VGLL1 in two negatively expressing cell lines.

Figure 4.4. Transduction of VGLL1 in two negatively expressing cell lines. VGLL1 was transduced in the pancreatic line, (**A**) PANC1 and the lung cancer line, H1975 (**B**). The lung cancer line, H1975 was also knocked down by esiRNA following overexpression.

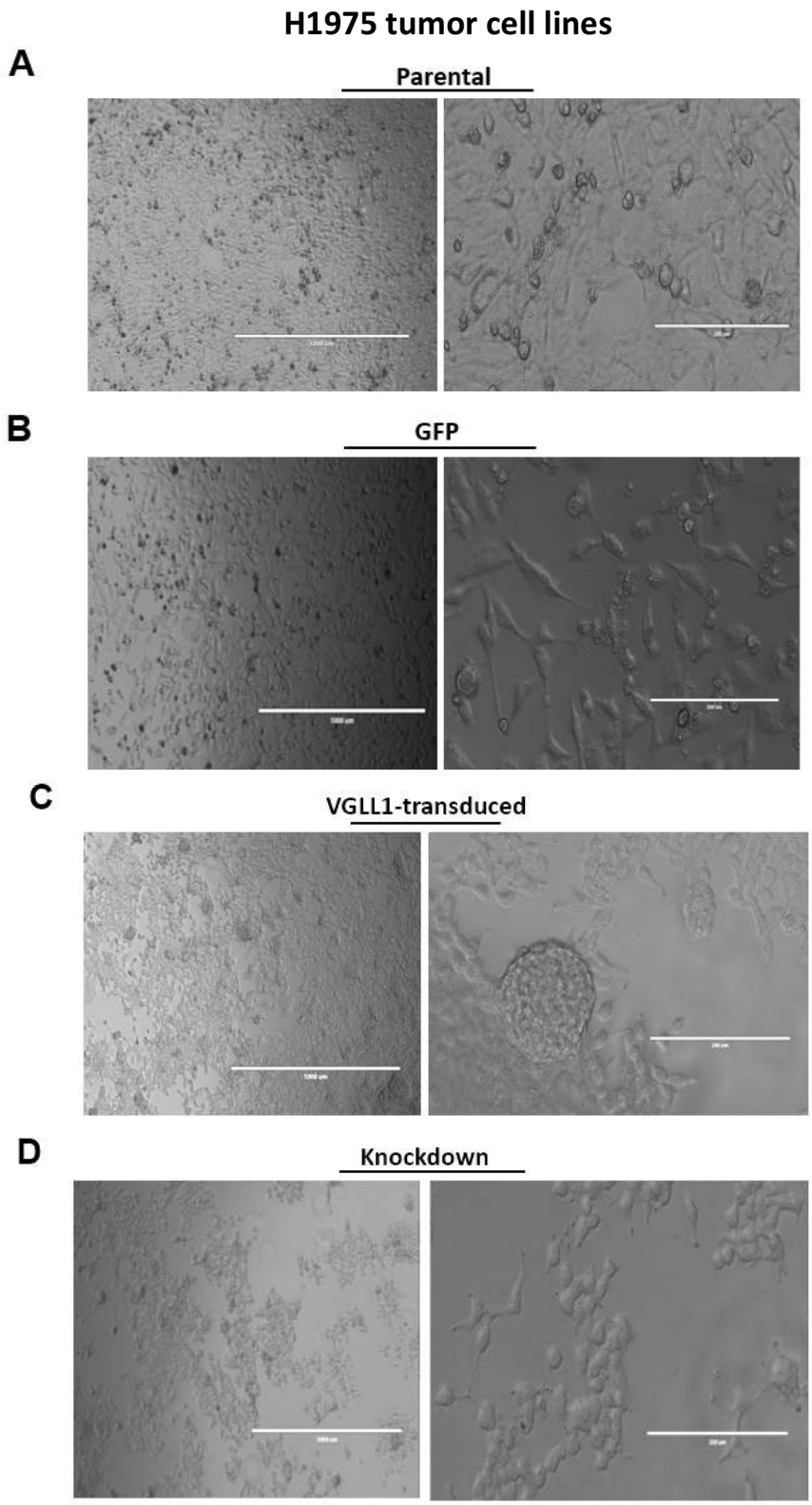

Figure 4.5. VGLL1 induces morphology changes following transduction in lung cancer cells.

Figure 4.5. VGLL1 induces morphology changes following transduction in lung cancer cells. VGLL1 was transduced into H1975 lung cancer cells. At 72hrs, the cells were analyzed by microscopy for morphological changes. (Shown 10X left, 100X right) No differences were seen in PANC1 (**A**) Parental, (**B**) GFP after 72 hrs. Following transduction, (**C**) VGLL1-expressing cells formed spherical colonies that were not observed in the un-transduced WT cell line. (**D**) Knockdown cells retained the same phenotype of the parental and GFP cells.

Proliferation of H195 tumor cells

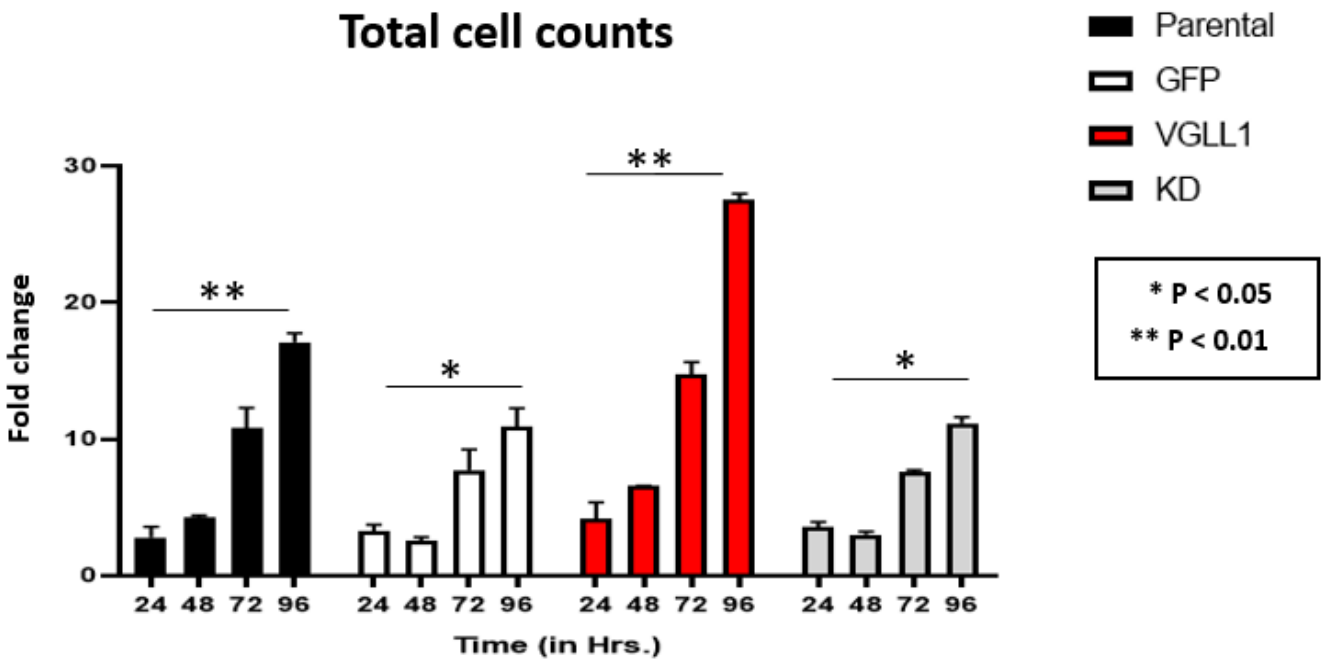

Figure 4.6 Total cell counts of H1975 tumor cells.

Figure 4.6 Total cell counts of H1975 tumor cells. Cells were played in triplicates on day 1 at 30,000 cells per well. Each day, the cells were harvested, counted, and the totals were then averaged. Total cell counts were averaged and compared to day 1 (24hrs) for fold change in GraphPad. Data is shown as mean ± STD *P <0.05 , **P<0.01.

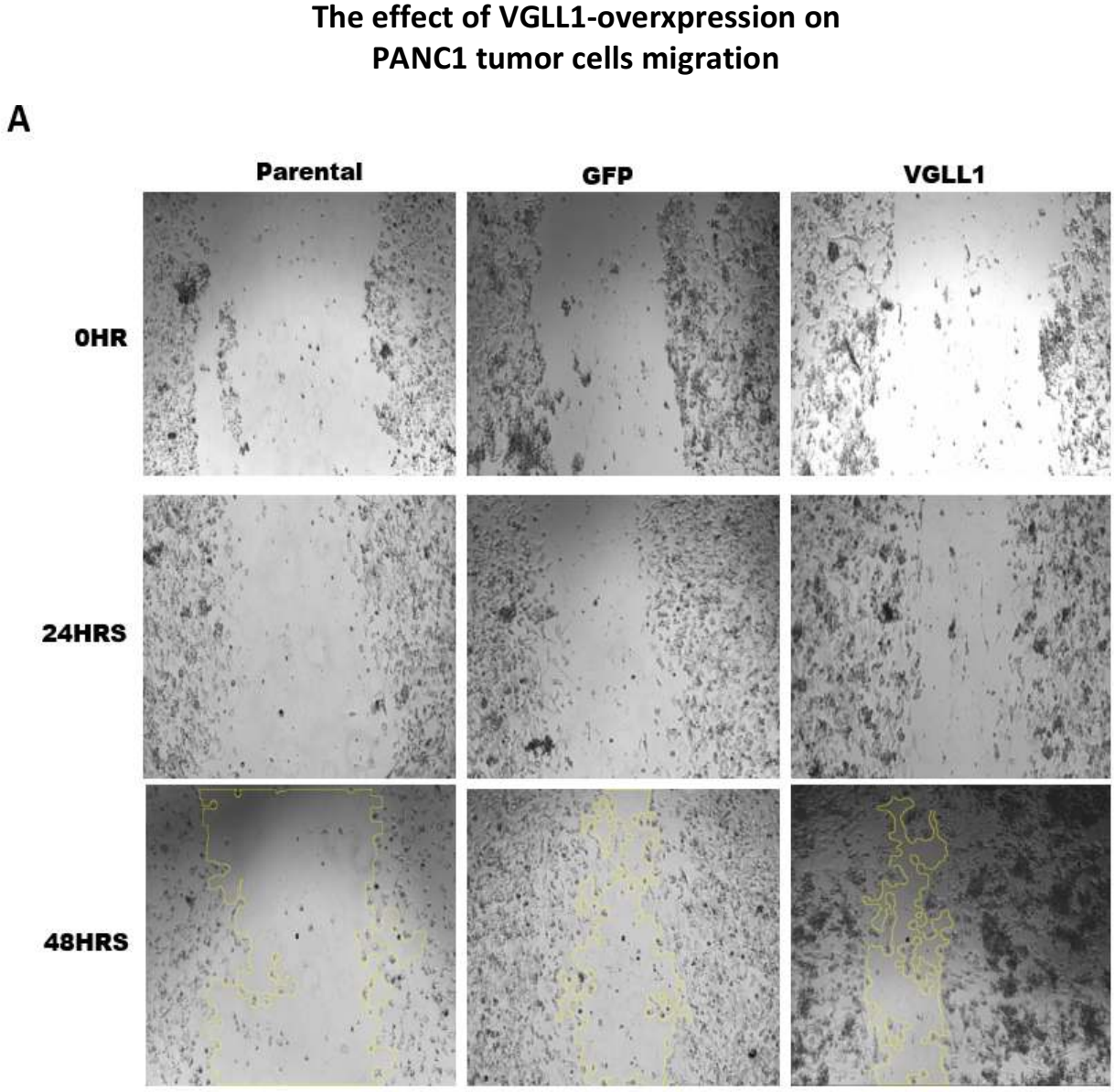

Figure 4.7 VGLL1 increases migration of PANC1 tumor cells following transduction.

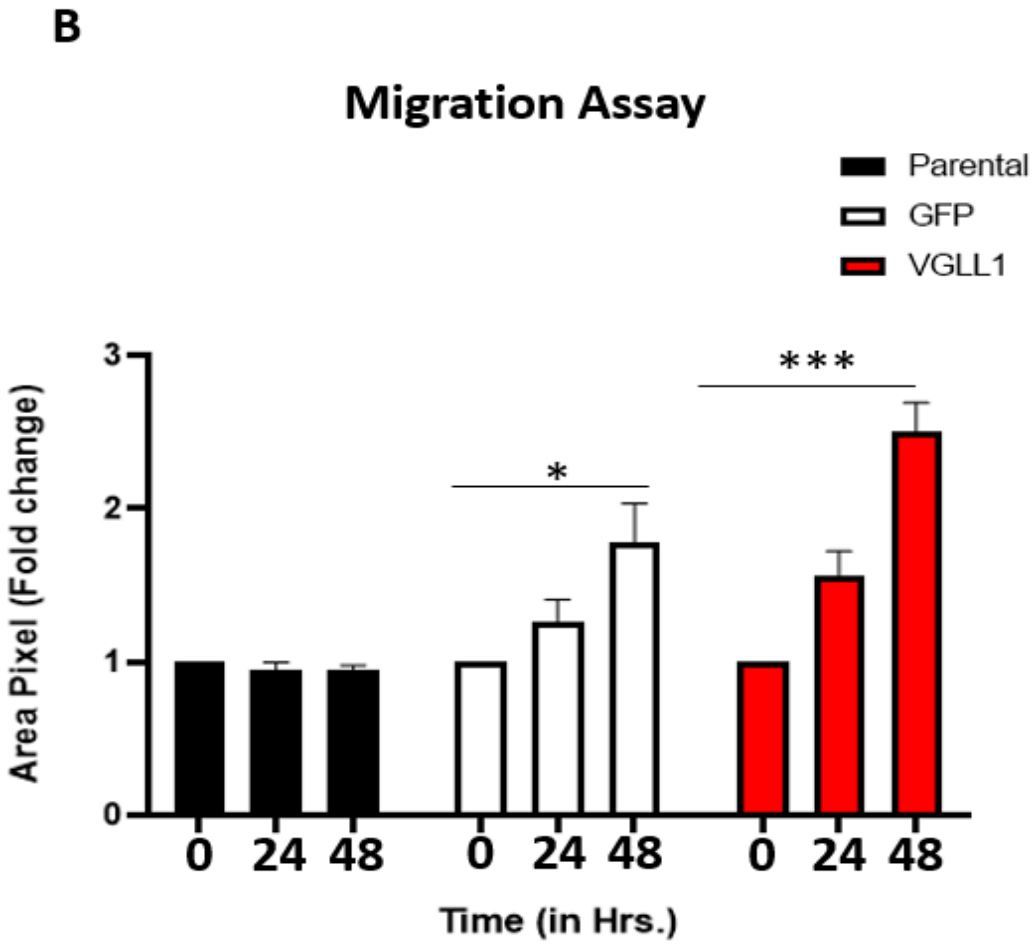

Figure 4.7 VGLL1 increases migration of PANC1 tumor cells following transduction.

Figure 4.7. VGLL1 increases migration of PANC1 tumor cells following transduction. **(A, B)** Representative image of the effect of VGLL1-overpexressing on the migration of PANC1 tumor cells. Cells were plated in triplicates, and the area of the wound was measured for all the fields of each well using Image J. Total migrated cell counts were averaged in GraphPad. Data is shown as mean ± STD *P<0.05 , *** P< 0.001.

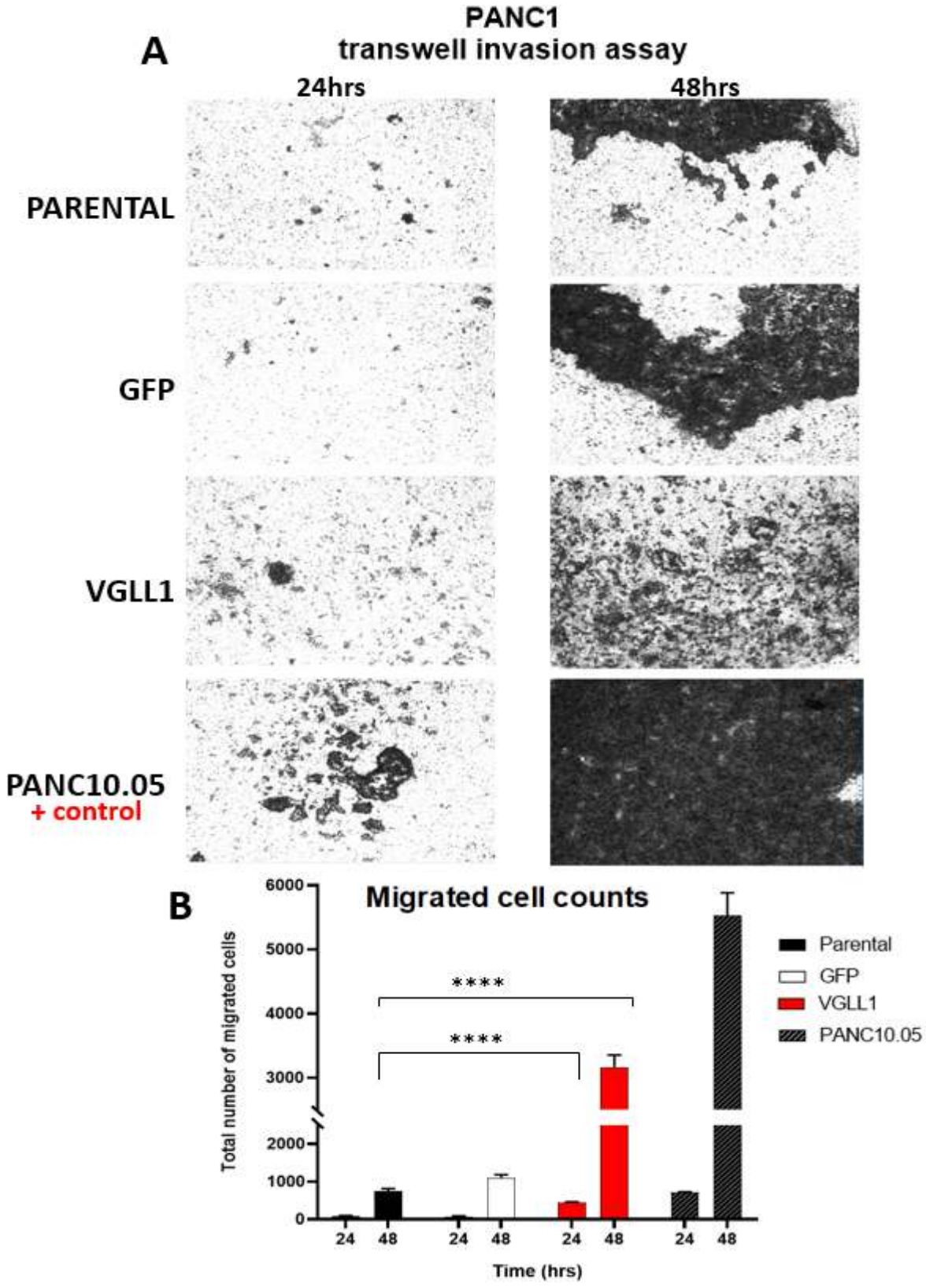

Figure 4.8. VGLL1 Transwell Invasion Assay.

FIGURE 4.8. PANC1 Transwell Invasion Assay. (A) Representative microscopic images of cells that migrated through the extra cellular matrix layer and clung to the bottom of the polycarbonate membrane. Cells were plated on the same day for two time points, 24hr and 48hr at 50,000 cells per well. The cells were harvested at each time point. (**B**) The quantification of the invasive cells was performed using image J for total migrated cells. Data from triplicates was averaged and analyzed by graphpad prism. Data is shown as mean ± STD ****P<0.0001.

4.4.) Discussion

The Hippo signaling pathway plays a critical role in cancer progression through the oncogenes YAP and TAZ [178]. These two genes are co-transcriptional activators to the TEADs within the Hippo signaling pathway. Cancers highjack this pathway and induce the expression of YAP/TAZ to promote downstream target gene expression that promotes the hallmarks of cancer [185]. These include genes involved in tumor cell proliferation, migration, and invasion [169, 179, 185]. Since VGLL1 shares considerable homology to YAP/TAZ, this prompted us to explore VGLL1's potential role in also increasing these 'hallmarks of cancers".

Through these studies, we were able to show that VGLL1 expression induces distinct morphological changes in pancreatic and lung tumor cells. The overexpression of VGLL1 induced both PANC1 and H1975 cells to exhibit aberrant growth patterns, in which cells grew in multiple small clusters with some attached and others detached from the culture plates. Despite being grown in 2D culture in traditional monolayers, the cells appeared to acquire the ability grow more like that of 3D culture cells. This differed significantly from what was observed in the parental and GFP-transduced tumor cells that retained normal growth patterns. This strongly suggests that VGLL1 does have a direct impact on tumor cell growth. VGLL1 can induce anchorage-independent growth in VGLL1-transduced prostate tumor cells [163, 189]. This pattern of growth is a marker used to assess the metastatic potential of tumors [186]. Malignant cells often acquire the ability to detach and continue to grow and proliferate without being attached to a substrate. The next step would be to perform a soft agar colony formation assay with VGLL1- transduced tumor cells. This assay specifically analyzes anchorage-independent growth and will help confirm this phenotype.

We showed that VGLL1 expression increased the proliferation rate of H1975 lung tumor cells (**Figure 4.6**). Furthermore, VGLL1 expression also significantly increased the migration and invasion of PANC1 pancreatic tumor cells (**Figure 4.8**). These results suggest that VGLL1 can induce many of the same phenotypes in tumor cells as YAP/TAZ. Additionally, according to the TCGA, VGLL1 and TAZ are not co-expressed, but rather are mutually exclusive. Since, VGLL1 is thought to compete for binding to the TEADs with YAP/TAZ, it may play a redundant role in cancer. However, more studies remain to be done to elucidate its role in cancer progression.

Moving beyond *in vitro* studies into mouse models will be necessary to answer many remaining questions. Mouse VGLL1 overexpression and knockdown plasmids have been prepared to transduce mouse cell lines. It is also important to note that mouse and human VGLL1 do not totally share overlapping symmetry; they only share 41% homology. The mouse VGLL1 protein sequence is also nearly twice as long the human VGLL1. Therefore, there may be some differences in their functions, but this still needs to be determined. Since human placenta has the highest expression of VGLL1, it will be important to determine if this is also the case in mice. Mouse placenta mRNA sequencing is planned to explore this question. Additionally, RNA sequencing and Nanostring of a panel of human and mouse tumor cell lines will be useful to determine what signaling pathways or genes may be associated with VGLL1 expression. The studies in this dissertation have revealed some intriguing results *in vitro*, but *in vivo* studies could substantially increase the significance of these results. Based on the current findings, VGLL1 appears to play a role in cancer progression similar to YAP/TAZ, but could also perform additional tasks that have yet to be discovered.

CHAPTER V:

OVERALL CONCLUSIONS AND FUTURE DIRECTIONS

V. Overall Conclusions and Future Studies.

5.1 Overall Conclusions

One of the major objectives of this dissertation was to identify a shared, targetable TAA to facilitate the development of a novel T cell based immunotherapy. By utilizing HLA immunoprecipitation, peptide elution, and MS-based tumor antigen discovery, we were successful in achieving our goal. Through our initial efforts working with ovarian tumor specimens, we identified a HLA-B*07:02-restricted MUC16-derived peptide. This MUC16-derived peptide, TPPGTQRSL, appeared to have great potential as a TAA (**Table 2.3**). However, after attempts at T cell generation failed, we opted to stop pursuing this antigen as a target (**Figure 2.9 and 2.10**).

T cell tolerance may be the reason why our efforts to generate T cells against MUC16 were unsuccessful. MUC16 is one of the largest surface glycoproteins at >22,000 amino acids. It also contains many tandem repeats that are shared among other surface mucins. Since MUC16 is primarily found in low abundance in female reproductive tissues, we utilized healthy male donor PBMCs in our attempts to try to isolate MUC16-specific T cells. While we were unsuccessful at expanding MUC16-specific T cells from this one male donor, it is possible that other donors would have given a different outcome. There is evidence that MUC16 peptides can be immunogenic, as shown in other studies [107]. However, cross-reactivity with other self-antigens may still be an issue should MUC16-specific T cell generation be successful in the future.

Since we also were working with pancreatic cancer tumor specimens simultaneously, we identified the novel epitope, LSELETPGKY, derived from the cancer placenta antigen VGLL1 (**Table 3.1**). This peptide was found in a pancreatic-patient derived tumor organoid cell line. This added to the novelty of our finding, because there are only a few established cancer-placenta antigens previously discovered [165]. Thus, VGLL1 is likely the first cancer placenta antigen to be targeted clinically with T cell based immunotherapies.

VGLL1 peptide specific CTLs were generated from this same patient, and expanded to >20 billion cells. This demonstrated that VGLL1 was immunogenic, further adding to its potential as TAA target. These cells were administered to the patient as a treatment, but by the time they received the T cells, the patient had lost tumor VGLL1 transcript expression (**Figure 3.13**). Despite the patient's loss of the VGLL1 gene target, this infusion showed that there were no adverse effects or toxic effects from receiving the VGLL1-specific T cells.

Further work revealed VGLL1 to be a promising shared TAA not just for pancreatic, but for multiple other cancers; including ovarian, bladder, lung, and breast cancers. We showed that VGLL1-specific T cells show minimal recognition of primary cell lines, with the exception of mammary cells. This may be the one area of caution for treatment of patients. However, the infused patient did not experience any apparent toxic off target reactivites, so this may not be a serious issue as our in vitro killing assay would suggest. Since, VGLL1 has now been approved for an MD Anderson clinical trial of ETC we will know soon if toxicities are seen in treated other patients.

The identification of VGLL1 also presented many additional questions pertaining to its role in cancer progression. As previously stated, very few studies have been published on

VGLL1 and most did not directly assess its function in cancer development. VGLL1 has minimal expression in normal tissues, with the exception of the placenta where it is expressed at over 200 TPMs on average (**Figure 4.1**) VGLL1 is expressed in cytothrophoblasts within the placenta, these cells are the responsible for implanting the placenta in the uterus, and forming the critical blood supply from the mother to the fetus [171]. Due to the function and nature of cytothrophoblasts, we speculate that VGLL1 may be involved in driving its high proliferation and invasive behavior.

Additionally, VGLL1 shares a similar binding motif to the well-characterized oncogenes YAP/TAZ, within the Hippo signaling pathway [169, 187]. This signaling pathway is the key regulator of organ size and development [184]. It appears that VGLL1 may compete for binding to the TEAD family of genes with YAP/TAZ. Once either of these genes bind to the TEADs, they act as co-transcriptional activators, inducing the expression of different cancer-promoting genes [174]. YAP/TAZ are linked to pancreatic, lung, and breast cancer progression by promoting factors that increase EMT transition, proliferation, chemoresistance, and immune evasion [169, 185, 190].

VGLL1 was specifically shown to upregulate anchorage-independent proliferation in a prostate cancer cell line following transduction [187]. Anchorage-independent growth is a key trait in cells transitioning into a metastatic state [186]. TAZ induces the migration, invasion, and tumorigenesis of breast cancer cells through the Hippo pathway [182]. Since VGLL1 may share similar characteristics to YAP/TAZ in the Hippo pathway, this led us to explore if VGLL1 expression could also induce a similar phenotype in pancreatic tumor cells. VGLL1 transduction indeed increased proliferation, migration, and invasion of pancreatic tumor cells (**Figure 4.5-4.8**). These provide evidence supporting the idea that

VGLL1 may play a role in driving cancer progression as well. We hypothesize that VGLL1 may be important for tumor cell proliferation and invasion early in tumorigenesis. This hypothesis is partly based on the observation of the pancreatic patient losing VGLL1 expression overtime, despite having high expression early on. We believe that VGLL1 may not be an essential driver in cancer, but rather an initiator, or potentially a stress dependent response. We observed in that cells that became close to 100% confluent in culture experienced a period of "crashing", and slow recovery after being re-plated. However, after that initial period they proliferated quickly again and became confluent. We think this may be due to VGLL1 expression being turned on only when it is needed for migration, but when cells begin to come in close contact, VGLL1 is downregulated to halt the growth of the tumor cells. This mechanism could be used by tumors to slow growth when space and resources become scarce, such as in low-nutrient environments. VGLL1-signaling in the Hippo pathway may be downregulated and other pathways may be upregulated to support the tumor during this time. The tumor microenvironment of pancreatic cancer controls abundant stroma that contribute to fibrosis, which limits oxygen and nutrients for the tumor cells [191]. Pancreatic tumor cells turn on scavenging pathways in order to survive these environments, and continue to thrive in times of low nutrients [191]. However, this is just one of the many possible explanations of for the aberrant changes in VGLL1 expressing-tumors *in vitro*. Performing experiments with mouse tumor models is the ideal next direction for our VGLL1 studies, in order to determine in vivo relevance.

5.2 Future Directions

To better understand the role of VGLL1 in disease progression, studying rare cancers that arise during gestation may help shed light on VGLL1's role in tumorigenesis.

Gestational trophoblastic disease (GTD) is a rare group of tumors that develop in the placenta during early pregnancy. These tumors includes invasive moles, choriocarcinoma (CCA), and the more aggressive placental site trophoblastic tumor and epithelioid trophoblastic tumor (PSTT/ETT) [192]. These tumors occur in due to abnormal growth of trophoblasts. Currently, the mechanism behind the development of these caners at a molecular level remains unknown. Since we know that VGLL1 is highly overexpressed in trophoblasts, and is likely important for the invasive nature of trophoblasts during the development of placenta, there may be a connection between VGLL1 expression and GTD development during pregnancy.

One of the ways we could access the role of VGLL1 in GTD is to examine a cohort of GTD patient tumor samples, and perform IHC staining to compare VGLL1 expression in normal placenta vs. GTD patient tumors. We could determine if VGLL1 is expressed more in GTD patient's vs normal tissue donors. This would aid in determining if VGLL1 is important for the initiation of GTD tumors. By identifying if VGLL1 is highly overexpressed in these tumors, we could next determine what is causing the aberrant expression of VGLL1 in the trophoblasts. We could achieve this by accessing if mutations within the Hippo signaling pathway may be connected to the activation of VGLL1 signaling by looking at upstream signaling partners of VGLL1 within in the Hippo pathway.

By performing genetic analysis on tumor samples, this may provide more in-depth insight into the mutational changes occurring that lead to what may be the constitutive activation Hippo signaling pathway mediated by VGLL1 upregulation. We could utilize RT-PCR or Real-Time PCR to look for mutations at the RNA level. We could also access differences at the DNA level, by performing micro array. In addition to looking specifically

at VGLL1, we could also determine if other major players may be involved in the initiation of GTD, such as YAP/TAZ, within in the Hippo signaling pathway.

Once targets have been identified, we could confirm their involvement with small molecule inhibitors of the Hippo signaling pathway to determine if proliferation of GTD tumor cells is reduced. By performing these set of studies we may be the first to show how GTD tumors arise and provide alternative forms of treatments for patients that fail to response to the front line therapy.

One approach to analyze proliferation, and migration, invasion would be to utilize an immunodeficent mouse model in which human VGLL1-expressing and non VGLL1-expressing tumors can be grown, monitoring the tumor site and metastasis over time. It will require more extensive studies to assess the role of VGLL1 in immune evasion that we cannot be explored in immunodeficent mice. Development of a mouse model to study VGLL1 function in vivo is currently in the very early stages. We have the plasmids constructed to create mouse VGLL1 overexpressing and knockdown cell lines. We have 3 different human pancreatic tumor lines that have been transduced to overexpress VGLL1, and human placenta cells that we plan to use for comparison of pathways associated with VGLL1 in primary tissues. Additionally, we are planning to explore pathways and gene expression that may be connected to mouse VGLL1 expression by utilizing nanostring and RNA sequencing. Nanostring and RNA sequencing will provide insights into the molecular mechanisms controlling VGLL1 expression or what is being controlled by VGLL1 expression. There is still so much to left to learn about VGLL1, and we still very much in the early stages of uncovering the significance of VGLL1 in cancer progression.

Together, this dissertation has unveiled a novel shared TAA that shows great promise as a therapeutic target for multiple cancers. VGLL1 is relatively uncharacterized in cancer, but its homology to YAP/TAZ makes a compelling case to continue studies of this gene. If the role of VGLL1 in in cancer progression cancer can be determined, it may open the door to additional upstream or downstream therapeutic targets of VGLL1.With much to be discovered, it is a very exciting point in research on VGLL1. We hope work will continue to build on the foundation outlined in this dissertation, and in turn affect cancer patient's lives for the better in the future.

CHAPTER VI:

MATERIALS AND METHODS

Cell Lines. Human cancer cell lines demonstrating *VGLL1* mRNA expression were identified using the Cancer Cell Line Encyclopedia (CCLE) microarray-based gene expression analysis. HLA-A*0101-expressing cancer cell lines PANC10.05, CAPAN-1 OAW28, HT1197, HT1376, BXPC3, UBCL-1, and primary cell lines were obtained from commercial sources (ATCC and Sigma-Aldrich). Two VGLL1 negative cells lines were also collected, the pancreatic cell line PANC1 and the lung cancer line H1975 was obtained from (ATCC). The patient-derived organoid cell line MP015-Org (hMIA2D) was generated by the Tuveson lab at Cold Spring Harbor Labs as previously described (29599906). The patient-derived organoid cell line MP081-Org was generated by the Maitra lab from tumor tissue derived from a wedge biopsy. The gastric cancer cell lines GT-5 and MKN74 were a kind gift from Dr. Lee Ellis. WM793, MKN74, PANC1005, GT-5, and OAW28 cells were cultured in RPMI 1640 medium (GIBCO), containing 10% fetal bovine serum, 1% penicillin-streptomycin (Pen-Strep) (Cellgrow), and 1% Insulin-Transferrin-Seleum-A (GIBCO). BT20 and bladder cell lines were cultured in equal parts DMEM F12K and MEM Alpha, with FBS, Pen-Strep, and 1% sodium pyruvate (GIBCO). All other cell lines were cultured in RPMI 1640, FBS, and Penn-strep, with the addition of HEPES (GIBCO) and Glutamax (GIBCO).

Lentiviral Transductions. Some HLA-A*0101-negative tumor cell lines that naturally expressed VGLL1 protein were transduced with a lentiviral gene transfer vector to express HLA-A*0101 driven by the human PGK promoter, as previously described [193]. Ectopic cell surface expression of A*0101 was assessed by staining with anti-human HLA-A1-biotin and streptavidin-FITC (US Biological) and measuring fluorescence using a FACScanto II flow cytometer (BD Biosciences). Tumor cells expressing physiological and comparable

levels of surface HLA-A*0101 were isolated by cell sorting and used in subsequent experiments. To conduct proliferation and invasion assays WT cell lines with no VGLL1 expression were compared to lenti-viral overexpressed cell lines. For cell lines with no VGLL1 expression, the origene plasmid was used to generate a lentivirus (RC600200L1V, Origene). WT VGLL1 negative cell lines were transduced to express VGLL1 and protein expression was validated by western blot analysis.

VGLL1 Protein Expression. VGLL1 protein expression was confirmed in all cell lines by Western blot analysis. Cell lysates from tumor and primary cell lines were prepared and protein content normalized using the BCA method (Thermo-Fisher). Using standard Western blot techniques, cell lysates were run by polyacrylamide gel electrophoresis, transferred, and membranes probed with VGLL1-specific rabbit polyclonal antibody (TA322329, OriGene). VGLL1 protein was visualized using an enzyme-linked anti-rabbit mAb with the Scientific Pierce Fast Western Blot Kit, according to the manufacturer's instructions.

Peptide Identification, Selection and Validation. Patient-derived laparoscopic wedge biopsies, xenografts (PDX), or cell lines were lysed using Triton X-100 and cell lysates incubated overnight at 4^{o}C with 1μg of pan-HLA-ABC specific mAb W6/32 for every 10 mg of protein. Protein A/G Ultralink resin beads were used to immunoprecipate HLA class I molecules and HLA-bound peptides were then eluted with 0.1M acetic acid. HLA-A,B,C isolation was confirmed by Western blot analysis, then HLA-positive elutes were analyzed by tandem mass spectrometry (MS/MS). HLA class I protein recovery was semi-quantitatively assessed by rating Western blot band intensity on a scale from 0 (not

detectable) to 4 (highest intensity). Tumor-associated HLA-bound peptides were injected onto HPLC system (Dionex 3000 RSLC), and separated by reverse-phase chromatography in 0.1% formic acid water-acetonitrile on 1.8μm C18 (Agilent Technologies) in the MS/MS discovery phase. Peptides were analyzed on an Orbitrap Elite mass spectrometer (Thermo-Fisher) using data-dependent acquisition. To analyze the acquired MS/MS spectra, the Mascot algorithm was utilized to search the spectra against the SwissProt complete human protein database (updated 9/2018), which provided potential matches to conventionally annotated peptides.

Individual peptide matches underwent quality assessment by reference to multiple orthogonal parameters, including Mascot Ion score, MS1 measured differential to the calculated peptide mass (delta mass), and predicted binding to the patient's HLA allotypes as determined by high-resolution genetic sequencing and the NetMHC and NetMHCpan algorithms [100],[101]. High-confidence peptide matches were analyzed by BLAST searches to identify all potential source genes, which were then cross-referenced to RNAseq data derived from individual tumor samples to provide further validation of peptide identity (validation requiring a minimum source gene expression of 0.3 transcripts per million, TPM). Eluted TAA peptides were screened for safety as potential CTL targets by applying sequential RNA transcript expression filters to eliminate peptides most likely to elicit autoimmune toxicities due to normal tissue expression (GTex Portal RNAseq data, http://cancergenome.nih.gov/). Excluding testis and placenta, source gene transcript expression of 30 TPM maximum was allowed in non-essential tissues (listed in Table S2), 10 TPM in "caution" tissues, 3 TPM in "hazard" tissues and 1 TPM in highly essential "danger" tissues (such as heart and brain). Putative TAA genes were also screened for expression and

prevalence in different cancer types through analysis of TCGA RNAseq data (http://cancergenome.nih.gov/). In selected cases, targeted-MS/MS analysis was performed to confirm TAA peptide identity. For these analyses, retention-time windows for $^{13}C/^{15}N$ isotope-labeled synthetic peptide standards were pre-determined by MS analysis of the synthetic peptides, then targeted methods for searching TAA peptides were constructed using mass windows of 3 Da around each m/z.

Gene Expression Analysis and Patient Survival. Whole transcriptome sequencing (RNAseq) analysis was performed on RNA derived from all PDAC tumor specimens, xenografts, and organoid cell lines using the Illumina TruSeq Stranded Total RNA kit with Ribo-Zero Gold with approximately 200 million paired-end reads for each tumor RNA sample (Avera Institute for Human Genetics). Gene expression profiles of *VGLL1* and other cancer placenta antigens were determined by compiling RNAseq data derived from normal human primary tissues (GTex Portal) and tumor tissues (TCGA). Kaplan-Meier curves were generated from survival data of TCGA cancer patients when stratified by tumor *VGLL1* transcript expression.

Isolation and expansion of antigen-specific CD8 T cells. We generated three antigen-specific T cells. A MART-1 HLA-A*0201 restricted peptide was used as our control antigen. The MUC16 B0702-restricted peptide TPGGTRQSL, and the VGLL1 peptide HLA-A*0101 restricted peptide LSELETPGKY were both our experimental test antigens. Antigen–specific CTLs were generated as previously described [194], [195], [196]. To generate T cells against both the A2-restricted MART-1 derived peptide, and MUC16 B7-restricted peptide, we begin with the same healthy donor. This donor was both HLA-A2*0201 and

HLA-B*0702 positive. We isolated PBMCs from this healthy-donor. PBMCs derived from this this donor were stimulated in separate wells by MART-1 peptide and B7-restricted MUC16 peptide. After the stimulation, cultured cells were stained with either an MART-1/HLA*0201 or MUC16/HLA-B*0702-PE conjugated custom tetramer. (Fred Hutchinson Cancer Research Center), washed and then stained with APC-conjugated CD8 antibody. Cells were washed and analyzed by flow cytometry (LSRFortessa X-20 Analyzer). CD8 and tetramer double-positive cells were sorted by ARIA II and the VGLL1-specific CD8 T cells were expanded using the Rapid Expansion Protocol (REP) with PBMC and LCL feeder cells, as previously described.(16081794).

To generate VGLL1-specific T cells HLA-A*0101 positive patient- or healthy donor-derived PBMCs were stimulated twice by autologous dendritic cells (DCs) pulsed with the $VGLL1_{231-240}$ peptide LSELETPGKY. Six days after the second DC stimulation, cultured cells were stained with $VGLL1_{231-240}$ peptide/HLA-A*0101–PE-conjugated custom tetramer (Fred Hutchinson Cancer Research Center), washed and then stained with APC-conjugated CD8 antibody. Cells were washed and analyzed by flow cytometry (LSRFortessa X-20 Analyzer). CD8 and tetramer double-positive cells were sorted by ARIA II and the VGLL1-specific CD8 T cells were expanded using the Rapid Expansion Protocol (REP) with PBMC and LCL feeder cells, as previously described.(16081794) The TCR V_β repertoire of expanded CD8 T cells was assessed using the IOTest Beta Mark TCR-V_β Repertoire kit.

Cytotoxic T cell assays. Antitumor killing by VGLL1-specific CD8+ T cells was assessed using a standard chromium-51 (^{51}Cr) release assay. Target cells were labeled with 100μL of ^{51}Cr for 1 hour, then washed and plated at 2,000 target cells per well in triplicate. VGLL1-

specific CD8+ T cells were incubated with target cells at various effector-to-target (E:T) cell ratios for four hours. After the incubation period, supernatant was collected from the wells and ^{51}Cr was measured with a gamma radiation counter. The percentage of specific target cell lysis was calculated, correcting for background ^{51}Cr release and relative to a maximum ^{51}Cr release as measured by Triton X-100 lysed target cells.

esiRNA Knockdown. VGLL1 knockdown cells were generated using MISSION esiRNA (Cat. #EHU042561, Millipore). H1975-VGLL1 expressing cells were transfected with esiRNA two months after VGLL1 transduction. The cells were re-assessed by western blot analysis for VGLL1 over-expression prior to knockdown. 48hrs post-transfection, the cells were checked by western blot analysis for knockdown. Once knockdown was confirmed, they were immediately used in assays.

Proliferation Assays. H1975 VGLL1-transduced, GFP, and parental cells were plated in triplicates at 30,000 cells per well. Each line was plated in wells marked 0hr, 24hr, 72hr, and 96hrs. At each time point the cells were collected and counted by Nexcelom Cellometer. Cells counts were averaged at each time and the data was analyzed using graph pad prism.

Wound Healing Assay. The CytoSelect™ Wound Healing Kit from Millipore (Cat.# CBA-120) was used to perform the wound healing assay. The kit contained well inserts that created 0.9mm gaps. PANC1 VGLL1 transduced, GFP, and parental cell lines were plated at and collected after 24hrs. 500,000 cells were collected in media and 500 µL of the cell suspension was added to each well insert in triplicates. The cells were incubated overnight

and sterile forceps were used to remove the well inserts. The media was changed and the cells visualized under the microscope. We monitored the cells for an additional 48 hrs., taking images each day. Migration was assessed by the visualization and quantification of the wound at multiple areas within the well for each day. Data was analyzed by Image J and Graphpad Prism.

Transwell Invasion assays. Invasiveness of VGLL1 transduced, GFP, and parental PANC1 cells was accessed with the use of the QCM ECMatrix Cell Invasion Assay (Millipore Sigma, Cat. # ECM550). Cells were plated in triplicate in two time points, 24hr and 48hr at 50,000 cells per well in chamber inserts containing a thin-monolayer of extracellular membrane. RPMI with 10% FBS media was added to the well below. The cells were then left to incubate at their respective time points and were harvested at each point. The cells were stained with crystal violet stain following washing a cleaning of the ECM insert chamber. Cells attached to the ECM after washing were counted by first visualizing under a microscope and photos were analyzed by Image J. Cell count data was then further analyzed in Grahpad Prism.

Statistical analysis. Data analysis was performed using GraphPad Prism version 7.03. Normally distributed data were analyzed using parametric tests (ANOVA or unpaired t test). Kaplan-Meier survival curves were analyzed by log-rank tests. Test differences were considered statistically significant if $P<0.05$.

BIBLIOGRAPHY

[1] C.A. Janeway, Jr., How the immune system protects the host from infection, Microbes Infect, 3 (2001) 1167-1171.

[2] K. Murphy, C. Weaver, A. Mowat, L. Berg, D. Chaplin, Janeway's immunobiology, Garland Science, Taylor & Francis Group, New York, N.Y, 2017.

[3] J.S. Marshall, R. Warrington, W. Watson, H.L. Kim, An introduction to immunology and immunopathology, Allergy Asthma Clin Immunol, 14 (2018) 49.

[4] S.H. Kaufmann, Immunology's foundation: the 100-year anniversary of the Nobel Prize to Paul Ehrlich and Elie Metchnikoff, Nat Immunol, 9 (2008) 705-712.

[5] S.E. Turvey, D.H. Broide, Innate immunity, J Allergy Clin Immunol, 125 (2010) S24-32.

[6] F.A. Bonilla, H.C. Oettgen, Adaptive immunity, J Allergy Clin Immunol, 125 (2010) S33-40.

[7] J. Idoyaga, C. Fiorese, L. Zbytnuik, A. Lubkin, J. Miller, B. Malissen, D. Mucida, M. Merad, R.M. Steinman, Specialized role of migratory dendritic cells in peripheral tolerance induction, J Clin Invest, 123 (2013) 844-854.

[8] G.B. Challis, H.J. Stam, The spontaneous regression of cancer. A review of cases from 1900 to 1987, Acta Oncol, 29 (1990) 545-550.

[9] S. Oiseth, M. Aziz, Cancer immunotherapy: a brief review of the history, possibilities, and challenges ahead, Journal of Cancer Metastasis and Treatment, 3 (2017) 250.

[10] W.B. Coley, The treatment of malignant tumors by repeated inoculations of erysipelas. With a report of ten original cases. 1893, Clin Orthop Relat Res, (1991) 3-11.

[11] W.B. Coley, The Treatment of Inoperable Sarcoma by Bacterial Toxins (the Mixed Toxins of the Streptococcus erysipelas and the Bacillus prodigiosus), Proc R Soc Med, 3 (1910) 1-48.

[12] E.A. Carswell, L.J. Old, R.L. Kassel, S. Green, N. Fiore, B. Williamson, An endotoxin-induced serum factor that causes necrosis of tumors, Proc Natl Acad Sci U S A, 72 (1975) 3666-3670.

[13] C. Speil, R. Rzepka, Vaccines and vaccine adjuvants as biological response modifiers, Infect Dis Clin North Am, 25 (2011) 755-772.

[14] S. Kruger, M. Ilmer, S. Kobold, B.L. Cadilha, S. Endres, S. Ormanns, G. Schuebbe, B.W. Renz, J.G. D'Haese, H. Schloesser, V. Heinemann, M. Subklewe, S. Boeck, J. Werner, M. von Bergwelt-Baildon, Advances in cancer immunotherapy 2019 - latest trends, J Exp Clin Cancer Res, 38 (2019) 268.

[15] G. Schuler, B. Schuler-Thurner, R.M. Steinman, The use of dendritic cells in cancer immunotherapy, Curr Opin Immunol, 15 (2003) 138-147.

[16] F.M. Marincola, E. Wang, M. Herlyn, B. Seliger, S. Ferrone, Tumors as elusive targets of T-cell-based active immunotherapy, Trends Immunol, 24 (2003) 335-342.

[17] R.M. Steinman, Cytokines amplify the function of accessory cells, Immunol Lett, 17 (1988) 197-202.

[18] M. Bilusic, R.A. Madan, Therapeutic cancer vaccines: the latest advancement in targeted therapy, Am J Ther, 19 (2012) e172-181.

[19] P.J. DeMaria, M. Bilusic, Cancer Vaccines, Hematol Oncol Clin North Am, 33 (2019) 199-214.

[20] P.A. Ott, G. Dotti, C. Yee, S.L. Goff, An Update on Adoptive T-Cell Therapy and Neoantigen Vaccines, Am Soc Clin Oncol Educ Book, 39 (2019) e70-e78.

[21] B. Monzavi-Karbassi, T. Kieber-Emmons, Current concepts in cancer vaccine strategies, Biotechniques, 30 (2001) 170-172, 174, 176 passim.

[22] I. Kimiz-Gebologlu, S. Gulce-Iz, C. Biray-Avci, Monoclonal antibodies in cancer immunotherapy, Mol Biol Rep, 45 (2018) 2935-2940.

[23] A. Salmaninejad, S.F. Valilou, A.G. Shabgah, S. Aslani, M. Alimardani, A. Pasdar, A. Sahebkar, PD-1/PD-L1 pathway: Basic biology and role in cancer immunotherapy, J Cell Physiol, 234 (2019) 16824-16837.

[24] J.P. Allison, C. Chambers, A. Hurwitz, T. Sullivan, B. Boitel, S. Fournier, M. Brunner, M. Krummel, A role for CTLA-4-mediated inhibitory signals in peripheral T cell tolerance?, Novartis Found Symp, 215 (1998) 92-98; discussion 98-102, 186-190.

[25] J. Yuan, B. Ginsberg, D. Page, Y. Li, T. Rasalan, H.F. Gallardo, Y. Xu, S. Adams, N. Bhardwaj, K. Busam, L.J. Old, J.P. Allison, A. Jungbluth, J.D. Wolchok, CTLA-4 blockade increases antigen-specific CD8(+) T cells in prevaccinated patients with melanoma: three cases, Cancer Immunol Immunother, 60 (2011) 1137-1146.

[26] S.C. Wei, N.A.S. Anang, R. Sharma, M.C. Andrews, A. Reuben, J.H. Levine, A.P. Cogdill, J.J. Mancuso, J.A. Wargo, D. Pe'er, J.P. Allison, Combination anti-CTLA-4 plus anti-PD-1 checkpoint blockade utilizes cellular mechanisms partially distinct from monotherapies, Proc Natl Acad Sci U S A, (2019).

[27] S. Farajzadeh Valilou, N. Rezaei, Tumor Antigens, 2019, pp. 61-74.

[28] M.W. Rohaan, S. Wilgenhof, J. Haanen, Adoptive cellular therapies: the current landscape, Virchows Arch, 474 (2019) 449-461.

[29] R.T. Prehn, Tumor Specific Immunity to Nonviral Tumors, Proc Can Cancer Conf, 5 (1963) 387-395.

[30] R.T. Prehn, Tumor-specific antigens and the homograft reaction, Am J Surg, 105 (1963) 184-191.

[31] C.H. Lee, R. Yelensky, K. Jooss, T.A. Chan, Update on Tumor Neoantigens and Their Utility: Why It Is Good to Be Different, Trends Immunol, 39 (2018) 536-548.

[32] P.G. Coulie, P. Weynants, F. Lehmann, J. Herman, V. Brichard, T. Wolfel, A. Van Pel, E. De Plaen, F. Brasseur, T. Boon, Genes coding for tumor antigens recognized by human cytolytic T lymphocytes, J Immunother Emphasis Tumor Immunol, 14 (1993) 104-109.

[33] P. van der Bruggen, J.P. Szikora, P. Boel, C. Wildmann, M. Somville, M. Sensi, T. Boon, Autologous cytolytic T lymphocytes recognize a MAGE-1 nonapeptide on melanomas expressing HLA-Cw*1601, Eur J Immunol, 24 (1994) 2134-2140.

[34] E. Celis, J. Fikes, P. Wentworth, J. Sidney, S. Southwood, A. Maewal, M.F. Del Guercio, A. Sette, B. Livingston, Identification of potential CTL epitopes of tumor-associated antigen MAGE-1 for five common HLA-A alleles, Mol Immunol, 31 (1994) 1423-1430.

[35] O.L. Caballero, Y.T. Chen, Cancer/testis (CT) antigens: potential targets for immunotherapy, Cancer Sci, 100 (2009) 2014-2021.

[36] N. Ise, K. Omi, D. Nambara, S. Higashiyama, K. Goishi, Overexpressed HER2 in NSCLC is a possible therapeutic target of EGFR inhibitors, Anticancer Res, 31 (2011) 4155-4161.

[37] M.O. Holmstrom, H.C. Hasselbalch, M.H. Andersen, Neo-antigen specific memory T-cell responses in healthy individuals, Oncoimmunology, 8 (2019) 1599640.

[38] O.J. Finn, Human Tumor Antigens Yesterday, Today, and Tomorrow, Cancer Immunol Res, 5 (2017) 347-354.

[39] D.H. Suh, M. Kim, K.H. Lee, K.Y. Eom, M.K. Kjeldsen, M.R. Mirza, J.W. Kim, Major clinical research advances in gynecologic cancer in 2017, J Gynecol Oncol, 29 (2018) e31.

[40] Y. Yang, Y. Che, Y. Zhao, X. Wang, Prevention and treatment of cervical cancer by a single administration of human papillomavirus peptide vaccine with CpG oligodeoxynucleotides as an adjuvant in vivo, Int Immunopharmacol, 69 (2019) 279-288.

[41] S.A. Rosenberg, Development of cancer immunotherapies based on identification of the genes encoding cancer regression antigens, J Natl Cancer Inst, 88 (1996) 1635-1644.

[42] S.A. Rosenberg, Y. Kawakami, P.F. Robbins, R. Wang, Identification of the genes encoding cancer antigens: implications for cancer immunotherapy, Advances in cancer research, 70 (1996) 145-177.

[43] E. Wang, S. Tomei, F.M. Marincola, Reflections upon human cancer immune responsiveness to T cell-based therapy, Cancer Immunol Immunother, 61 (2012) 761-770.

[44] T. Wolfel, E. Klehmann, C. Muller, K.H. Schutt, K.H. Meyer zum Buschenfelde, A. Knuth, Lysis of human melanoma cells by autologous cytolytic T cell clones. Identification of human histocompatibility leukocyte antigen A2 as a restriction element for three different antigens, J Exp Med, 170 (1989) 797-810.

[45] P. van der Bruggen, C. Traversari, P. Chomez, C. Lurquin, E. De Plaen, B. Van den Eynde, A. Knuth, T. Boon, A gene encoding an antigen recognized by cytolytic T lymphocytes on a human melanoma, Science, 254 (1991) 1643-1647.

[46] G. Parmiani, C. Castelli, P. Dalerba, R. Mortarini, L. Rivoltini, F.M. Marincola, A. Anichini, Cancer immunotherapy with peptide-based vaccines: what have we achieved? Where are we going?, J Natl Cancer Inst, 94 (2002) 805-818.

[47] K. Falk, O. Rotzschke, S. Stevanovic, G. Jung, H.G. Rammensee, Allele-specific motifs revealed by sequencing of self-peptides eluted from MHC molecules, Nature, 351 (1991) 290-296.

[48] R.F. Wang, G. Zeng, S.F. Johnston, K. Voo, H. Ying, T cell-mediated immune responses in melanoma: implications for immunotherapy, Critical reviews in oncology/hematology, 43 (2002) 1-11.

[49] C. Yee, J.A. Thompson, D. Byrd, S.R. Riddell, P. Roche, E. Celis, P.D. Greenberg, Adoptive T cell therapy using antigen-specific CD8+ T cell clones for the treatment of patients with metastatic melanoma: in vivo persistence, migration, and antitumor effect of transferred T cells, Proc Natl Acad Sci U S A, 99 (2002) 16168-16173.

[50] C. Yee, Adoptive T cell therapy: points to consider, Curr Opin Immunol, 51 (2018) 197-203.

[51] A. Rotte, M. Bhandaru, Y. Zhou, K.J. McElwee, Immunotherapy of melanoma: present options and future promises, Cancer Metastasis Rev, 34 (2015) 115-128.

[52] S.A. Rosenberg, IL-2: the first effective immunotherapy for human cancer, J Immunol, 192 (2014) 5451-5458.

[53] C. Yee, G. Lizee, A.J. Schueneman, Endogenous T-Cell Therapy: Clinical Experience, Cancer J, 21 (2015) 492-500.

[54] C. Yee, Adoptive T-cell therapy for cancer: boutique therapy or treatment modality?, Clin Cancer Res, 19 (2013) 4550-4552.

[55] M.A. Forget, C. Haymaker, K.R. Hess, Y.J. Meng, C. Creasy, T. Karpinets, O.J. Fulbright, J. Roszik, S.E. Woodman, Y.U. Kim, D. Sakellariou-Thompson, A. Bhatta, A. Wahl, E. Flores, S.T. Thorsen, R.J. Tavera, R. Ramachandran, A.M. Gonzalez, C.L. Toth, S. Wardell, R. Mansaray, V. Patel, D.J. Carpio, C. Vaughn, C.M. Farinas, P.G. Velasquez, W.J. Hwu, S.P. Patel, M.A. Davies, A. Diab, I.C. Glitza, H. Tawbi, M.K. Wong, S. Cain, M.I. Ross, J.E. Lee, J.E. Gershenwald, A. Lucci, R. Royal, J.N. Cormier, J.A. Wargo, L.G. Radvanyi, C.A. Torres-Cabala, R. Beroukhim, P. Hwu, R.N. Amaria, C. Bernatchez, Prospective Analysis of Adoptive TIL Therapy in Patients with Metastatic Melanoma: Response, Impact of Anti-CTLA4, and Biomarkers to Predict Clinical Outcome, Clin Cancer Res, 24 (2018) 4416-4428.

[56] W. Si, C. Li, P. Wei, Synthetic immunology: T-cell engineering and adoptive immunotherapy, Synth Syst Biotechnol, 3 (2018) 179-185.

[57] C. Yee, Adoptive therapy using antigen-specific T-cell clones, Cancer J, 16 (2010) 367-373.

[58] C. Yee, S.R. Riddell, P.D. Greenberg, Prospects for adoptive T cell therapy, Curr Opin Immunol, 9 (1997) 702-708.

[59] G. Lizee, G. Basha, W.A. Jefferies, Tails of wonder: endocytic-sorting motifs key for exogenous antigen presentation, Trends Immunol, 26 (2005) 141-149.

[60] G. Lizee, G. Basha, J. Tiong, J.P. Julien, M. Tian, K.E. Biron, W.A. Jefferies, Control of dendritic cell cross-presentation by the major histocompatibility complex class I cytoplasmic domain, Nat Immunol, 4 (2003) 1065-1073.

[61] J. Neefjes, M.L. Jongsma, P. Paul, O. Bakke, Towards a systems understanding of MHC class I and MHC class II antigen presentation, Nature reviews. Immunology, 11 (2011) 823-836.

[62] J. Trowsdale, HLA genomics in the third millennium, Curr Opin Immunol, 17 (2005) 498-504.

[63] X. Cao, S.F. Cai, T.A. Fehniger, J. Song, L.I. Collins, D.R. Piwnica-Worms, T.J. Ley, Granzyme B and perforin are important for regulatory T cell-mediated suppression of tumor clearance, Immunity, 27 (2007) 635-646.

[64] M. Bassani-Sternberg, G. Coukos, Mass spectrometry-based antigen discovery for cancer immunotherapy, Curr Opin Immunol, 41 (2016) 9-17.

[65] J. Schmidt, P. Guillaume, D. Dojcinovic, J. Karbach, G. Coukos, I. Luescher, In silico and cell-based analyses reveal strong divergence between prediction and observation of T-cell-recognized tumor antigen T-cell epitopes, J Biol Chem, 292 (2017) 11840-11849.

[66] X. Liu, Q. Hu, S. Liu, L.J. Tallo, L. Sadzewicz, C.A. Schettine, M. Nikiforov, E.N. Klyushnenkova, Y. Ionov, Serum Antibody Repertoire Profiling Using In Silico Antigen Screen, PLoS One, 8 (2013) e67181.

[67] N.A. Bykova, D.B. Malko, G.A. Efimov, In Silico Analysis of the Minor Histocompatibility Antigen Landscape Based on the 1000 Genomes Project, Front Immunol, 9 (2018) 1819.

[68] E. Caron, D.J. Kowalewski, C. Chiek Koh, T. Sturm, H. Schuster, R. Aebersold, Analysis of Major Histocompatibility Complex (MHC) Immunopeptidomes Using Mass Spectrometry, Mol Cell Proteomics, 14 (2015) 3105-3117.

[69] A.L. Pritchard, M.L. Hastie, M. Neller, J.J. Gorman, C.W. Schmidt, N.K. Hayward, Exploration of peptides bound to MHC class I molecules in melanoma, Pigment Cell Melanoma Res, 28 (2015) 281-294.

[70] P. Jagtap, S. Bandhakavi, L. Higgins, T. McGowan, R. Sa, M.D. Stone, J. Chilton, E.A. Arriaga, S.L. Seymour, T.J. Griffin, Workflow for analysis of high mass accuracy salivary data set using MaxQuant and ProteinPilot search algorithm, Proteomics, 12 (2012) 1726-1730.

[71] C.T. Tan, N.P. Croft, N.L. Dudek, N.A. Williamson, A.W. Purcell, Direct quantitation of MHC-bound peptide epitopes by selected reaction monitoring, Proteomics, 11 (2011) 2336-2340.

[72] C. Hassan, M.G. Kester, G. Oudgenoeg, A.H. de Ru, G.M. Janssen, J.W. Drijfhout, R.M. Spaapen, C.R. Jimenez, M.H. Heemskerk, J.H. Falkenburg, P.A. van Veelen, Accurate quantitation of MHC-bound peptides by application of isotopically labeled peptide MHC complexes, J Proteomics, 109 (2014) 240-244.

[73] E. Boutet, D. Lieberherr, M. Tognolli, M. Schneider, P. Bansal, A.J. Bridge, S. Poux, L. Bougueleret, I. Xenarios, UniProtKB/Swiss-Prot, the Manually Annotated Section of the UniProt KnowledgeBase: How to Use the Entry View, Methods Mol Biol, 1374 (2016) 23-54.

[74] E. Boutet, D. Lieberherr, M. Tognolli, M. Schneider, A. Bairoch, UniProtKB/Swiss-Prot, Methods Mol Biol, 406 (2007) 89-112.

[75] S. Jarmalavicius, Y. Welte, P. Walden, High immunogenicity of the human leukocyte antigen peptidomes of melanoma tumor cells, J Biol Chem, 287 (2012) 33401-33411.

[76] S. Kreiter, M. Vormehr, N. van de Roemer, M. Diken, M. Lower, J. Diekmann, S. Boegel, B. Schrors, F. Vascotto, J.C. Castle, A.D. Tadmor, S.P. Schoenberger, C. Huber, O. Tureci, U. Sahin, Mutant MHC class II epitopes drive therapeutic immune responses to cancer, Nature, 520 (2015) 692-696.

[77] M.C. Dange, H.S. Bhonsle, R.K. Godbole, S.K. More, S.M. Bane, M.J. Kulkarni, R.D. Kalraiya, Mass spectrometry based identification of galectin-3 interacting proteins potentially involved in lung melanoma metastasis, Mol Biosyst, 13 (2017) 2303-2309.

[78] P. Shepherd, K.L. Sheath, S.T. Tin, P. Khwaounjoo, P.S. Aye, A. Li, G.R. Laking, N.J. Kingston, C.A. Lewis, J. Mark Elwood, D.R. Love, M.J. McKeage, Lung cancer mutation testing: a clinical retesting study of agreement between a real-time PCR and a mass spectrometry test, Oncotarget, 8 (2017) 101437-101451.

[79] J. Park, A.H. Talukder, S.A. Lim, K. Kim, K. Pan, B. Melendez, S.D. Bradley, K.R. Jackson, J.S. Khalili, J. Wang, C. Creasy, B.F. Pan, S.E. Woodman, C. Bernatchez, D. Hawke, P. Hwu, K.M. Lee, J. Roszik, G. Lizee, C. Yee, SLC45A2: A Melanoma Antigen with High Tumor Selectivity and Reduced Potential for Autoimmune Toxicity, Cancer Immunol Res, 5 (2017) 618-629.

[80] E. Ghisoni, M. Imbimbo, S. Zimmermann, G. Valabrega, Ovarian Cancer Immunotherapy: Turning up the Heat, Int J Mol Sci, 20 (2019).

[81] J. Wang, G.S. Wu, Role of autophagy in cisplatin resistance in ovarian cancer cells, J Biol Chem, 289 (2014) 17163-17173.

[82] J.M. Hansen, R.L. Coleman, A.K. Sood, Targeting the tumour microenvironment in ovarian cancer, Eur J Cancer, 56 (2016) 131-143.

[83] K.R. Cho, M. Shih Ie, Ovarian cancer, Annu Rev Pathol, 4 (2009) 287-313.

[84] R.L. Siegel, K.D. Miller, A. Jemal, Cancer statistics, 2019, CA Cancer J Clin, 69 (2019) 7-34.

[85] R.A. Steinman, I.O. De Castro, M. Shrayyef, V. Chengazi, E. Giampoli, P. Van Der Sloot, L.M. Calvi, S.D. Wittlin, S.R. Hammes, R. Hou, Two cases of malignant struma ovarii with metastasis to pelvic bone, Gynecol Obstet Invest, 75 (2013) 139-144.

[86] K.D. Miller, L. Nogueira, A.B. Mariotto, J.H. Rowland, K.R. Yabroff, C.M. Alfano, A. Jemal, J.L. Kramer, R.L. Siegel, Cancer treatment and survivorship statistics, 2019, CA Cancer J Clin, 69 (2019) 363-385.

[87] K. Oda, J. Hamanishi, K. Matsuo, K. Hasegawa, Genomics to immunotherapy of ovarian clear cell carcinoma: Unique opportunities for management, Gynecol Oncol, 151 (2018) 381-389.

[88] C.W. McCloskey, G.M. Rodriguez, K.J.C. Galpin, B.C. Vanderhyden, Ovarian Cancer Immunotherapy: Preclinical Models and Emerging Therapeutics, Cancers (Basel), 10 (2018).

[89] M.R. Mirza, S. Pignata, J.A. Ledermann, Latest clinical evidence and further development of PARP inhibitors in ovarian cancer, Ann Oncol, 29 (2018) 1366-1376.

[90] L. Zhang, J.R. Conejo-Garcia, D. Katsaros, P.A. Gimotty, M. Massobrio, G. Regnani, A. Makrigiannakis, H. Gray, K. Schlienger, M.N. Liebman, S.C. Rubin, G. Coukos, Intratumoral T cells, recurrence, and survival in epithelial ovarian cancer, N Engl J Med, 348 (2003) 203-213.

[91] G.M. Rodriguez, K.J.C. Galpin, C.W. McCloskey, B.C. Vanderhyden, The Tumor Microenvironment of Epithelial Ovarian Cancer and Its Influence on Response to Immunotherapy, Cancers (Basel), 10 (2018).

[92] C. Hermans, D. Anz, J. Engel, T. Kirchner, S. Endres, D. Mayr, Analysis of FoxP3+ T-regulatory cells and CD8+ T-cells in ovarian carcinoma: location and tumor infiltration patterns are key prognostic markers, PLoS One, 9 (2014) e111757.

[93] J.C. Yang, S.A. Rosenberg, Adoptive T-Cell Therapy for Cancer, Adv Immunol, 130 (2016) 279-294.

[94] M.R. Raspollini, F. Castiglione, D. Rossi Degl'innocenti, G. Amunni, A. Villanucci, F. Garbini, G. Baroni, G.L. Taddei, Tumour-infiltrating gamma/delta T-lymphocytes are correlated with a brief disease-free interval in advanced ovarian serous carcinoma, Ann Oncol, 16 (2005) 590-596.

[95] Y. Aoki, K. Takakuwa, S. Kodama, K. Tanaka, M. Takahashi, A. Tokunaga, T. Takahashi, Use of adoptive transfer of tumor-infiltrating lymphocytes alone or in combination with cisplatin-containing chemotherapy in patients with epithelial ovarian cancer, Cancer Res, 51 (1991) 1934-1939.

[96] P.P. Santoiemma, D.J. Powell, Jr., Tumor infiltrating lymphocytes in ovarian cancer, Cancer Biol Ther, 16 (2015) 807-820.

[97] G.P. Linette, E.A. Stadtmauer, M.V. Maus, A.P. Rapoport, B.L. Levine, L. Emery, L. Litzky, A. Bagg, B.M. Carreno, P.J. Cimino, G.K. Binder-Scholl, D.P. Smethurst, A.B. Gerry, N.J. Pumphrey, A.D. Bennett, J.E. Brewer, J. Dukes, J. Harper, H.K. Tayton-Martin, B.K. Jakobsen, N.J. Hassan, M. Kalos, C.H. June, Cardiovascular toxicity and titin cross-reactivity of affinity-enhanced T cells in myeloma and melanoma, Blood, 122 (2013) 863-871.

[98] R.A. Morgan, N. Chinnasamy, D. Abate-Daga, A. Gros, P.F. Robbins, Z. Zheng, M.E. Dudley, S.A. Feldman, J.C. Yang, R.M. Sherry, G.Q. Phan, M.S. Hughes, U.S. Kammula,

A.D. Miller, C.J. Hessman, A.A. Stewart, N.P. Restifo, M.M. Quezado, M. Alimchandani, A.Z. Rosenberg, A. Nath, T. Wang, B. Bielekova, S.C. Wuest, N. Akula, F.J. McMahon, S. Wilde, B. Mosetter, D.J. Schendel, C.M. Laurencot, S.A. Rosenberg, Cancer regression and neurological toxicity following anti-MAGE-A3 TCR gene therapy, J Immunother, 36 (2013) 133-151.

[99] M.C. Panelli, M.P. Bettinotti, K. Lally, G.A. Ohnmacht, Y. Li, P. Robbins, A. Riker, S.A. Rosenberg, F.M. Marincola, A tumor-infiltrating lymphocyte from a melanoma metastasis with decreased expression of melanoma differentiation antigens recognizes MAGE-12, J Immunol, 164 (2000) 4382-4392.

[100] V. Jurtz, S. Paul, M. Andreatta, P. Marcatili, B. Peters, M. Nielsen, NetMHCpan-4.0: Improved Peptide-MHC Class I Interaction Predictions Integrating Eluted Ligand and Peptide Binding Affinity Data, J Immunol, 199 (2017) 3360-3368.

[101] M. Nielsen, M. Andreatta, NetMHCpan-3.0; improved prediction of binding to MHC class I molecules integrating information from multiple receptor and peptide length datasets, Genome Med, 8 (2016) 33.

[102] R. Giambruno, M. Mihailovich, T. Bonaldi, Mass Spectrometry-Based Proteomics to Unveil the Non-coding RNA World, Front Mol Biosci, 5 (2018) 90.

[103] J. Lv, P. Li, Mesothelin as a biomarker for targeted therapy, Biomark Res, 7 (2019) 18.

[104] M. Akce, M.Y. Zaidi, E.K. Waller, B.F. El-Rayes, G.B. Lesinski, The Potential of CAR T Cell Therapy in Pancreatic Cancer, Front Immunol, 9 (2018) 2166.

[105] M. Miyazawa, M. Iwahashi, T. Ojima, M. Katsuda, M. Nakamura, M. Nakamori, K. Ueda, T. Naka, K. Hayata, T. Iida, H. Yamaue, Dendritic cells adenovirally-transduced with

full-length mesothelin cDNA elicit mesothelin-specific cytotoxicity against pancreatic cancer cell lines in vitro, Cancer Lett, 305 (2011) 32-39.

[106] G.L. Beatty, M.H. O'Hara, S.F. Lacey, D.A. Torigian, F. Nazimuddin, F. Chen, I.M. Kulikovskaya, M.C. Soulen, M. McGarvey, A.M. Nelson, W.L. Gladney, B.L. Levine, J.J. Melenhorst, G. Plesa, C.H. June, Activity of Mesothelin-Specific Chimeric Antigen Receptor T Cells Against Pancreatic Carcinoma Metastases in a Phase 1 Trial, Gastroenterology, 155 (2018) 29-32.

[107] H. Schuster, J.K. Peper, H.C. Bosmuller, K. Rohle, L. Backert, T. Bilich, B. Ney, M.W. Loffler, D.J. Kowalewski, N. Trautwein, A. Rabsteyn, T. Engler, S. Braun, S.P. Haen, J.S. Walz, B. Schmid-Horch, S.Y. Brucker, D. Wallwiener, O. Kohlbacher, F. Fend, H.G. Rammensee, S. Stevanovic, A. Staebler, P. Wagner, The immunopeptidomic landscape of ovarian carcinomas, Proc Natl Acad Sci U S A, 114 (2017) E9942-E9951.

[108] J.M. Niloff, R.C. Knapp, E. Schaetzl, C. Reynolds, R.C. Bast, Jr., CA125 antigen levels in obstetric and gynecologic patients, Obstet Gynecol, 64 (1984) 703-707.

[109] C. Theriault, M. Pinard, M. Comamala, M. Migneault, J. Beaudin, I. Matte, M. Boivin, A. Piche, C. Rancourt, MUC16 (CA125) regulates epithelial ovarian cancer cell growth, tumorigenesis and metastasis, Gynecol Oncol, 121 (2011) 434-443.

[110] M. Felder, A. Kapur, J. Gonzalez-Bosquet, S. Horibata, J. Heintz, R. Albrecht, L. Fass, J. Kaur, K. Hu, H. Shojaei, R.J. Whelan, M.S. Patankar, MUC16 (CA125): tumor biomarker to cancer therapy, a work in progress, Molecular cancer, 13 (2014) 129.

[111] J.M. Niloff, T.L. Klug, E. Schaetzl, V.R. Zurawski, Jr., R.C. Knapp, R.C. Bast, Jr., Elevation of serum CA125 in carcinomas of the fallopian tube, endometrium, and endocervix, Am J Obstet Gynecol, 148 (1984) 1057-1058.

[112] H. Sekine, D.F. Hayes, T. Ohno, K.A. Keefe, E. Schaetzl, R.C. Bast, R. Knapp, D.W. Kufe, Circulating DF3 and CA125 antigen levels in serum from patients with epithelial ovarian carcinoma, J Clin Oncol, 3 (1985) 1355-1363.

[113] J.A. Gubbels, J. Belisle, M. Onda, C. Rancourt, M. Migneault, M. Ho, T.K. Bera, J. Connor, B.K. Sathyanarayana, B. Lee, I. Pastan, M.S. Patankar, Mesothelin-MUC16 binding is a high affinity, N-glycan dependent interaction that facilitates peritoneal metastasis of ovarian tumors, Molecular cancer, 5 (2006) 50.

[114] O. Kaneko, L. Gong, J. Zhang, J.K. Hansen, R. Hassan, B. Lee, M. Ho, A binding domain on mesothelin for CA125/MUC16, J Biol Chem, 284 (2009) 3739-3749.

[115] A. Rump, Y. Morikawa, M. Tanaka, S. Minami, N. Umesaki, M. Takeuchi, A. Miyajima, Binding of ovarian cancer antigen CA125/MUC16 to mesothelin mediates cell adhesion, J Biol Chem, 279 (2004) 9190-9198.

[116] S.H. Chen, W.C. Hung, P. Wang, C. Paul, K. Konstantopoulos, Mesothelin binding to CA125/MUC16 promotes pancreatic cancer cell motility and invasion via MMP-7 activation, Sci Rep, 3 (2013) 1870.

[117] C. Fang, Y. Cao, X. Liu, X.T. Zeng, Y. Li, Serum CA125 is a predictive marker for breast cancer outcomes and correlates with molecular subtypes, Oncotarget, 8 (2017) 63963-63970.

[118] Q. Yuan, J. Song, W. Yang, H. Wang, Q. Huo, J. Yang, X. Yu, Y. Liu, C. Xu, H. Bao, The effect of CA125 on metastasis of ovarian cancer: old marker new function, Oncotarget, 8 (2017) 50015-50022.

[119] Y.C. Zeng, R. Wu, S.L. Wang, F. Chi, R. Xing, W.S. Cai, G.L. Fan, Y.C. Fan, W.Z. Zhong, L.N. Wu, X.D. Chen, H.H. Chen, Y.P. Xiao, Serum CA125 level predicts prognosis

in patients with multiple brain metastases from non-small cell lung cancer before and after treatment of whole-brain radiotherapy, Med Oncol, 31 (2014) 48.

[120] V.P. Balachandran, M. Luksza, J.N. Zhao, V. Makarov, J.A. Moral, R. Remark, B. Herbst, G. Askan, U. Bhanot, Y. Senbabaoglu, D.K. Wells, C.I.O. Cary, O. Grbovic-Huezo, M. Attiyeh, B. Medina, J. Zhang, J. Loo, J. Saglimbeni, M. Abu-Akeel, R. Zappasodi, N. Riaz, M. Smoragiewicz, Z.L. Kelley, O. Basturk, I. Australian Pancreatic Cancer Genome, R. Garvan Institute of Medical, H. Prince of Wales, H. Royal North Shore, G. University of, H. St Vincent's, Q.B.M.R. Institute, C.f.C.R. University of Melbourne, I.f.M.B. University of Queensland, H. Bankstown, H. Liverpool, C.O.B.L. Royal Prince Alfred Hospital, H. Westmead, H. Fremantle, H. St John of God, H. Royal Adelaide, C. Flinders Medical, P. Envoi, H. Princess Alexandria, H. Austin, I. Johns Hopkins Medical, A.R.-N.C.f.A.R.o. Cancer, M. Gonen, A.J. Levine, P.J. Allen, D.T. Fearon, M. Merad, S. Gnjatic, C.A. Iacobuzio-Donahue, J.D. Wolchok, R.P. DeMatteo, T.A. Chan, B.D. Greenbaum, T. Merghoub, S.D. Leach, Identification of unique neoantigen qualities in long-term survivors of pancreatic cancer, Nature, 551 (2017) 512-516.

[121] S. Bellone, S. Anfossi, T.J. O'Brien, M.J. Cannon, D.A. Silasi, M. Azodi, P.E. Schwartz, T.J. Rutherford, S. Pecorelli, A.D. Santin, Generation of CA125-specific cytotoxic T lymphocytes in human leukocyte antigen-A2.1-positive healthy donors and patients with advanced ovarian cancer, Am J Obstet Gynecol, 200 (2009) 75 e71-10.

[122] A. Aithal, S. Rauth, P. Kshirsagar, A. Shah, I. Lakshmanan, W.M. Junker, M. Jain, M.P. Ponnusamy, S.K. Batra, MUC16 as a novel target for cancer therapy, Expert Opin Ther Targets, 22 (2018) 675-686.

[123] O. Hiraike, T. Yano, Y. Taketani, [The characteristics of CA125/MUC16], Nihon Rinsho, 68 Suppl 7 (2010) 681-684.

[124] A.M. Varghese, M.A. Lowery, K.H. Yu, E.M. O'Reilly, Current management and future directions in metastatic pancreatic adenocarcinoma, Cancer, 122 (2016) 3765-3775.

[125] A. McGuigan, P. Kelly, R.C. Turkington, C. Jones, H.G. Coleman, R.S. McCain, Pancreatic cancer: A review of clinical diagnosis, epidemiology, treatment and outcomes, World J Gastroenterol, 24 (2018) 4846-4861.

[126] S.T. Chari, K. Kelly, M.A. Hollingsworth, S.P. Thayer, D.A. Ahlquist, D.K. Andersen, S.K. Batra, T.A. Brentnall, M. Canto, D.F. Cleeter, M.A. Firpo, S.S. Gambhir, V.L. Go, O.J. Hines, B.J. Kenner, D.S. Klimstra, M.M. Lerch, M.J. Levy, A. Maitra, S.J. Mulvihill, G.M. Petersen, A.D. Rhim, D.M. Simeone, S. Srivastava, M. Tanaka, A.I. Vinik, D. Wong, Early detection of sporadic pancreatic cancer: summative review, Pancreas, 44 (2015) 693-712.

[127] K. Polireddy, Q. Chen, Cancer of the Pancreas: Molecular Pathways and Current Advancement in Treatment, J Cancer, 7 (2016) 1497-1514.

[128] E.M. Van Allen, D. Miao, B. Schilling, S.A. Shukla, C. Blank, L. Zimmer, A. Sucker, U. Hillen, M.H.G. Foppen, S.M. Goldinger, J. Utikal, J.C. Hassel, B. Weide, K.C. Kaehler, C. Loquai, P. Mohr, R. Gutzmer, R. Dummer, S. Gabriel, C.J. Wu, D. Schadendorf, L.A. Garraway, Genomic correlates of response to CTLA-4 blockade in metastatic melanoma, Science, 350 (2015) 207-211.

[129] O. Strobel, J. Neoptolemos, D. Jager, M.W. Buchler, Optimizing the outcomes of pancreatic cancer surgery, Nat Rev Clin Oncol, 16 (2019) 11-26.

[130] S.C. Wei, C.R. Duffy, J.P. Allison, Fundamental Mechanisms of Immune Checkpoint Blockade Therapy, Cancer Discov, 8 (2018) 1069-1086.

[131] N.A. Rizvi, M.D. Hellmann, A. Snyder, P. Kvistborg, V. Makarov, J.J. Havel, W. Lee, J. Yuan, P. Wong, T.S. Ho, M.L. Miller, N. Rekhtman, A.L. Moreira, F. Ibrahim, C. Bruggeman, B. Gasmi, R. Zappasodi, Y. Maeda, C. Sander, E.B. Garon, T. Merghoub, J.D. Wolchok, T.N. Schumacher, T.A. Chan, Cancer immunology. Mutational landscape determines sensitivity to PD-1 blockade in non-small cell lung cancer, Science, 348 (2015) 124-128.

[132] M.E. Dudley, J.R. Wunderlich, J.C. Yang, R.M. Sherry, S.L. Topalian, N.P. Restifo, R.E. Royal, U. Kammula, D.E. White, S.A. Mavroukakis, L.J. Rogers, G.J. Gracia, S.A. Jones, D.P. Mangiameli, M.M. Pelletier, J. Gea-Banacloche, M.R. Robinson, D.M. Berman, A.C. Filie, A. Abati, S.A. Rosenberg, Adoptive cell transfer therapy following non-myeloablative but lymphodepleting chemotherapy for the treatment of patients with refractory metastatic melanoma, J Clin Oncol, 23 (2005) 2346-2357.

[133] L.G. Radvanyi, C. Bernatchez, M. Zhang, P.S. Fox, P. Miller, J. Chacon, R. Wu, G. Lizee, S. Mahoney, G. Alvarado, M. Glass, V.E. Johnson, J.D. McMannis, E. Shpall, V. Prieto, N. Papadopoulos, K. Kim, J. Homsi, A. Bedikian, W.J. Hwu, S. Patel, M.I. Ross, J.E. Lee, J.E. Gershenwald, A. Lucci, R. Royal, J.N. Cormier, M.A. Davies, R. Mansaray, O.J. Fulbright, C. Toth, R. Ramachandran, S. Wardell, A. Gonzalez, P. Hwu, Specific lymphocyte subsets predict response to adoptive cell therapy using expanded autologous tumor-infiltrating lymphocytes in metastatic melanoma patients, Clin Cancer Res, 18 (2012) 6758-6770.

[134] E. Tran, M. Ahmadzadeh, Y.C. Lu, A. Gros, S. Turcotte, P.F. Robbins, J.J. Gartner, Z. Zheng, Y.F. Li, S. Ray, J.R. Wunderlich, R.P. Somerville, S.A. Rosenberg, Immunogenicity of somatic mutations in human gastrointestinal cancers, Science, 350 (2015) 1387-1390.

[135] N. Zacharakis, H. Chinnasamy, M. Black, H. Xu, Y.C. Lu, Z. Zheng, A. Pasetto, M. Langhan, T. Shelton, T. Prickett, J. Gartner, L. Jia, K. Trebska-McGowan, R.P. Somerville, P.F. Robbins, S.A. Rosenberg, S.L. Goff, S.A. Feldman, Immune recognition of somatic mutations leading to complete durable regression in metastatic breast cancer, Nat Med, 24 (2018) 724-730.

[136] C.S. Hinrichs, S.A. Rosenberg, Exploiting the curative potential of adoptive T-cell therapy for cancer, Immunol Rev, 257 (2014) 56-71.

[137] A.G. Chapuis, I.M. Roberts, J.A. Thompson, K.A. Margolin, S. Bhatia, S.M. Lee, H.L. Sloan, I.P. Lai, E.A. Farrar, F. Wagener, K.C. Shibuya, J. Cao, J.D. Wolchok, P.D. Greenberg, C. Yee, T-Cell Therapy Using Interleukin-21-Primed Cytotoxic T-Cell Lymphocytes Combined With Cytotoxic T-Cell Lymphocyte Antigen-4 Blockade Results in Long-Term Cell Persistence and Durable Tumor Regression, J Clin Oncol, 34 (2016) 3787-3795.

[138] A.G. Chapuis, S.M. Lee, J.A. Thompson, I.M. Roberts, K.A. Margolin, S. Bhatia, H.L. Sloan, I. Lai, F. Wagener, K. Shibuya, J. Cao, J.D. Wolchok, P.D. Greenberg, C. Yee, Combined IL-21-primed polyclonal CTL plus CTLA4 blockade controls refractory metastatic melanoma in a patient, J Exp Med, 213 (2016) 1133-1139.

[139] P.F. Robbins, S.H. Kassim, T.L. Tran, J.S. Crystal, R.A. Morgan, S.A. Feldman, J.C. Yang, M.E. Dudley, J.R. Wunderlich, R.M. Sherry, U.S. Kammula, M.S. Hughes, N.P. Restifo, M. Raffeld, C.C. Lee, Y.F. Li, M. El-Gamil, S.A. Rosenberg, A pilot trial using lymphocytes genetically engineered with an NY-ESO-1-reactive T-cell receptor: long-term follow-up and correlates with response, Clin Cancer Res, 21 (2015) 1019-1027.

[140] I. Tawara, S. Kageyama, Y. Miyahara, H. Fujiwara, T. Nishida, Y. Akatsuka, H. Ikeda, K. Tanimoto, S. Terakura, M. Murata, Y. Inaguma, M. Masuya, N. Inoue, T. Kidokoro, S. Okamoto, D. Tomura, H. Chono, I. Nukaya, J. Mineno, T. Naoe, N. Emi, M. Yasukawa, N. Katayama, H. Shiku, Safety and persistence of WT1-specific T-cell receptor gene-transduced lymphocytes in patients with AML and MDS, Blood, 130 (2017) 1985-1994.

[141] R.A. Morgan, M.E. Dudley, J.R. Wunderlich, M.S. Hughes, J.C. Yang, R.M. Sherry, R.E. Royal, S.L. Topalian, U.S. Kammula, N.P. Restifo, Z. Zheng, A. Nahvi, C.R. de Vries, L.J. Rogers-Freezer, S.A. Mavroukakis, S.A. Rosenberg, Cancer regression in patients after transfer of genetically engineered lymphocytes, Science, 314 (2006) 126-129.

[142] K. Young, D.J. Hughes, D. Cunningham, N. Starling, Immunotherapy and pancreatic cancer: unique challenges and potential opportunities, Ther Adv Med Oncol, 10 (2018) 1758835918816281.

[143] D. Kabacaoglu, K.J. Ciecielski, D.A. Ruess, H. Algul, Immune Checkpoint Inhibition for Pancreatic Ductal Adenocarcinoma: Current Limitations and Future Options, Front Immunol, 9 (2018) 1878.

[144] M. Yarchoan, A. Hopkins, E.M. Jaffee, Tumor Mutational Burden and Response Rate to PD-1 Inhibition, N Engl J Med, 377 (2017) 2500-2501.

[145] P. Bailey, D.K. Chang, K. Nones, A.L. Johns, A.M. Patch, M.C. Gingras, D.K. Miller, A.N. Christ, T.J. Bruxner, M.C. Quinn, C. Nourse, L.C. Murtaugh, I. Harliwong, S. Idrisoglu, S. Manning, E. Nourbakhsh, S. Wani, L. Fink, O. Holmes, V. Chin, M.J. Anderson, S. Kazakoff, C. Leonard, F. Newell, N. Waddell, S. Wood, Q. Xu, P.J. Wilson, N. Cloonan, K.S. Kassahn, D. Taylor, K. Quek, A. Robertson, L. Pantano, L. Mincarelli, L.N. Sanchez, L. Evers, J. Wu, M. Pinese, M.J. Cowley, M.D. Jones, E.K. Colvin, A.M. Nagrial,

E.S. Humphrey, L.A. Chantrill, A. Mawson, J. Humphris, A. Chou, M. Pajic, C.J. Scarlett, A.V. Pinho, M. Giry-Laterriere, I. Rooman, J.S. Samra, J.G. Kench, J.A. Lovell, N.D. Merrett, C.W. Toon, K. Epari, N.Q. Nguyen, A. Barbour, N. Zeps, K. Moran-Jones, N.B. Jamieson, J.S. Graham, F. Duthie, K. Oien, J. Hair, R. Grutzmann, A. Maitra, C.A. Iacobuzio-Donahue, C.L. Wolfgang, R.A. Morgan, R.T. Lawlor, V. Corbo, C. Bassi, B. Rusev, P. Capelli, R. Salvia, G. Tortora, D. Mukhopadhyay, G.M. Petersen, I. Australian Pancreatic Cancer Genome, D.M. Munzy, W.E. Fisher, S.A. Karim, J.R. Eshleman, R.H. Hruban, C. Pilarsky, J.P. Morton, O.J. Sansom, A. Scarpa, E.A. Musgrove, U.M. Bailey, O. Hofmann, R.L. Sutherland, D.A. Wheeler, A.J. Gill, R.A. Gibbs, J.V. Pearson, N. Waddell, A.V. Biankin, S.M. Grimmond, Genomic analyses identify molecular subtypes of pancreatic cancer, Nature, 531 (2016) 47-52.

[146] E.D. Foucher, C. Ghigo, S. Chouaib, J. Galon, J. Iovanna, D. Olive, Pancreatic Ductal Adenocarcinoma: A Strong Imbalance of Good and Bad Immunological Cops in the Tumor Microenvironment, Front Immunol, 9 (2018) 1044.

[147] E. Tran, P.F. Robbins, Y.C. Lu, T.D. Prickett, J.J. Gartner, L. Jia, A. Pasetto, Z. Zheng, S. Ray, E.M. Groh, I.R. Kriley, S.A. Rosenberg, T-Cell Transfer Therapy Targeting Mutant KRAS in Cancer, N Engl J Med, 375 (2016) 2255-2262.

[148] I.M. Stromnes, T.M. Schmitt, A. Hulbert, J.S. Brockenbrough, H. Nguyen, C. Cuevas, A.M. Dotson, X. Tan, J.L. Hotes, P.D. Greenberg, S.R. Hingorani, T Cells Engineered against a Native Antigen Can Surmount Immunologic and Physical Barriers to Treat Pancreatic Ductal Adenocarcinoma, Cancer Cell, 28 (2015) 638-652.

[149] M. Koneru, R. O'Cearbhaill, S. Pendharkar, D.R. Spriggs, R.J. Brentjens, A phase I clinical trial of adoptive T cell therapy using IL-12 secreting MUC-16(ecto) directed chimeric antigen receptors for recurrent ovarian cancer, J Transl Med, 13 (2015) 102.

[150] M.R. Parkhurst, J.C. Yang, R.C. Langan, M.E. Dudley, D.A. Nathan, S.A. Feldman, J.L. Davis, R.A. Morgan, M.J. Merino, R.M. Sherry, M.S. Hughes, U.S. Kammula, G.Q. Phan, R.M. Lim, S.A. Wank, N.P. Restifo, P.F. Robbins, C.M. Laurencot, S.A. Rosenberg, T cells targeting carcinoembryonic antigen can mediate regression of metastatic colorectal cancer but induce severe transient colitis, Mol Ther, 19 (2011) 620-626.

[151] A.H. Morrison, K.T. Byrne, R.H. Vonderheide, Immunotherapy and Prevention of Pancreatic Cancer, Trends Cancer, 4 (2018) 418-428.

[152] P. Vaudin, R. Delanoue, I. Davidson, J. Silber, A. Zider, TONDU (TDU), a novel human protein related to the product of vestigial (vg) gene of Drosophila melanogaster interacts with vertebrate TEF factors and substitutes for Vg function in wing formation, Development, 126 (1999) 4807-4816.

[153] E. Simon, C. Faucheux, A. Zider, N. Theze, P. Thiebaud, From vestigial to vestigial-like: the Drosophila gene that has taken wing, Dev Genes Evol, 226 (2016) 297-315.

[154] M.A. Castilla, M.A. Lopez-Garcia, M.R. Atienza, J.M. Rosa-Rosa, J. Diaz-Martin, M.L. Pecero, B. Vieites, L. Romero-Perez, J. Benitez, A. Calcabrini, J. Palacios, VGLL1 expression is associated with a triple-negative basal-like phenotype in breast cancer, Endocr Relat Cancer, 21 (2014) 587-599.

[155] L. Cheng, S. Zhang, R. Alexander, G.T. Maclennan, K.B. Hodges, B.T. Harrison, A. Lopez-Beltran, R. Montironi, Sarcomatoid carcinoma of the urinary bladder: the final

common pathway of urothelial carcinoma dedifferentiation, Am J Surg Pathol, 35 (2011) e34-46.

[156] F. Soncin, M. Khater, C. To, D. Pizzo, O. Farah, A. Wakeland, K. Arul Nambi Rajan, K.K. Nelson, C.W. Chang, M. Moretto-Zita, D.R. Natale, L.C. Laurent, M.M. Parast, Comparative analysis of mouse and human placentae across gestation reveals species-specific regulators of placental development, Development, 145 (2018).

[157] X.Y. Dong, J.R. Peng, Y.J. Ye, H.S. Chen, L.J. Zhang, X.W. Pang, Y. Li, Y. Zhang, S. Wang, M.E. Fant, Y.H. Yin, W.F. Chen, Plac1 is a tumor-specific antigen capable of eliciting spontaneous antibody responses in human cancer patients, Int J Cancer, 122 (2008) 2038-2043.

[158] R.A. Wolff, A. Wang-Gillam, H. Alvarez, H. Tiriac, D. Engle, S. Hou, A.F. Groff, A. San Lucas, V. Bernard, K. Allenson, J. Castillo, D. Kim, F. Mulu, J. Huang, B. Stephens, Wistuba, II, M. Katz, G. Varadhachary, Y. Park, J. Hicks, A. Chinnaiyan, L. Scampavia, T. Spicer, C. Gerhardinger, A. Maitra, D. Tuveson, J. Rinn, G. Lizee, C. Yee, A.J. Levine, Dynamic changes during the treatment of pancreatic cancer, Oncotarget, 9 (2018) 14764-14790.

[159] R.J. Torphy, Y. Zhu, R.D. Schulick, Immunotherapy for pancreatic cancer: Barriers and breakthroughs, Ann Gastroenterol Surg, 2 (2018) 274-281.

[160] Q.J. Wang, Z. Yu, K. Griffith, K. Hanada, N.P. Restifo, J.C. Yang, Identification of T-cell Receptors Targeting KRAS-Mutated Human Tumors, Cancer Immunol Res, 4 (2016) 204-214.

[161] F.F. Gonzalez-Galarza, L.Y. Takeshita, E.J. Santos, F. Kempson, M.H. Maia, A.L. da Silva, A.L. Teles e Silva, G.S. Ghattaoraya, A. Alfirevic, A.R. Jones, D. Middleton, Allele

frequency net 2015 update: new features for HLA epitopes, KIR and disease and HLA adverse drug reaction associations, Nucleic Acids Res, 43 (2015) D784-788.

[162] M. Uhlen, L. Fagerberg, B.M. Hallstrom, C. Lindskog, P. Oksvold, A. Mardinoglu, A. Sivertsson, C. Kampf, E. Sjostedt, A. Asplund, I. Olsson, K. Edlund, E. Lundberg, S. Navani, C.A. Szigyarto, J. Odeberg, D. Djureinovic, J.O. Takanen, S. Hober, T. Alm, P.H. Edqvist, H. Berling, H. Tegel, J. Mulder, J. Rockberg, P. Nilsson, J.M. Schwenk, M. Hamsten, K. von Feilitzen, M. Forsberg, L. Persson, F. Johansson, M. Zwahlen, G. von Heijne, J. Nielsen, F. Ponten, Proteomics. Tissue-based map of the human proteome, Science, 347 (2015) 1260419.

[163] A.V. Pobbati, S.W. Chan, I. Lee, H. Song, W. Hong, Structural and functional similarity between the Vgll1-TEAD and the YAP-TEAD complexes, Structure, 20 (2012) 1135-1140.

[164] J. Chen, X.W. Pang, F.F. Liu, X.Y. Dong, H.C. Wang, S. Wang, Y. Zhang, W.F. Chen, [PLAC1/CP1 gene expression and autologous humoral immunity in gastric cancer patients], Beijing Da Xue Xue Bao Yi Xue Ban, 38 (2006) 124-127.

[165] W.A. Silva, Jr., S. Gnjatic, E. Ritter, R. Chua, T. Cohen, M. Hsu, A.A. Jungbluth, N.K. Altorki, Y.T. Chen, L.J. Old, A.J. Simpson, O.L. Caballero, PLAC1, a trophoblast-specific cell surface protein, is expressed in a range of human tumors and elicits spontaneous antibody responses, Cancer Immun, 7 (2007) 18.

[166] Q. Li, M. Liu, M. Wu, X. Zhou, S. Wang, Y. Hu, Y. Wang, Y. He, X. Zeng, J. Chen, Q. Liu, D. Xiao, X. Hu, W. Liu, PLAC1-specific TCR-engineered T cells mediate antigen-specific antitumor effects in breast cancer, Oncol Lett, 15 (2018) 5924-5932.

[167] R. Shi, X. Yu, Y. Wang, J. Sun, Q. Sun, W. Xia, G. Dong, A. Wang, Z. Gao, F. Jiang, L. Xu, Expression profile, clinical significance, and biological function of insulin-like growth factor 2 messenger RNA-binding proteins in non-small cell lung cancer, Tumour Biol, 39 (2017) 1010428317695928.

[168] Y. Zhou, T. Huang, H.L. Siu, C.C. Wong, Y. Dong, F. Wu, B. Zhang, W.K. Wu, A.S. Cheng, J. Yu, K.F. To, W. Kang, IGF2BP3 functions as a potential oncogene and is a crucial target of miR-34a in gastric carcinogenesis, Mol Cancer, 16 (2017) 77.

[169] D. Ansari, H. Ohlsson, C. Althini, M. Bauden, Q. Zhou, D. Hu, R. Andersson, The Hippo Signaling Pathway in Pancreatic Cancer, Anticancer Res, 39 (2019) 3317-3321.

[170] J.D. Aplin, Implantation, trophoblast differentiation and haemochorial placentation: mechanistic evidence in vivo and in vitro, J Cell Sci, 99 (Pt 4) (1991) 681-692.

[171] E.P. Kam, L. Gardner, Y.W. Loke, A. King, The role of trophoblast in the physiological change in decidual spiral arteries, Human reproduction, 14 (1999) 2131-2138.

[172] P. Bischof, A. Meisser, A. Campana, Paracrine and autocrine regulators of trophoblast invasion--a review, Placenta, 21 Suppl A (2000) S55-60.

[173] Y. Chang-Qing, L. Jie, Z. Shi-Qi, Z. Kun, G. Zi-Qian, X. Ran, L. Hui-Meng, Z. Ren-Bin, Z. Gang, Y. Da-Chuan, Z. Chen-Yan, Recent treatment progress of triple negative breast cancer, Prog Biophys Mol Biol, (2019).

[174] Y. Mesrouze, J.C. Hau, D. Erdmann, C. Zimmermann, P. Fontana, T. Schmelzle, P. Chene, The surprising features of the TEAD4-Vgll1 protein-protein interaction, Chembiochem, 15 (2014) 537-542.

[175] I.M. Moya, G. Halder, Hippo-YAP/TAZ signalling in organ regeneration and regenerative medicine, Nat Rev Mol Cell Biol, (2018).

[176] X. Zhang, H. Zhao, Y. Li, D. Xia, L. Yang, Y. Ma, H. Li, The role of YAP/TAZ activity in cancer metabolic reprogramming, Mol Cancer, 17 (2018) 134.

[177] Y. Zhou, T. Huang, A.S. Cheng, J. Yu, W. Kang, K.F. To, The TEAD Family and Its Oncogenic Role in Promoting Tumorigenesis, Int J Mol Sci, 17 (2016).

[178] S.W. Plouffe, K.C. Lin, J.L. Moore, 3rd, F.E. Tan, S. Ma, Z. Ye, Y. Qiu, B. Ren, K.L. Guan, The Hippo pathway effector proteins YAP and TAZ have both distinct and overlapping functions in the cell, J Biol Chem, 293 (2018) 11230-11240.

[179] Z. Li, Y. Wang, Y. Zhu, C. Yuan, D. Wang, W. Zhang, B. Qi, J. Qiu, X. Song, J. Ye, H. Wu, H. Jiang, L. Liu, Y. Zhang, L.N. Song, J. Yang, J. Cheng, The Hippo transducer TAZ promotes epithelial to mesenchymal transition and cancer stem cell maintenance in oral cancer, Molecular oncology, 9 (2015) 1091-1105.

[180] S. Yang, L. Zhang, V. Purohit, S.K. Shukla, X. Chen, F. Yu, K. Fu, Y. Chen, J. Solheim, P.K. Singh, W. Song, J. Dong, Active YAP promotes pancreatic cancer cell motility, invasion and tumorigenesis in a mitotic phosphorylation-dependent manner through LPAR3, Oncotarget, 6 (2015) 36019-36031.

[181] W. Zhang, N. Nandakumar, Y. Shi, M. Manzano, A. Smith, G. Graham, S. Gupta, E.E. Vietsch, S.Z. Laughlin, M. Wadhwa, M. Chetram, M. Joshi, F. Wang, B. Kallakury, J. Toretsky, A. Wellstein, C. Yi, Downstream of mutant KRAS, the transcription regulator YAP is essential for neoplastic progression to pancreatic ductal adenocarcinoma, Sci Signal, 7 (2014) ra42.

[182] S.W. Chan, C.J. Lim, K. Guo, C.P. Ng, I. Lee, W. Hunziker, Q. Zeng, W. Hong, A role for TAZ in migration, invasion, and tumorigenesis of breast cancer cells, Cancer Res, 68 (2008) 2592-2598.

[183] Q. Zhang, X. Han, J. Chen, X. Xie, J. Xu, Y. Zhao, J. Shen, L. Hu, P. Xu, H. Song, L. Zhang, B. Zhao, Y.J. Wang, Z. Xia, Yes-associated protein (YAP) and transcriptional coactivator with PDZ-binding motif (TAZ) mediate cell density-dependent proinflammatory responses, J Biol Chem, 293 (2018) 18071-18085.

[184] Z. Taha, H.J. Janse van Rensburg, X. Yang, The Hippo Pathway: Immunity and Cancer, Cancers (Basel), 10 (2018).

[185] H.J. Janse van Rensburg, T. Azad, M. Ling, Y. Hao, B. Snetsinger, P. Khanal, L.M. Minassian, C.H. Graham, M.J. Rauh, X. Yang, The Hippo Pathway Component TAZ Promotes Immune Evasion in Human Cancer through PD-L1, Cancer Res, 78 (2018) 1457-1470.

[186] S. Mori, J.T. Chang, E.R. Andrechek, N. Matsumura, T. Baba, G. Yao, J.W. Kim, M. Gatza, S. Murphy, J.R. Nevins, Anchorage-independent cell growth signature identifies tumors with metastatic potential, Oncogene, 28 (2009) 2796-2805.

[187] Ajaybabu V. Pobbati, Siew W. Chan, I. Lee, H. Song, W. Hong, Structural and Functional Similarity between the Vgll1-TEAD and the YAP-TEAD Complexes, Structure, 20 (2012) 1135-1140.

[188] C.R. Justus, N. Leffler, M. Ruiz-Echevarria, L.V. Yang, In vitro cell migration and invasion assays, J Vis Exp, (2014).

[189] F. Du, X. Zhao, D. Fan, Soft Agar Colony Formation Assay as a Hallmark of Carcinogenesis, Bio-protocol, 7 (2017) e2351.

[190] S. Noguchi, A. Saito, M. Horie, Y. Mikami, H.I. Suzuki, Y. Morishita, M. Ohshima, Y. Abiko, J.S. Mattsson, H. Konig, M. Lohr, K. Edlund, J. Botling, P. Micke, T. Nagase, An

integrative analysis of the tumorigenic role of TAZ in human non-small cell lung cancer, Clin Cancer Res, 20 (2014) 4660-4672.

[191] B.T. Finicle, V. Jayashankar, A.L. Edinger, Nutrient scavenging in cancer, Nat Rev Cancer, 18 (2018) 619-633.

[192] A. Braga, P. Mora, A.C. de Melo, A. Nogueira-Rodrigues, J. Amim-Junior, J. Rezende-Filho, M.J. Seckl, Challenges in the diagnosis and treatment of gestational trophoblastic neoplasia worldwide, World J Clin Oncol, 10 (2019) 28-37.

[193] S.D. Bradley, Z. Chen, B. Melendez, A. Talukder, J.S. Khalili, T. Rodriguez-Cruz, S. Liu, M. Whittington, W. Deng, F. Li, C. Bernatchez, L.G. Radvanyi, M.A. Davies, P. Hwu, G. Lizee, BRAFV600E Co-opts a Conserved MHC Class I Internalization Pathway to Diminish Antigen Presentation and CD8+ T-cell Recognition of Melanoma, Cancer Immunol Res, 3 (2015) 602-609.

[194] Y. Li, M. Bleakley, C. Yee, IL-21 influences the frequency, phenotype, and affinity of the antigen-specific CD8 T cell response, J Immunol, 175 (2005) 2261-2269.

[195] Y. Li, C. Yee, IL-21 mediated Foxp3 suppression leads to enhanced generation of antigen-specific CD8+ cytotoxic T lymphocytes, Blood, 111 (2008) 229-235.

[196] A.G. Chapuis, G.B. Ragnarsson, H.N. Nguyen, C.N. Chaney, J.S. Pufnock, T.M. Schmitt, N. Duerkopp, I.M. Roberts, G.L. Pogosov, W.Y. Ho, S. Ochsenreither, M. Wolfl, M. Bar, J.P. Radich, C. Yee, P.D. Greenberg, Transferred WT1-reactive CD8+ T cells can mediate antileukemic activity and persist in post-transplant patients, Sci Transl Med, 5 (2013) 174ra127.

VITA

Sherille Denaé Bradley was born in Mid-West City, Oklahoma. She is the daughter of Debra and Thomas Bradley. She earned her high school diploma in 2006 from George Bush High school, in Richmond. She then attended Texas State University in San Marcos, Texas. Sherille received her Bachelors of Science degree with a major in microbiology and a minor in biochemistry from Texas State University in 2011. After graduating, she began her graduate studies at The MD Anderson Cancer Center UTHealth Graduate School of Biomedical Sciences. There she completed her master's degree in 2014, followed by her Ph.D. in 2019.

Email address:

Sherillebradley@gmail.com